Dissipation-induced Luttinger liquids in the Caldeira-Leggett formalism

Master's thesis

Sam Eigenhuis

Supervisors:

prof. dr. Cristiane de Morais Smith

dr. Giandomenico Palumbo

Institute for Theoretical Physics

Utrecht University

December 2016

Abstract

It is well known that dissipation usually induces decoherence in quantum systems. However, recently it has been employed to engineer zero-energy Majorana modes on the boundary of a one-dimensional fermionic chain by using the Lindblad master equation [1]. In this thesis, by employing the Caldeira-Leggett theory of quantum dissipation, we study the equivalence between a particle on a one-dimensional lattice coupled to a thermal bath, and the massless Luttinger liquid with an impurity on the boundary in a closed system [2–4]. In particular, the Luttinger liquid with a single impurity at the boundary of a semi-infinite chain is bosonized into the boundary sine-Gordon theory. Here, a zero-energy Majorana mode appears at the boundary when the Luttinger parameter $K = 1/2$. The equivalence is shown to apply also in the case of helical Luttinger liquids, which play an important role in topological insulators. This equivalence is then generalized to the full sine-Gordon theory, such that massive Luttinger liquids can be mapped to a single-particle one-dimensional tunneling Hamiltonian with a dissipative Ohmic Caldeira-Leggett bath.

Contents

1 Introduction **1**

1.1 Historical background 1

1.2 This thesis 2

1.3 Outline 3

2 Topological states of matter **5**

2.1 Introduction 5

2.2 Topological insulators and the quantum Hall effect 6

2.2.1 Insulators and conductors 6

2.2.2 Superconductors 6

2.3 Topological states of matter 7

2.3.1 Quantum Hall effect and topological insulators 7

2.3.2 Characterization of the topological phase 12

2.3.3 Symmetries 15

2.4 Topological superconductors 18

2.4.1 Introduction 18

2.4.2 The Kitaev chain 20

2.4.3 Topological invariant 22

2.4.4 Majorana modes 23

2.4.5 QFT approach of Hamiltonians in Class D 25

2.4.6 Applications 25

3 Dissipation in quantum systems **27**

3.1 Introduction 27

3.2 Caldeira-Leggett model 28

3.2.1 Introduction 28

3.2.2 The model 29

3.2.3 Integrating out the bath 33

4 Bosonization of the Luttinger liquid **39**
4.1 Introduction . . . 39
4.2 Bosonization . . . 41
4.2.1 Introduction . . . 41
4.2.2 Dictionary . . . 41
4.3 Luttinger liquid . . . 48
4.3.1 Noninteracting spinless electrons . . . 48
4.3.2 Interactions . . . 52
4.3.3 Luttinger liquid . . . 55
4.3.4 Impurity in the spinless Luttinger liquid . . . 56
4.3.5 Chiral and helical Luttinger liquid . . . 58
4.4 Boundary sine-Gordon model . . . 59
4.4.1 Sine-Gordon theory . . . 60
4.4.2 Partition function of the BSG . . . 60
4.4.3 Majorana mode in the BSG model . . . 62

5 Equivalence between the boundary sine-Gordon theory and Caldeira-Leggett model **65**
5.1 Introduction . . . 65
5.2 Intuitive approach . . . 65
5.3 Mode expansion . . . 67
5.3.1 Cosine interaction . . . 68
5.3.2 Non-interacting part . . . 68
5.4 Rotation of basis . . . 71
5.4.1 First and second term . . . 72
5.4.2 Third term . . . 73
5.4.3 Result . . . 76
5.5 Mapping the variables . . . 76
5.5.1 First and second term . . . 76
5.5.2 Third term . . . 77
5.5.3 Final result . . . 78
5.6 Conclusion . . . 79

6 Extension to the helical Luttinger liquid **81**
6.1 Introduction . . . 81
6.2 Helical Luttinger liquid . . . 81
6.3 Conclusion . . . 83

7 Extension to the sine-Gordon theory **85**
7.1 Introduction 85
7.2 Equivalence in the sine-Gordon theory 85
7.2.1 Mode expansion 86
7.2.2 Basis rotation 86
7.2.3 Mapping the variables 89

8 Conclusion and outlook **91**

9 Nederlandse samenvatting **95**

References **103**

Chapter 1

Introduction

1.1 Historical background

The field of condensed matter physics exhibits a rich variety of phenomena, which recently have been embellished by a connection to the mathematical branch of topology, the study of properties that are preserved through deformations of objects. In 2005, Kane and Mele [5] and Bernevig, Hughes, and Zhang [6] proposed models for a two-dimensional quantum spin Hall insulator, which realizes the quantum spin Hall effect (QSHE). Here, the edge states carry a quantized spin Hall current, in contrast to the insulating bulk states. A strong spin-orbit coupling and time-reversal invariance protect the edge states from scattering due to disorder in the material. This system is an example of a topological insulator, a system that is insulating in the bulk, but has protected conducting states at the edges. Its physical observables depend on its topological properties. In 2007, the group of Molenkamp found experimental evidence of the QSHE in mercury-telluride quantum wells [7]. Similarly to topological insulators, the existence of topological superconductors also has been theoretically investigated. In 2001, Kitaev proposed a model of a one-dimensional chain of spinless fermions, where a superconducting energy gap leads to a state that supports zero-energy Majorana modes at the edges of the chain [8]. These brought an impulse to the field of topological quantum computation, as their topological protection shields them from decoherence. Experimental signatures of zero-energy Majorana modes have been found by the groups led by Kouwenhoven [9] and Marcus [10]. These developments have given a large impetus to the field of condensed-matter physics.

Contrary to the superconducting Kitaev model, the Luttinger-liquid theory describes conventional one-dimensional fermionic systems [11]. This low-energy theory includes density-density interactions between electrons, and can be rewritten in terms of a free-bosonic theory. It is the paradigm of the method of bosonization, a non-perturbative method used to

switch between fermionic and bosonic language to describe one-dimensional systems [2]. In its bosonized form, the Hamiltonian is Gaussian. If impurities or other types of electron-electron interactions are added, a cosine interaction appears. Together, they constitute a Hamiltonian corresponding to the sine-Gordon equation. A local interaction or an impurity at the boundary of the system leads to the boundary sine-Gordon equation.

Dissipation, the exchange of energy corresponding to the interaction of a system with its environment, usually is highly detrimental to quantum-mechanical systems. The transition from a pure quantum state to a mixed state, i.e. decoherence, is one of the common culprits that prevent creating a stable qubit in quantum computation. The paradigmatic model to describe quantum dissipative systems is the Caldeira-Leggett model [12, 13]. Here, the system of interest is studied together with a reservoir, responsible for its energy losses. The reservoir is modelled as a set of harmonic oscillators, linearly coupled to the system of interest. In the classical limit, this model correctly reproduces the Langevin equation, used to classically characterize open systems. The model has been used in the ‘80s and ‘90s to successfully describe Josephson junctions and superconducting quantum interference devices. However, dissipation also does have another face. In 2011, Diehl et al. have proposed how to use dissipation as a mean to engineer topological states in quantum systems [1]. Using the Lindblad formalism, a general dynamical description of open quantum systems, they showed that at the edges of a one-dimensional chain of spinless fermions, zero-energy Majorana modes appear as a consequence of dissipation. The analogy of this model with the Kitaev chain is clear, whilst it differs in the sense that in the latter the origin of the zero-energy Majorana modes lies in the Cooper pairing terms in the Hamiltonian, instead of dissipation as in the former model. This indicates that dissipation can play a constructive role in quantum systems as well. This is very promising, because experimentally it is very difficult to simulate systems that are truly isolated from their environment.

1.2 This thesis

The research thesis reports on the study of dissipation effects in the Kitaev chain using the Caldeira-Leggett formalism. The central question is: how can dissipation on a lattice, represented by the Caldeira-Leggett formalism, be connected to the appearance of zero-energy Majorana modes in a fermionic chain? Instrumental in this thesis is the equivalence between a dissipative particle on a one-dimensional lattice, in the Caldeira-Leggett model with Ohmic bath, and the boundary sine-Gordon equation, as reported by Guinea, Hakim, and Muramatsu [3, 4], and later by Gogolin, Nersesyan, and Tsvelik [2].

The equivalence can be extended from the boundary sine-Gordon equation to several kinds of Luttinger liquids. Initially, it will be shown for an impurity at the boundary of a semi-infinite chain for both fermionic left- and right-moving modes. Subsequently, the chiral Luttinger liquid is considered, containing electrons moving in a single direction, and the helical Luttinger liquid, where the spin variable is added, but the spin orientation is locked to the direction of motion. It is shown that the boundary sine-Gordon equation hosts a zero-energy Majorana mode a the boundary of the chain. Furthermore, the correspondence may be generalized to the full sine-Gordon theory, where a cosine interaction term is present at each lattice site. This allows the application of the equivalence to a much wider range of Luttinger liquids.

1.3 Outline

This thesis can be divided in two parts. The first part, Chapters 2-4, serves as an introduction to the topic, and provides background for the models used in the equivalence presented in Chapter 5. The second part, Chapters 5-7, reveals the equivalence between a dissipative particle on a one-dimensional lattice with Ohmic bath and the boundary sine-Gordon equation, as well as several extensions and generalizations of this equivalence. Chapter 5 is the core of this thesis. Chapters 6 and 7 concern the analytic application of this theory to related quantum systems, and represent own work of the author.

The first part starts with Chapter 2, where topological insulators and topological superconductors are discussed. The integer quantum Hall effect and the quantum spin Hall effect are briefly reviewed. Also, their behaviour and classification are discussed. Then we look in detail into the Kitaev chain, a one-dimensional superconductor that supports zero-energy Majorana modes at its edges, and say a few words about its possible practical applications. Chapter 3 covers the topic of quantum dissipation and how to treat it mathematically, with a strong focus on the Caldeira-Leggett model. Chapter 4 deals with the theory of fermionic systems in one dimension, the Luttinger liquid, and explains the method of bosonization. Finally, it is shown that the interacting Luttinger liquid after bosonization has the form of the sine-Gordon equation. In the last section, it is shown that, for a specific parameter choice, a zero-energy Majorana mode appears at the boundary of a semi-infinite chain, described by the boundary sine-Gordon equation.

The second part begins with Chapter 5, where the central equivalence of this thesis is proved. It follows in detail the outline provided by Ref. [2]. Some intuition for the correspondence is provided, and it includes the calculations showing the equivalence. The differences with Refs. [3, 4] are briefly adressed. Furthermore, the boundary sine-Gordon

equation is linked to the Luttinger liquid with an impurity at the boundary. In Chapter 6, it is shown that the equivalence also applies to the helical Luttinger liquid, describing edge states in the quantum spin Hall effect. In Chapter 7 the same procedure is used as in Chapter 5, but starting from the sine-Gordon theory. The procedure ensures that a Caldeira-Legget dissipative contribution appears. This case also may be mapped to a dissipative particle on a, albeit different, lattice.

In Chapter 8, the main contents of this thesis are summarized, and an outlook into further research is provided.

Finally, in Chapter 9, I provide a Dutch summary of the work for the non-expert reader.

Chapter 2

Topological states of matter

2.1 Introduction

It is well known that most of the phases of matter and their quantum phase transitions have been classified according to Landau's theory of spontaneous symmetry breaking [14]. The phase transition between liquid and solid can be understood from the breaking of rotational invariance and continuous translational symmetry. A ferromagnetic system abruptly loses its long-range order for temperatures higher than its Curie temperature. Superconductivity is caused by a condensate of Cooper pairs, which spontaneously break the U(1)-gauge symmetry. However, in the 1980's the quantum version of the Hall effect was discovered. Here, for a specific parameter regime, the insulating bulk was found to be surrounded by gapless edge states. This proved the classification based on geometrical properties to be insufficient, since the physical observables of this new quantum state instead depended on its topological properties. Since then, other types of topological materials have been unveiled, like topological insulators and topological superconductors [5, 6, 8, 15].

In this chapter, first we will briefly discuss conventional insulators and superconductors. Then we examine topological phases of matter, such as topological insulators, the quantum Hall effect, topological superconductors, and their properties. The difference between topological and trivial phases of matter can be explained by looking at the Hamiltonian of a system. Two Hamiltonians are topologically equivalent if they can be adiabatically transformed into each other without closing the energy gap. As a consequence, gapped band structures can be classified according to the symmetries that their Hamiltonians possess. We will also look briefly into possible applications of these topological states of matter. Finally, we will analyze one of the most basic topological superconductors: the Kitaev chain, which supports topologically protected Majorana zero modes on its edges.

2.2 Topological insulators and the quantum Hall effect

2.2.1 Insulators and conductors

In solid-state physics, the electronic-band theory has successfully been used to understand many properties of solids, such as electrical conductivity. Whereas individual atoms have an energy spectrum with discrete energies, when they are grouped into larger structures, the spectrum consists of separate energy bands, which group several energy levels together. Due to the fermionic character of electrons, at low temperatures all consecutive energy levels above the ground state will be occupied, until the Fermi level, which is the highest occupied energy level in the system. The highest fully-filled band and the one above are named the valence and conduction bands, respectively. The insulating and conducting properties of a material can be understood in terms of the relation between the Fermi energy and these bands, as represented in Fig. 2.1. In conducting materials, like metals, the Fermi energy lies within a band, such that the conduction and valence band overlap and there is no band gap. Electrons can be moved to slightly higher-energy levels, thus leading to an electric current. Insulators, however, have a Fermi energy between the completely filled valence band and the empty conduction band, such that in order to be excited, electrons will have to cross the intermediate energy gap. Typically, these gaps are of the order of electron volts or ionization energies, which is a large energy on the atomic scale. In semiconductors, the band gap is much smaller, such that thermal or other excitations can bridge the gap [16].

2.2.2 Superconductors

In 1911, Heike Kamerlingh Onnes discovered superconductivity. He observed that when he cooled mercury below 4 K, the resistivity of the metal suddenly dropped to zero. This is one of the characteristics of the superconducting phase, together with the Meissner effect, which is the screening of a magnetic field by the Cooper pairs that leads to a zero magnetic field inside the superconductor. In 1957, Bardeen, Cooper, and Schrieffer (BCS) proposed a successful mean-field theory of superconductivity [18], for which they were awarded the Nobel Prize in 1972. They described superconductivity as a superfluid of Cooper pairs, i.e. bosons created by the interactions between electrons and phonons. Importantly, in the ‘80s superconducting materials were discovered at very high temperatures, which could not be explained anymore by the BCS theory [19].

One can distinguish different kinds of superconductivity by looking at the pairing symmetries. The quantum mechanical wavefunction that describes a superconducting Cooper pair has both a spin and orbital angular-momentum components. The spin can be in a singlet

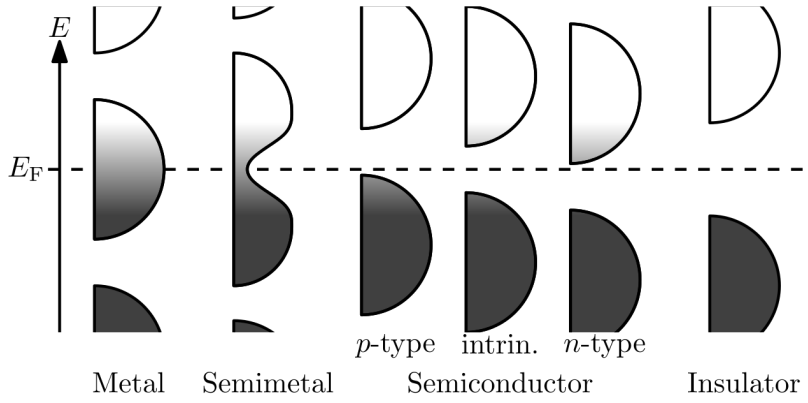

Figure 2.1 Band filling diagram for different types of conductors and insulators. The y-axis shows the energy of bands, and the x-axis shows how these bands are positioned with respect to the Fermi level E_F. The filling of these bands is indicated by the shaded region, where the dark regions correspond to fully occupied energy levels. The most left band structure belongs to a metal, where electrons can easily access higher energy levels as the conduction and valence bands are connected, and likewise for the semimetal. However, the conduction and valence bands are separated by a gap for semiconductors and insulators. A p-type semiconductor has a larger concentration of holes than electrons, and vice versa for a n-type semiconductor. Figure taken from Ref. [17].

or in a triplet state, with total spin 0 and 1, respectively. The orbital component depends on the angular momentum, with $l = 0, 1, 2, ...$, or respectively electron orbitals s,p,d,f, et cetera. Because the wavefunction obeys the Fermi-Dirac statistics and is odd under exchange of particles, an antisymmetric singlet-spin state must be accompanied by a symmetric orbital part. A s-wave superconductor has $s = 0$, $l = 0$, a p-wave $s = 1$, $l = 1$, and a d-wave $s = 0$ and $l = 2$. Conventional superconductivity, which can be explained by BCS theory, is described in terms of s-wave Cooper pairs. Here, the superconducting gap, the energy needed to create a Cooper pair, is independent of the pair momentum. All standard superconductors, such as Al, Nb, and Pb, fall into this class. Cuprate high-temperature superconductors are typically d-wave, while Sr_2RuO_4 is a p-wave superconductor [20].

2.3 Topological states of matter

2.3.1 Quantum Hall effect and topological insulators

The Hall effect

The classical Hall effect was discovered by Edwin Hall in 1879 [21]. In the experimental setup, graphically represented in Fig. 2.2, a potential V_x leads to an electric current J_x that

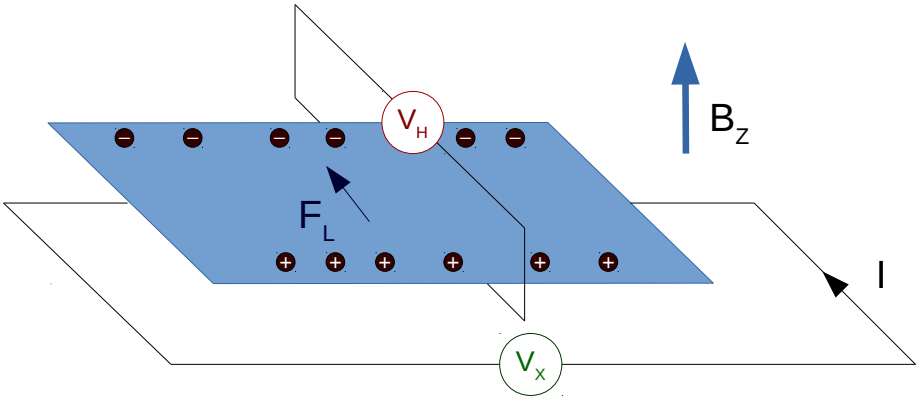

Figure 2.2 The Hall effect. Electrons are moving in a two-dimensional plane because of a electric potential difference V_x, and a perpendicular homogeneous magnetic field B_z is applied. As a consequence, the electrons experience a Lorentz force F_L which causes them to deflect, leading to a transverse Hall voltage V_H.

flows through a conducting sheet of material in the x-direction. A homogeneous magnetic field B_z is applied perpendicularly to the sheet. Electrons in a magnetic field experience a Lorentz force F_L, which causes them to orbit with frequency $\omega_B = eB/m$, where B is the magnetic field strength, m the electron mass, and e the electric charge. By adding a friction term to account for interactions with electrons or impurities, we arrive at a model known in literature as the Drude model, with the equation of motion given by

$$m\frac{\mathrm{d}\mathbf{v}}{\mathrm{d}t} = -e\mathbf{E} + e\mathbf{v}\times\mathbf{B} - \frac{m\mathbf{v}}{\tau}, \tag{2.1}$$

where $\mathbf{E}$ is the electric field corresponding to the potential difference V_x, and the last term denotes the friction and depends on the average velocity $\mathbf{v}$ and the scattering time τ, which can be interpreted as the average time between collisions.

Physically speaking, initially the electrons are moving in the x-direction, but due to the Lorentz force they are deflected towards the transverse direction. This causes a charge build-up at the edges of the sheet, producing a transverse electric field E_y. This transverse electric field gives rise to a voltage difference between the two sides, the so-called Hall voltage V_H. The longitudinal conductivity σ_x and Hall conductivity σ_H can be calculated and read [22]

$$\sigma_x = \frac{ne^2\tau}{m}, \quad \sigma_H = \frac{ne}{B}, \tag{2.2}$$

with n the density of charge carriers. Thus, in the classical picture, the Hall conductivity scales inversely proportional with the magnetic field B.

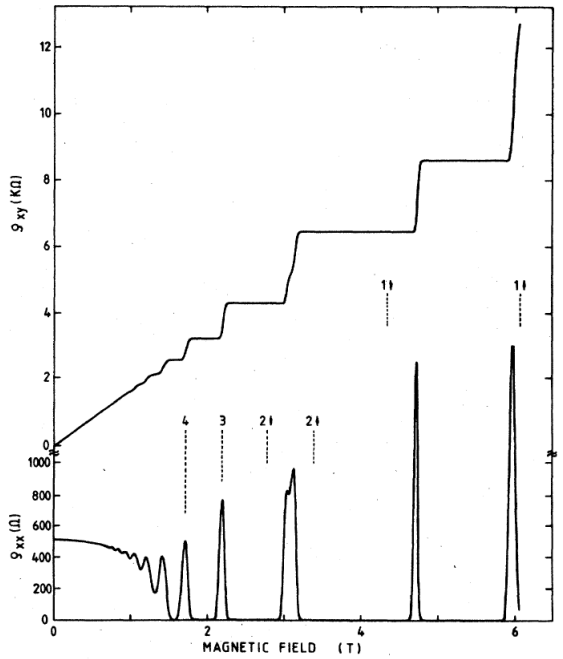

Figure 2.3 Experimental results in measuring the integer quantum Hall effect [23]. The Hall resistivity (ρ_{xy}) versus the applied magnetic field is depicted at a temperature of 8 mK, and its quantized behaviour is clearly visible.

Integer quantum Hall effect

In 1980, the quantum version of the Hall effect (integer quantum Hall effect, IQHE) was discovered by Klaus von Klitzing [15]. For this discovery, he was awarded the Nobel Prize in 1985. He investigated the Hall effect in a two-dimensional electron gas at temperatures of the order of $1K$, and observed a quantized Hall resistivity, unlike what would be expected classically from Eq. (2.2). More recent results for the Hall resistivity (inverse conductivity) and the longitudinal resistivity are shown in Fig. 2.3. On the plateaus, the electric Hall conductivity goes as

$$\sigma_H = \frac{e^2}{h}\nu, \quad \nu \in \mathbb{Z}, \tag{2.3}$$

where ν is the filling factor. It is worth noting that the value of the constant e^2/h has been measured with extraordinary precision, up till 10^{-9}, and is referred to as the Von Klitzing constant. In the middle of each plateau, the magnetic field is

$$B = \frac{hn}{\nu e} = \frac{n}{\nu}\Phi_0, \tag{2.4}$$

where $\Phi_0 = h/e$ is defined as the flux quantum. It is possible to describe these quantum states through the Hamiltonian for a charged particle moving in a magnetic field. The corresponding

energy levels are given by

$$E_n = \hbar\omega_B \left(n + \frac{1}{2}\right), \quad n \in \mathbb{N}, \tag{2.5}$$

where $\omega_B = eB/m$ is the cyclotron frequency. These equally spaced energy levels are the so-called Landau levels, which are degenerate with respect to the quantum number $k_x = 2\pi p/L$, with p integer and L the length of the system. Remarkable behaviour occurs at the edges of the material. Adding an electric field to the system causes the energy levels to tilt slightly and lifts the degeneracy, as the energy levels now depend linearly on k_x. The current in the x-direction of one Landau level is given by

$$I_n = -\frac{e}{L}\sum_{k_x} v_{k_x}, \tag{2.6}$$

where v_{k_x} represents the average single mode velocity,

$$v_{k_x} = \frac{1}{\hbar}\frac{\partial E_{nk_x}}{\partial k_x} = \frac{1}{\hbar}\frac{\Delta E_{nk_x}}{\Delta k_x} = \frac{L}{2\pi\hbar}\Delta E_{nk_x}. \tag{2.7}$$

The energy difference between two Landau levels is $\Delta E_{nk_x} = \Delta E_{n,k_x+1} - \Delta E_{n,k_x}$, such that

$$I_n = -\frac{e}{h}\left(E_{n,k_{max}} - E_{n,k_{min}}\right). \tag{2.8}$$

A voltage difference V between the two sides of the material gives $E_{n,k_{max}} - E_{n,k_{min}} = -eV$, such that we find

$$I_n = \frac{e^2}{h}V. \tag{2.9}$$

Pictorially, we can understand this in the following way. Due to the magnetic field, the electrons obey cyclotron motion, say for example in the clockwise direction. The electrons in the bulk do not contribute to the current. However, near the edges, the electrons are reflected at the boundary and propagate in the x-direction. These modes are called chiral edge modes. Usually, if electrons in the material encounter an impurity, they would scatter in various directions. However, for chiral modes the scattering is not possible, as the movement along the boundary is the only allowed movement there is. This means that chiral edge modes are highly immune to scattering off impurities [24]. Now, we will generalize the previous discussion for a single Landau level to all energy levels. The Landau levels are completely

filled up till level ν [22]. The total current then reads

$$I_{tot} = \sum_{n=0}^{\nu-1} I_n = \nu \frac{e^2}{h} V, \tag{2.10}$$

and for the quantized Hall conductivity

$$\sigma_H = \frac{1}{\rho_H} = \frac{I_{tot}}{V} = \nu \frac{e^2}{h}, \tag{2.11}$$

which is indeed Eq. (2.3) [25]. We can briefly anticipate the next section, and explain why the IQHE is a topological phase. In the next section, we will discuss the fact that ν is a topological invariant, called the Chern number [26].

Its robustness against disorder would make this topological phase extremely useful for applications in semiconductor devices, but at the same time the low temperatures and strong magnetic field that are required leave the possibilities for practical applications limited. However, there exist novel topological phases called Chern insulators, where time-reversal symmetry is broken and a finite Berry phase leads to the IQHE even in the absence of an external magnetic field. In these materials, we can still observe the quantization of the electric conductivity without the presence of any external magnetic field [27].

In 1998, another Nobel prize was awarded to Tsui, Störmer and Laughlin for the discovery and theoretical description of the fractional quantum Hall effect (FQHE) [28, 29]. In this phenomenon, the Hall conductance shows quantized behaviour as in Eq. (2.3), but now with $\nu \in \mathbb{Q}$. Whereas the IQHE can be explained by the theory of free electrons, interactions between electrons need to be incorporated to account for the FQHE.

Quantum spin Hall effect and two-dimensional topological insulators

In 2005, Kane and Mele [5], and Zhang, Bernevig, and Hughes [6] predicted the existence of the quantum spin Hall effect (QSHE), which was indeed later found experimentally in HgTe quantum wells by Molenkamp's group [7]. In these systems, the magnetic field is no longer the driving mechanism, but instead a strong spin-orbit coupling triggers a quantized spin Hall conductance. They are now also well known under the name of topological insulators. A topological invariant $\mathbb{Z}_2$ distinguishes the ordinary insulator from the quantum spin-Hall phase [30]. The QSHE effect is analogous to the IQHE, which is characterized by insulating behaviour in the bulk accompanied by metallic gapless electron states at the edges. The main difference is that here the edge states are helical and spin up and down counter-propagate, contrarily to the chiral states that characterize the QHE, where the time-reversal symmetry is

broken. As a result, the net charge current is zero, but the spin current is quantized. Second, the IQHE requires a strong magnetic field, which breaks time-reversal invariance of the system. The QSHE however, is time-reversal invariant and does not require any magnetic field [31].

Besides the two-dimensional mercury telluride quantum wells, topological insulators also have been discovered in three-dimensional materials, such as Bi_2Se_3 and Bi_2Te_3 bulk crystals [31, 32].

What makes these systems topological insulators?

Two Hamiltonians are said to be topologically equivalent if they can be continuously transformed into each other, without closing the energy gap. The set of all topologically equivalent Hamiltonians are charcterized by a topological invariant. A topological invariant is a number that does not change under continuous transformations inside the set of gapped Hamiltonians.

To give an example, a conventional insulator could be transformed into a semi-conductor, by smoothly (without closing the energy gap) decreasing the gap size in the Hamiltonian. In this sense, conventional conductors and semi-conductors belong to the same phase. In fact, they are topologically equivalent to the vacuum. Now, if one would transform the Hamiltonian and close the energy gap, the topological invariant (e.g. the Chern number, discussed below) changes, and therefore the topological phase of the material changes.

We can apply this idea now, for instance, to the IQHE. Usually, the conductivity of a system depends on the microscopic details of the system. For the quantum Hall state this is different. In 1982, Thouless, Kohmoto, Nightingale, and Den Nijs (TKNN) showed that the Hall conductivity is a topological invariant of the system [26], and therefore can be characterized by an integer. This topological quantity is the Chern number, which will be introduced in section 2.3.2. This explains the quantized behaviour of the Hall conductance. As for the edge states, we have seen the IQHE supports chiral edge states between the insulating bulk and the vacuum. We explain in the next section that these are highly robust to scattering due to their topological protection, called the bulk-boundary correspondence [24].

2.3.2 Characterization of the topological phase

Berry phase and curvature

Some topological invariants can be calculated from the Berry phase and curvature. An example is the TKNN invariant in the IQHE, where the Hall conductance is calculated from the Berry curvature [26]. The Berry phase can be measured experimentally [33]. In this section, I will follow the introduction to the Berry phase by Bernevig [34].

Consider a Hamiltonian $H(\mathbf{R})$, depending on parameters $R_1, R_2, ...$ as magnetic field, electric field, and so on. The parameters R depend on time, but for notational clarity we will leave this out. Here, the eigenstates read

$$H(\mathbf{R})\,|n(\mathbf{R})\rangle = E_n(\mathbf{R})\,|n(\mathbf{R})\rangle\,, \tag{2.12}$$

and the time evolution of the system is given by Schrödinger's equation

$$H(\mathbf{R}(t))\,|\psi(t)\rangle = i\hbar\frac{d}{dt}\,|\psi(t)\rangle\,. \tag{2.13}$$

The state of the system is written as $|\psi(t)\rangle = e^{-i\theta(t)}\,|n(\mathbf{R}(t))\rangle$ with phase $\theta(t)$. Using the eigenvalue equation

$$E_n(\mathbf{R})\,|n(\mathbf{R})\rangle = \hbar\left(\frac{d}{dt}\theta(t)\right)|n(\mathbf{R})\rangle + i\hbar\frac{d}{dt}\,|n(\mathbf{R})\rangle\,, \tag{2.14}$$

we take the scalar product with $\langle n(\mathbf{R})|$ and assuming that the state is normalized, $\langle n(\mathbf{R})|n(\mathbf{R})\rangle = 1$, we find

$$E_n(\mathbf{R}) - i\hbar\,\langle n(\mathbf{R}(t))|\,\frac{d}{dt}\,|n(\mathbf{R}(t))\rangle = \hbar\frac{d}{dt}\theta(t), \tag{2.15}$$

which leads to the solution for the phase

$$\theta(t) = \frac{1}{\hbar}\int_0^t E_n(\mathbf{R}(t'))dt' - i\int_0^t \langle n(\mathbf{R}(t'))|\,\frac{d}{dt}\,|n(\mathbf{R}(t'))\rangle\,dt'. \tag{2.16}$$

The first term is the conventional dynamical phase, and the second is the Berry phase γ_n

$$\gamma_n = i\int_0^t \langle n(\mathbf{R}(t'))|\,\frac{d}{dt}\,|n(\mathbf{R}(t'))\rangle\,dt', \tag{2.17}$$

which arises because the states at t and $t+dt$ are not the same. Interestingly, we can make an analogy with electromagnetism by considering the Berry phase as the magnetic flux in parameter space. If the parameters $\mathbf{R}$ are varied along a path $\mathscr{C}$ in parameter space, we rewrite it as an integral over $\mathbf{R}$,

$$\gamma_n = i\oint_{\mathscr{C}} \langle n(\mathbf{R})|\,\nabla_{\mathbf{R}}\,|n(\mathbf{R})\rangle\,d\mathbf{R} = i\oint_{\mathscr{C}} d\mathbf{R}\cdot\mathbf{A}_n(\mathbf{R}), \tag{2.18}$$

with the Berry connection (or, analogously, the Berry vector potential) $\mathbf{A}_n$,

$$\mathbf{A}_n(\mathbf{R}) = i\,\langle n(\mathbf{R})|\,\nabla_{\mathbf{R}}\,|n(\mathbf{R})\rangle\,. \tag{2.19}$$

For a three-dimensional integral, we apply Stokes' theorem to find

$$\gamma_n = \int_{\mathscr{S}} dS \cdot F_n(\mathbf{R}), \quad F(\mathbf{R}) = \nabla_{\mathbf{R}} \times \mathbf{A}_n(\mathbf{R}), \tag{2.20}$$

with $F_n(\mathbf{R})$ the Berry curvature, which is the curl of the Berry potential (or the magnetic field in parameter space).

Chern number

From the Berry curvature, the topological invariant Chern number can be calculated. It is used to distinguish between the trivial and topological phases of systems.

The Chern invariant is the total Berry flux in the Brillouin zone, which is integer,

$$m_n = \frac{1}{2\pi} \int \mathrm{d}^2\mathbf{k}\, F_n(k), \tag{2.21}$$

and summing over all occupied bands gives the total Chern number,

$$m = \sum_n m_n, \tag{2.22}$$

with $m \in \mathbb{Z}$. The special thing is that this number is invariant, as long the energy gap is not closed. Thus, it can be used to classify Hamiltonians according to their topology.

In the case of the integer quantum Hall state, the Chern number is the same as the integer ν appearing in Eq. (2.3), the so-called TKNN invariant [26]. The topological character then explains the robust quantization of the Hall resistivity.

We are now ready to discuss another intriguing property of topological materials: the bulk-boundary correspondence. It relates the topological structure of the bulk to the existence of gapless modes at the surface. For two-dimensional insulators, for example, the topological invariant Chern number in the bulk is connected to the number of edge states. The dispersion of the conducting edge states connects the conduction and valence bands. The energy can be deformed such that it crosses the Fermi energy multiple times. However, the difference between the number of left- and right-moving modes at the edge, N_L and N_R, does not change. It can be related to the topological invariant of the bulk,

$$N_R - N_L = \Delta n, \tag{2.23}$$

where Δn is the difference in Chern number across the interface [24].

2.3.3 Symmetries

Discrete symmetries play a central role in the classification of different types of topological systems. The symmetries present in the Hamiltonians define the possible topological invariants associated to their bulk. We consider three important types of intrinsic symmetries: time-reversal, particle-hole, and sublattice or chiral symmetry. Note however that the overview of topological invariants and symmetries in this section is not complete: firstly, it applies only to free-fermion models, and secondly, spatial symmetries, e.g. related to the cristalline structure of a material, can give rise to so-called cristalline topological insulators, and are not included in the discussion [35].

Time-reversal symmetry

Time reversal is a transformation that reverses the arrow of time, and time-reversal symmetry (TRS) indicates that the Hamiltonian stays unchanged with respect to this transformation. Let Θ be the time-reversal operator, such that

$$\Theta : t \to -t, \quad |\alpha\rangle \to \Theta |\alpha\rangle , \tag{2.24}$$

where $\Theta|\alpha\rangle$ denotes the time-reversed state. Time-reversal invariance dictates that

$$[H, \Theta] = 0. \tag{2.25}$$

The operator Θ is anti-unitary, such that $\Theta^* \Theta = -1$. This can be seen from the Schrödinger equation for a time-reversal invariant system

$$i\hbar \frac{\partial}{\partial t} \Psi(x,t) = H\Psi(x,t), \tag{2.26}$$

with $\Theta \partial_t \Theta^{-1} = \partial_{-t}$. The position operator x is not changed by this operation, but the momentum operator $p = i\hbar \frac{d}{dx}$ is

$$\Theta x \Theta^{-1} = x, \quad \Theta p \Theta^{-1} = -p. \tag{2.27}$$

The anti-unitary operator can be written as the product of a unitary matrix times the complex conjugation operator: $\Theta = UK$.

We consider now time-reversal for systems with spin $\frac{1}{2}$. Interestingly, by applying the time-reversal operator twice does not necessarily yield the original result. For spin-$\frac{1}{2}$ systems,

the time-reversal operation is

$$\Theta\sigma_j\Theta^{-1} = -\sigma_j, \tag{2.28}$$

with the label $j = x, y, z$, and σ_j the Pauli matrices

$$\sigma_x = \begin{pmatrix} 0 & 1 \\ 1 & 0 \end{pmatrix}, \quad \sigma_y = \begin{pmatrix} 0 & -i \\ i & 0 \end{pmatrix}, \quad \sigma_z = \begin{pmatrix} 1 & 0 \\ 0 & -1 \end{pmatrix}.$$

Note that

$$\sigma_y\sigma_x\sigma_y = -\sigma_x, \tag{2.29}$$

$$\sigma_y\sigma_y\sigma_y = +\sigma_y, \tag{2.30}$$

$$\sigma_y\sigma_z\sigma_y = -\sigma_z. \tag{2.31}$$

Since $\sigma_{x,z}$ are real-valued and σ_y is complex-valued, we have that $K\sigma_x = \sigma_x K$ and $K\sigma_y = -\sigma_y K$. Combining this, we write the time-reversal operator as

$$\Theta = -i\sigma_y K = e^{-i\pi S_y/\hbar}K, \tag{2.32}$$

with spin matrix $S_y = \frac{\hbar}{2}\sigma_y$, and using that

$$e^{-i\pi S_y/\hbar} = \sum_{k=0}^{\infty} \frac{1}{k!}\left(\frac{-i\pi\sigma_y}{2}\right)^k = \cos\left(\frac{\pi}{2}\right)\begin{pmatrix} 1 & 0 \\ 0 & 1 \end{pmatrix} + \sin\left(\frac{\pi}{2}\right)\begin{pmatrix} 0 & -1 \\ 1 & 0 \end{pmatrix} = -i\sigma_y. \tag{2.33}$$

For general angular momentum J_y, we have

$$\Theta = e^{-i\pi J_y/\hbar}K, \tag{2.34}$$

which satisfies

$$\Theta^2 = -1. \tag{2.35}$$

Kramer's theorem states that in a TRS-invariant system, if $\Theta^2 = -1$, all energy states must be at least doubly degenerate. This holds for any system with an odd total number of fermions, and can be seen by proving that $\Theta|\psi\rangle \neq |\psi\rangle$, even when both states have the same energy. Thus, if $\Theta|\psi\rangle = e^{i\phi}|\psi\rangle$, then $\Theta^2|\psi\rangle = e^{-i\phi}e^{i\phi}|\psi\rangle = |\psi\rangle$. But, this is in contradiction with $\Theta^2|\psi\rangle = -|\psi\rangle$. Hence, the fermionic states $\Theta|\psi\rangle$ and $|\psi\rangle$ are not equivalent, but have the same energy, so the corresponding energy level must be doubly degenerate.

The time-reversal transformation of the Hamiltonian reads

$$i\sigma_y H^T(-i\sigma_y) = H. \tag{2.36}$$

For integer-spin particles, the time-reversal operator is unitary, such that $\Theta^2 = 1$, and the transformation becomes

$$H^T = H. \tag{2.37}$$

Particle-hole symmetry

Particle-hole symmetry (PHS) appears in superconducting systems and refers to viewing creation operators for electrons as annihilation operators for holes. The transformation is represented by

$$(\sigma_x K)H(\sigma_x K)^{-1} = -H. \tag{2.38}$$

Because of this symmetry, the spectrum is symmetric around the Fermi energy. The particle-hole symmetry is of central importance in the Kitaev chain, as we will see in section 2.4.

Chiral symmetry

Chiral or sublattice symmetry (CS) arises when the lattice can be divided into two sublattices, as in the honeycomb carbon lattice of graphene. The symmetry operation is

$$\sigma_z H^T \sigma_z = -H. \tag{2.39}$$

All energy eigenstates come in pairs $(E_n, -E_n)$.

In fact, a system with both PHS and TRS also automatically has CS. However, also when neither of those symmetries are present, the CS can hold. An example of this is the AIII class of topological insulators, introduced in the next paragraph.

Classification

Crucially, the features of topological states of matter can be classified according to their symmetries. In 2009, Schnyder et al. published an exhaustive classification of topological phases of insulators and superconductors based on the above symmetries [36]. This classification is based on two types of symmetry operations P and C, given by

$$P : H = -PHP^{-1}, \quad PP^\dagger = 1, \quad P^2 = 1, \tag{2.40a}$$

$$C : H = -\varepsilon_c CHC^{-1}, \quad CC^\dagger = 1, \quad C^T = \eta_c C, \tag{2.40b}$$

where H represents the single-particle Hamiltonian, $\varepsilon_c = \pm 1$ and $\eta_c = \pm 1$.

The C-type symmetry represents a TRS operation when $\varepsilon_c = +1$ and a PHS operation when $\varepsilon_c = -1$. More specifically, $(\varepsilon_c, \eta_c) = (1,1)$ corresponds to a TRS for integer spin or spinless particles, and $(\varepsilon_c, \eta_c) = (1,-1)$ corresponds to a TRS for half-integer spin particles. Furthermore, $(\varepsilon_c, \eta_c) = (-1,1)$ represents a PHS for a triplet pairing Bogoliubov-de Gennes (BdG) Hamiltonian, and $(\varepsilon_c, \eta_c) = (-1,-1)$ represents a PHS for a singlet pairing BdG Hamiltonian.

The classification scheme is given in Table 2.1 [37]. The different classes are identified following the Altland-Zirnbauer classification [38] in the first column. The next three columns correspond to the symmetries present in these classes. The symbol 0 denotes the absence of the regarding symmetry. The presence of a given symmetry is indicated by ± 1, depending on whether the symmetry operator squares to $+1$ or -1. The other columns on the right show whether topologically non-trivial ground states exist for the given symmetries as a function of spatial dimension d. The symbols $\mathbb{Z}$ and $\mathbb{Z}_2$ denote whether the topologically distinct phases within a given symmetry class are characterized by an integer topological invariant, such as the Chern number, or by an invariant which is either 0 or 1, such as the Fu-Kane invariant [30], respectively, and the 0 indicates that all quantum ground state are topologically equivalent to the trivial state. Note that the table does not cover topological semi-metals like Weyl-semimetals, that also support gapless excitations, so-called Fermi arcs [39]. Extensions of this classification scheme with mirror or inversion symmetries can be found in Ref. [35].

The AII class covers the well-known topological insulators, such as HgTe in 2D and BiSe in 3D. The quantum Hall effect and Chern insulators belong to class A in 2D. The topological superconducting Kitaev chain in class D is characterized by a $\mathbb{Z}_2$ topological number, as shown in the next section.

2.4 Topological superconductors

2.4.1 Introduction

In the mean-field BCS theory of superconducting materials, a superconductor has a superconducting gap in the bulk, which corresponds to the energy needed to create a Cooper pair. For a specific parameter regime, a topological superconductor supports topologically protected zero-energy Majorana modes at its edges, as predicted by Kitaev [8]. In contrast to the QHE and QHSE which are single-particle phenomena, here the interactions need to be incorporated into the model in order to have a superconducting phase. However, at mean-field level, the

Table 2.1 Symmetry classification of non-interacting free-fermion Hamiltonians of topological insulators and superconductors, as a function of the spatial dimension d. Table taken from Ref. [37].

AZ class	TRS	PHS	CS	$d=0$	$d=1$	$d=2$	$d=3$	$d=4$	$d=5$	$d=6$	$d=7$
A	0	0	0	$\mathbb{Z}$	0	$\mathbb{Z}$	0	$\mathbb{Z}$	0	$\mathbb{Z}$	0
AIII	0	0	1	0	$\mathbb{Z}$	0	$\mathbb{Z}$	0	$\mathbb{Z}$	0	$\mathbb{Z}$
AI	1	0	0	$\mathbb{Z}$	0	0	0	$2\mathbb{Z}$	0	$\mathbb{Z}_2$	$\mathbb{Z}_2$
BDI	1	1	1	$\mathbb{Z}_2$	$\mathbb{Z}$	0	0	0	$2\mathbb{Z}$	0	$\mathbb{Z}_2$
D	0	1	0	$\mathbb{Z}_2$	$\mathbb{Z}_2$	$\mathbb{Z}$	0	0	0	$2\mathbb{Z}$	0
DIII	-1	1	1	0	$\mathbb{Z}_2$	$\mathbb{Z}_2$	$\mathbb{Z}$	0	0	0	$2\mathbb{Z}$
AII	-1	0	0	$2\mathbb{Z}$	0	$\mathbb{Z}_2$	$\mathbb{Z}_2$	$\mathbb{Z}$	0	0	0
CII	-1	-1	1	0	$2\mathbb{Z}$	0	$\mathbb{Z}_2$	$\mathbb{Z}_2$	$\mathbb{Z}$	0	0
C	0	-1	0	0	0	$2\mathbb{Z}$	0	$\mathbb{Z}_2$	$\mathbb{Z}_2$	$\mathbb{Z}$	0
CI	1	-1	1	0	0	0	$2\mathbb{Z}$	0	$\mathbb{Z}_2$	$\mathbb{Z}_2$	$\mathbb{Z}$

model becomes equivalent to a free-fermion system described by a Bogoliubov-de Gennes Hamiltonian, where the particle-hole symmetry plays a central role.

Hence, topological superconductors are closely connected to the phenomenon of Majorana modes [40, 41]. In 1937, Majorana predicted that real wavefunctions also satisfy the Dirac equation, which correspond to particles that are equal to their own antiparticles [42]. However, experimentally still no fundamental particles have been found to be Majorana fermions, though a possible candidate might be the neutrino. On the other hand, in the area of condensed matter, where ions, electrons, and their interactions are the main objects of study, quasiparticles may arise that satisfy the Majorana character. The operators that mathematically create these electrons, dressed with interactions, are equivalent to the ones that annihilate them, thus leading to a zero-energy Majorana mode. The Kitaev chain (Ref. [8]) is an example of a topological superconductor that hosts these Majorana modes, and will be discussed extensively in section 2.4. Apart from providing a fundamental understanding of the rich behaviour of one-dimensional topological superconductors, Majorana modes have attracted much theoretical interest because their alleged practical applications, see section 2.4.6. Recently, signatures of Majorana modes in topological superconductors have been found experimentally [9, 43].

A superconductor is called topological if any topological number that can be associated to the occupied states is nonzero [39]. This can be explained by making the above more precise. At the ends of a one-dimensional superconductor, bound states can be present. If so, then for every state with energy E, there also exists a state with energy $-E$. These finite-energy pairs are not topologically protected. Smooth transformations of the Hamiltonian can push

these states out of the energy gap. However, if the bound state has energy $E = 0$, this single unpaired state is topologically protected, as it cannot move away from $E = 0$. The topological invariant of these systems is a $\mathbb{Z}_2 = \{0, 1\}$ quantity. Though this number is calculated from the bulk properties, it indicates whether such a zero-energy mode exists. These are the Majorana modes discussed in the above, each comprising half a Dirac fermion. Since they always come in pairs (there are two edges), the states together define a degenerate two-level system, where quantum information can be stored non-locally [24, 41].

2.4.2 The Kitaev chain

In 2001, Kitaev showed that a 1D quantum wire of spinless fermions can host zero-energy states at the edges of the chain [8]. These edge states are called Majorana zero modes because they can be rewritten in terms of operators that equal their Hermitian conjugate. Kitaev's model is described by a tight-binding Hamiltonian with p-wave pairing on a one-dimensional lattice, given by

$$H = -\mu \sum_{j=1}^{N} n_j - \sum_{j=1}^{N-1} \left[t \left(c_j^\dagger c_{j+1} + c_{j+1}^\dagger c_j \right) + \frac{\Delta}{2} \left(c_j c_{j+1} + c_{j+1}^\dagger c_j^\dagger \right) \right]. \tag{2.41}$$

Here, $c_j^\dagger$ (c_j) is the fermionic creation (annihilation) operator acting on site j, and $n_j = c_j^\dagger c_j$ the occupation number operator, μ the chemical potential, $t \geq 0$ the hopping amplitude, and $\Delta = < c_j^\dagger c_{j+1}^\dagger >$ the superconducting pairing amplitude, giving rise to the Cooper pairs (note that BCS is a mean-field theory). For p-waves, typically the energy gap is dependent on the momentum, whereas for s-wave it is a constant. This will become apparent when we write the Hamiltonian in k-space.

In other words, the first term counts the number of particles present in the system. The second tight-binding term describes the energy gain of a particle hopping to an adjacent site. The third term describes the formation of nearest-neighbour electron pairs, and corresponds to the formation of superconducting Cooper pairs.

We rewrite the Hamiltonian in the momentum space by introducing the Fourier transforms

$$c_j^\dagger = \frac{1}{\sqrt{N}} \sum_k e^{-ikaj} c_k^\dagger, \quad c_j = \frac{1}{\sqrt{N}} \sum_k e^{ikaj} c_k, \tag{2.42}$$

with a the atomic lattice spacing, $-\pi m/aN \leq k \leq \pi m/aN$ denoting the first Brillouin zone, and $|m| \leq N/2$. The first term of Eq. (2.41) reads

$$-\mu \sum_{j=1}^{N} n_j = -\frac{\mu}{N} \sum_{j=1}^{N} \sum_{k,k'} e^{-i(k-k')aj} c_k^\dagger c_{k'} = -\mu \sum_k c_k^\dagger c_k, \tag{2.43}$$

where we used the definition of the delta function

$$\sum_{j=1}^{N} e^{-i(k-k')aj} = N\delta_{k,k'}. \tag{2.44}$$

Similarly, the second term becomes

$$\begin{aligned} &-t \sum_{j=1}^{N-1} \left(c_j^\dagger c_{j+1} + c_{j+1}^\dagger c_j \right) = -\frac{t}{N} \sum_{j=1}^{N-1} \sum_{k,k'} c_k^\dagger c_{k'} e^{-i(k-k')aj} \left(e^{-ika} + e^{ik'a} \right) \\ &= -t\frac{N-1}{N} \sum_k c_k^\dagger c_k \left(e^{-ika} + e^{ika} \right) = -2t \sum_k c_k^\dagger c_k \cos(ka), \end{aligned} \tag{2.45}$$

where in the last step we took the limit $N \to \infty$. The third term yields

$$\begin{aligned} &\frac{\Delta}{2} \sum_{j=1}^{N-1} \left(c_j c_{j+1} + c_{j+1}^\dagger c_j^\dagger \right) = \frac{\Delta}{2} \frac{1}{N} \sum_{j=1}^{N-1} \left(\sum_{k,k'} c_k c_{k'} e^{i(k+k')aj + ik'a} + \sum_{k,k'} c_k^\dagger c_{k'}^\dagger e^{-i(k+k')aj - ika} \right) \\ &= \frac{\Delta}{2} \frac{N-1}{N} \sum_k \left(c_k c_{-k} e^{-ika} + c_k^\dagger c_{-k}^\dagger e^{-ika} \right). \end{aligned} \tag{2.46}$$

In the last expression, we take again the limit $N \to \infty$, and we set $k = -k$ in the first term. Combining all terms, we obtain

$$H = \sum_k \varepsilon_k c_k^\dagger c_k + \frac{\Delta}{2} \sum_k \left(c_{-k} c_k e^{ika} + c_k^\dagger c_{-k}^\dagger e^{-ika} \right), \tag{2.47}$$

with

$$\varepsilon_k = -\mu - 2t\cos(ka). \tag{2.48}$$

Introducing the two-component Nambu spinor $N_k^\dagger = \left(c_k^\dagger, c_{-k} \right)$, we rewrite the Hamiltonian in the standard Bogoliubov-de Gennes form [40], with $\tilde{\Delta}_k = \Delta e^{ika}$,

$$H = \frac{1}{2} \sum_k N_k^\dagger H_k N_k, \quad H_k = \begin{pmatrix} \varepsilon_k & \tilde{\Delta}_k^* \\ \tilde{\Delta}_k & -\varepsilon_{-k} \end{pmatrix}. \tag{2.49}$$

Furthermore, using $e^{\pm ika} = \cos(ka) \pm i\sin(ka)$, we find

$$H_k = \Delta\cos(ka)\sigma_1 + \Delta\sin(ka)\sigma_2 + \varepsilon_k\sigma_3 = \vec{\sigma}\cdot\vec{d}(\vec{k}) \tag{2.50}$$

with σ_i the Pauli spin matrices.

Note that by introducing the Nambu spinors, we have doubled the number of degrees of freedom. The reason behind this is the equal footing on which electrons and holes can be treated, resulting in a particle-hole symmetry of our Hamiltonian.

The particle-hole symmetry can be used to perform a Bogoliubov transformation on the Hamiltonian. This transformation describes excitations above the superconducting ground state as new quasi-particles, which are a superposition of electrons and holes [40]. The new quasiparticle operators are given by

$$a_k = u_k c_k + v_k c^\dagger_{-k}, \tag{2.51}$$

$$u_k = \frac{\tilde{\Delta}_k}{|\tilde{\Delta}_k|}\frac{\sqrt{E_{\text{bulk}} + \varepsilon}}{\sqrt{2E_{\text{bulk}}}}, \tag{2.52}$$

$$v_k = \left(\frac{E_{\text{bulk}} - \varepsilon}{\tilde{\Delta}_k}\right), \tag{2.53}$$

and the bulk excitation energies read

$$E_{\text{bulk}} = \sqrt{\varepsilon_k^2 + |\tilde{\Delta}_k|^2}. \tag{2.54}$$

2.4.3 Topological invariant

The Kitaev Hamiltonian belongs to class D (particle-hole symmetry, no time-reversal symmetry), and the topological and trivial phases are distinguished by a $\mathbb{Z}_2$ invariant. In the same paper where Kitaev proposes the topological superconductor [8], he introduces the Majorana number, given by

$$M(H) = \pm 1, \tag{2.55}$$

associated with the Hamiltonian H. It is related to the fermionic parity of the ground state of a closed chain with length L, denoted by $P(H(L))$,

$$P(H(L_1 + L_2)) = M(H)P(H(L_1))P(H(L_2)). \tag{2.56}$$

where the invariant can be expressed as

$$M(H) = (-1)^{\frac{\Delta\varphi}{\pi}}, \tag{2.57}$$

where $\Delta\varphi$ denotes a phase change, which can be calculated by a winding integral over half of the Brillouin zone,

$$\Delta\varphi = i\int_0^{\pi} \left\{\partial_k \log\left[\tilde{W}(k)\right]\right\} \mathrm{d}k, \tag{2.58}$$

where $\tilde{W}(k)$ is Fourier transform of the transformation matrix W that brings the Majorana representation matrix of the Hamiltonian B into the form

$$WBW^T = \mathrm{diag}_\lambda \begin{pmatrix} 0 & \varepsilon_\lambda \\ -\varepsilon_\lambda & 0 \end{pmatrix}, \tag{2.59}$$

where ε_λ are the eigenvalues of B.

In 2013, Budich and Ardonne showed that the invariant $M(H)$ is equivalent to the topological invariant calculated with the quantized Zak-Berry phase Φ_{ZB} in the Bogoliubov-de Gennes mean field description of superconductivity [44], as

$$\Phi_{\mathrm{ZB}} = \int_{-\pi}^{\pi} \mathrm{d}k A(k) = \Delta\varphi, \tag{2.60}$$

with $A(k)$ the Berry connection as defined in Eq. (2.19).

2.4.4 Majorana modes

In this section, we show how to write the Kitaev chain in terms of Majorana operators. We write the fermionic creation (annihilation) operators $c_j^\dagger$ (c_j) with $\left\{c_j, c_{j'}^\dagger\right\} = \delta_{j,j'}$ in terms of Majorana operators η_j and γ_j as

$$c_j = \frac{1}{2}\left(\eta_j + i\gamma_j\right), \quad c_j^\dagger = \frac{1}{2}\left(\eta_j - i\gamma_j\right), \tag{2.61}$$

with $\eta_j^\dagger = \eta_j$ and $\gamma_j^\dagger = \gamma_j$, such that Majoranas always come in even numbers. Equivalently,

$$\eta_j = c_j + c_j^\dagger, \quad \gamma_j = -i\left(c_j - c_j^\dagger\right) \tag{2.62}$$

From this, we find the anticommutator and the squares of the operators, namely

$$\left\{\eta_j, \gamma_j\right\} = \left\{\left(c_j + c_j^\dagger\right), -i\left(c_j - c_j^\dagger\right)\right\} = 0, \tag{2.63}$$

$$\left(\eta_j\right)^2 = \left(c_j + c_j^\dagger\right)^2 = \left\{c_j, c_j^\dagger\right\} = 1, \tag{2.64}$$

$$\left(\gamma_j\right)^2 = -\left(c_j - c_j^\dagger\right)^2 = \left\{c_j, c_j^\dagger\right\} = 1. \tag{2.65}$$

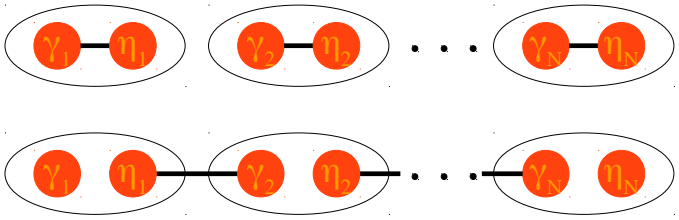

Figure 2.4 Schematic representation of the Kitaev Hamiltonian in Eq. (2.66), for (top) $\mu < 0$, $t = \Delta = 0$, and (bottom) $\mu = 0$ and $t = \frac{\Delta}{2} \neq 0$. In the former, representing the trivial phase, the Majorana operators pair at the same lattice site, whereas in the latter, representing the topological phase, they pair with their adjacent lattice sites, leaving two unpaired operators at the boundaries γ_1 and η_N.

By introducing the Majarana operators given in Eq. (2.61), the Hamiltonian becomes

$$H = -\frac{\mu}{2}\sum_{j=1}^{N}\left(1+i\eta_j\gamma_j\right) - \frac{i}{4}\sum_{j=1}^{N-1}\left[\left(\frac{\Delta}{2}+t\right)\eta_j\gamma_{j+1} + \left(\frac{\Delta}{2}-t\right)\gamma_j\eta_{j+1}\right]. \tag{2.66}$$

We consider two interesting limits, represented schematically in Fig. 2.4. First, take $\mu \neq 0$ and $t = \Delta = 0$. The Hamiltonian given in Eq. (2.41) reduces to

$$H = -\frac{\mu}{2}\sum_{j=1}^{N}\left(1+i\eta_j\gamma_j\right). \tag{2.67}$$

This is the trivial case. The Majorana operators η_j and γ_j from the same site j are paired together. The ground state corresponds to the empty chain. The spectrum is gapped, since the cost of adding a particle is $|\mu|$.

Second, take $\mu = 0$ and $t = \frac{\Delta}{2} \neq 0$. The Hamiltonian becomes

$$H = -\frac{it}{2}\sum_{j=1}^{N-1}\eta_j\gamma_{j+1}. \tag{2.68}$$

Here, the topological phase appears. The Majorana operators η_j and γ_{j+1} of adjacent physical sites $j, j+1$ are paired together.

Note that this last Hamiltonian does not depend on the operators γ_1, η_N, which obey $\gamma_1^\dagger = \gamma_1$ and $\eta_N^\dagger = \eta_N$. Since these sites do not contribute to the Hamiltonian, we recognize them as zero-energy Majorana modes.

2.4.5 QFT approach of Hamiltonians in Class D

The symmetry class D contains Hamiltonians with PHS, but no TRS and CS. In this case, we need to fulfill

$$H(k) = -CH^*(-k)C^{-1}, \quad CC^\dagger = 1, \quad C^T = C, \tag{2.69}$$

such that we need a symmetric unitary representation of C.

We can easily show now that the particle-hole symmetric topological superconductor is described by the $1+1$-dimensional Dirac Lagrangian in Minkowski spacetime [45], given by

$$\mathscr{L} = \bar{\psi} i\gamma^\mu \partial_\mu \psi - m\bar{\psi}\psi - im_5 \bar{\psi}\gamma^5 \psi, \tag{2.70}$$

with m the normal mass and m_5 the axial mass, $\{\gamma^\mu, \gamma^\nu\} = \eta^{\mu\nu}$, $\eta^{\mu\nu} = \mathrm{diag}(1,-1)$. The Dirac matrices are chosen real $\gamma^0 \equiv \sigma_x$, $\gamma^1 \equiv -i\sigma_y$, $\gamma^5 \equiv \gamma^0\gamma^1 = \sigma_x$. The corresponding Hamiltonian

$$H = -i\gamma^0\gamma^1\partial_1 + m\gamma^0 + im_5\gamma^0\gamma^5 \tag{2.71}$$

is then Hermitian because $\left\{\gamma^\mu, \gamma^5\right\} = 0$, and reads in momentum space

$$H(k) = \gamma^0\gamma^1 k + m\gamma^0 + im_5\gamma^0\gamma^5. \tag{2.72}$$

Since

$$-H^*(-k) = \gamma^0\gamma^1 k - m\gamma^0 + im_5\gamma^0\gamma^5, \tag{2.73}$$

we choose $C = \mathbb{I}$ if $m = 0$, and $C = \gamma^5$ if $m_5 = 0$, such that the requirements are fullfilled. Thus, the Hamiltonian $H(k)$ describes a class D system. In fact, all the topological phases in Table 2.1 can be mapped to Dirac Hamiltonians, which can be classified in terms of their underlying Clifford algebras [36].

2.4.6 Applications

Topological insulators are interesting for applications in electronic circuits and thermoelectrics due to their electronic band structure and topological protection of the edge states. Furthermore, the QSHE might be very interesting in the context of spintronics [6].

One of the most important contributions of topological systems will be in the implementation of a new quantum computer. Whereas the classical bit only can take values 0 and 1, the quantum qubit represents the linear superposition of the states $|0\rangle$ and $|1\rangle$. Furthermore, the system state is a superposition of the individual qubits, the so-called entangled states. This highly increases the number of possible states, and thus its computing power compared

to current machines using classical bits (2^n to $2n$ for n (qu)bits). Furthermore, qubits are evolved by quantum gates, which are operations that change one quantum state into any other. However, in order to build a reliable quantum computer, qubits must be configured, evolved and read very precisely. Quantum measurement errors and unavoidable environmental perturbations (quantum decoherence) make the conditions very difficult to realize experimentally. At this point, the aforementioned topological robustness might be a solution to this problem. For example, topological superconductors support zero-energy Majorana modes at their edges, which could act as a stable qubit. These quasi-particles are non-abelian anyons, meaning that their statistics are neither fermionic nor bosonic, and that the order in which they are multiplied is important as the operation of multiplication is not commutative. Logical gates are formed by using braiding, the exchange of particles, and fusion, which corresponds to bringing two anyons together and using their collective behaviour. Hence, topological systems could prove to be essential in building a fault-tolerant quantum computer [46, 47].

Chapter 3

Dissipation in quantum systems

3.1 Introduction

Usual quantum mechanics deals with closed systems, for which a Hamiltonian can be constructed. Systems in the real world, however, can hardly be regarded as truly isolated from their environment. Systems constantly interact and exchange energy with their environment. To study this dissipative behaviour in the quantum context, one has to go beyond the Hamiltonian formalism, in which the total energy always is conserved and, take the dissipation somehow into account. The paradigmatic example of a classical open system is Brownian motion. This refers to the dynamics of a macroscopic particle constantly exchanging thermal energy with its environment, for example a nanoparticle in a fluid. If a nonexternal force is applied, the average displacement is zero, whereas the average squared displacement obeys $\langle(\Delta x)^2\rangle \neq 0$. Theoretically, Brownian motion is described by the Langevin equation in one dimension [48]

$$M\ddot{q} + \eta\dot{q} + V'(q) = f(t), \quad \langle f(t)\rangle = 0, \quad \langle f(t)f(t')\rangle = 2\eta k_{\mathrm{B}}T\delta(t-t'), \tag{3.1}$$

in which $q(t)$ is the coordinate of the macroscopic particle, M is the particle mass, η is a constant parametrizing how much the particle is slowed down by its surroundings (friction), $V(q)$ is some external potential, and $k_{\mathrm{B}}T$ is the thermal energy. The equation of motion can be generalized to higher dimensions by using the same equation for each direction individually. The most important term is the fluctuating force $f(t)$, which represents the influence of the environment on the particle. Similar to the displacement of a random walk, the mean of $f(t)$ is zero, but the mean of the square is some nonzero quantity, dependent on the friction coefficient and on the temperature of the system. The Langevin equation assumes

that the particle mass M is much larger than that of the particles making up the viscous fluid, and that the time scale t is much larger than the typical time between molecular collisions.

Next to the paradigm of classical Brownian motion, the Langevin equation appears in other systems as well. For example, in an RLC circuit, which is a circuit with a resistance R, a capacitor C, and a non-linear element L connected in parallel, the dynamics of magnetic flux obey to the following equations

$$C\ddot{\phi} + \frac{RC}{L}\dot{\phi} + \frac{\phi}{L} = I_f(t), \quad \langle I_f(t)\rangle = 0, \quad \langle I_f(t)I_f(t')\rangle = \frac{2RCk_{\mathrm{B}}T}{L}\delta(t-t'), \tag{3.2}$$

with $I_f(t)$ some fluctuating current. An important example of such a system is a superconducting ring closed with a weak contact, the so-called superconducting quantum interference device (SQUID) [49].

The Langevin equation (3.1) is purely classical. The interesting thing is now to study open systems in the quantum regime. In order to find a proper quantum description, the quantum model should reduce to the Langevin equation in the classical limit. There are roughly three ways of doing this. Firstly, one can try to generalize the canonical commutation relations such that dissipation on the quantum level can be described. However, there is no safe way to do this [12]. The second way is to consider the environment together with the system of interest, such that the entire system is closed again. One can now model the environment and its coupling to the system of interest to study dissipation. This procedure was proposed by Caldeira and Leggett in the 80's [12, 13]. A third way is to use probabilistic processes, as happens in the Lindblad formalism [50]. In 2011, Diehl and others showed that topologically protected Majorana modes appear in open quantum systems [1]. The key feature in the approach was engineered dissipation for a spinless quantum wire, which is coupled to a bath with dissipative behaviour, governed by the Lindblad master equation. In this chapter, the emphasis lies on the discussion of the successful Caldeira-Leggett formalism.

3.2 Caldeira-Leggett model

3.2.1 Introduction

The basic idea in the study of dissipative quantum systems is to separate the system in two parts: the first one represents the main system of interest, and the second one is some bath, where the energy can flow to. The simplest way to do this splitting is by coupling the system of interest to an infinite bath of harmonic oscillators, as suggested by Feynman and Vernon in 1963 [51]. In 1983, Caldeira and Leggett proposed a model that was able to reproduce

the Langevin equation in the classical limit in one dimension [12, 13]. They modelled the environment as a set of simple quantum harmonic oscillators, which are coupled linearly to the main system. The Caldeira-Leggett model has been very helpful in many applications, including dissipative quantum tunneling and quantum decoherence [49].

3.2.2 The model

The Caldeira-Leggett model is based on the following Lagrangian

$$L = L_S + L_I + L_R + L_{CT}, \tag{3.3}$$

where

$$\begin{aligned} L_S &= \frac{1}{2}M\dot{q}^2 - V(q), \quad L_I = -\sum_k C_k q_k q, \\ L_R &= \sum_k \frac{1}{2}m_k\dot{q}_k^2 - \sum_k \frac{1}{2}m_k\omega_k^2 q_k^2, \quad L_{CT} = -\sum_k \frac{1}{2}\frac{C_k^2}{m_k\omega_k^2}q^2, \end{aligned} \tag{3.4}$$

are the Lagrangian of the main system, interaction term, reservoir, and counter-term, respectively. The first and third terms need no further explanation. They have the standard form of a particle interacting with an external potential $V(q)$ and a harmonic oscillator, respectively, for simplicity all living in one spatial dimension. Note that the interaction is bilinear in the positions of the oscillators and of the particle, but obviously other choices can be made too. The last term might seem odd at first glance, but it has an important physical explanation. Generally, a coupling to the oscillators in the bath modifies the natural frequency of the system. This causes a change in $V(q)$, up till the point that original minima are rendered unstable. These are called frequency-renormalization effects, and in order to account for these effects, the counter-term is added [12]. As a final remark, one can define a canonical transformation to get rid of the counter-term [49]. However, in this chapter we study the Caldeira-Leggett theory in its original formulation.

First, we calculate the equations of motion for both the particle and the SHO's, by using the corresponding Euler-Lagrange equations

$$M\ddot{q} = -V'(q) + \sum_k C_k q_k - q\sum_k \frac{C_k^2}{m_k\omega_k}, \tag{3.5}$$

$$m_k\ddot{q}_k = -m_k\omega_k^2 q_k + C_k q. \tag{3.6}$$

Next, we use the Laplace transform, which is defined by

$$F(s) = \int_0^\infty e^{-st} f(t) \mathrm{d}t, \tag{3.7}$$

and its inverse transform

$$f(t) = \frac{1}{2\pi i} \lim_{T\to\infty} \int_{\gamma-iT}^{\gamma+iT} e^{st} F(s) \mathrm{d}s, \tag{3.8}$$

where $s \in \mathbb{C}$. The Laplace transform of the second equation of motion then reads

$$\begin{aligned} m_k \int \mathrm{d}t e^{-st} \ddot{q}_k(t) &= -m_k \omega_k^2 \int \mathrm{d}t e^{-st} q_k(t) + C_k \int \mathrm{d}t e^{-st} q(t) \\ &= -m_k \omega_k^2 \tilde{q}_k(s) + C_k \tilde{q}(s). \end{aligned} \tag{3.9}$$

By partially integrating the left-hand side twice, we obtain

$$\begin{aligned} m_k \int \mathrm{d}t e^{-st} \ddot{q}_k(t) &= m_k \left[e^{-st} \dot{q}_k(t) \right]_{t=0}^{t=\infty} + m_k \int \mathrm{d}t s e^{-st} \dot{q}_k(t) \\ &= -m_k \dot{q}_k(0) + m_k \left[s e^{-st} q_k(t) \right]_{t=0}^{t=\infty} + m_k \int \mathrm{d}t s^2 e^{-st} q_k(t) \\ &= -m_k \dot{q}_k(0) - m_k s q_k(0) + m_k s^2 \tilde{q}_k(s). \end{aligned} \tag{3.10}$$

We put now Eqs. (3.9) and (3.10) together, and we find

$$\tilde{q}_k(s) = \frac{\dot{q}_k(0)}{s^2+\omega_k^2} + \frac{s q_k(0)}{s^2+\omega_k^2} + \frac{C_k \tilde{q}(s)}{m_k (s^2+\omega_k^2)}. \tag{3.11}$$

By taking the inverse Laplace transform of the above, and by substituting this into the first equation of motion, we have

$$\begin{aligned} &M\ddot{q} + V'(q) + q \sum_k \frac{C_k^2}{m_k \omega_k} = \sum_k C_k q_k \\ =&\frac{1}{2\pi i} \int_{\gamma-i\infty}^{\gamma+i\infty} e^{st} \left\{ \sum_k C_k \left[\frac{\dot{q}_k(0)}{s^2+\omega_k^2} + \frac{s q_k(0)}{s^2+\omega_k^2} \right] \right\} \mathrm{d}s + \sum_k \frac{C_k^2}{m_k} \frac{1}{2\pi i} \int_{\gamma-i\infty}^{\gamma+i\infty} e^{st} \frac{\tilde{q}(s)}{s^2+\omega_k^2} \mathrm{d}s. \end{aligned} \tag{3.12}$$

We use that

$$\frac{1}{s^2+\omega_k^2} = \frac{1}{\omega_k^2} \left(1 - \frac{s^2}{s^2+\omega_k^2} \right). \tag{3.13}$$

Due to the inverse Laplace transform, the last term on the right-hand side of Eq. (3.12) generates two terms, one of which cancels the last term on the left-hand side.

Summarizing, so far we have

$$M\ddot{q}+V'(q)+\sum_k \frac{C_k^2}{m_k\omega_k^2}\frac{1}{2\pi i}\int_{\gamma-i\infty}^{\gamma+i\infty} \mathrm{d}s e^{st}\frac{s^2\tilde{q}(s)}{s^2+\omega_k^2} = \frac{1}{2\pi i}\int_{\gamma-i\infty}^{\gamma+i\infty}\mathrm{d}s\, e^{st}\left\{\sum_k C_k\left[\frac{\dot{q}_k(0)}{s^2+\omega_k^2}+\frac{sq_k(0)}{s^2+\omega_k^2}\right]\right\}. \tag{3.14}$$

Inspecting the last term on the left-hand side, we note that it can be written as a total time derivative. By subsequently using the convolution theorem [49], it reduces to the Laplace transform of a simple cosine,

$$\begin{aligned}\sum_k \frac{C_k^2}{m_k\omega_k^2}\frac{1}{2\pi i}\int_{\gamma-i\infty}^{\gamma+i\infty}\mathrm{d}s e^{st}\frac{s^2\tilde{q}(s)}{s^2+\omega_k^2} &= \frac{d}{dt}\left[\sum_k \frac{C_k^2}{m_k\omega_k^2}\frac{1}{2\pi i}\int_{\gamma-i\infty}^{\gamma+i\infty}\mathrm{d}s\, e^{st}\frac{s\tilde{q}(s)}{s^2+\omega_k^2}\right]\\ &= \frac{d}{dt}\left\{\sum_k \frac{C_k^2}{m_k\omega_k^2}\int_0^t \mathrm{d}t'\cos[\omega_k(t-t')]q(t')\right\}.\end{aligned} \tag{3.15}$$

In order to replace the summation over k with an integral, we introduce the spectral function $J(\omega)$,

$$J(\omega)\equiv\frac{\pi}{2}\sum_k\frac{C_k^2}{m_k\omega_k}\delta(\omega-\omega_k). \tag{3.16}$$

This allows us to rewrite

$$\sum_k\frac{C_k^2}{m_k\omega_k^2}\cos[\omega_k(t-t')]=\frac{2}{\pi}\int_0^\infty \mathrm{d}\omega\frac{J(\omega)}{\omega}\cos[\omega(t-t')]. \tag{3.17}$$

Note that the spectral function is the imaginary part of the Fourier transform of the retarded dynamical susceptibility of the bath [49]. We now assume that $J(\omega)$ is *Ohmic*,

$$J(\omega)=\begin{cases}\eta\omega & \text{if } \omega<\Omega\\ 0 & \text{if } \omega>\Omega,\end{cases} \tag{3.18}$$

where Ω is some high-frequency cut-off. Then, for the Ohmic case we find

$$\begin{aligned}\sum_k\frac{C_k^2}{m_k\omega_k^2}\cos[\omega_k(t-t')] &= \frac{2\eta}{\pi}\lim_{\Omega\to\infty}\int_0^\Omega \mathrm{d}\omega\cos[\omega(t-t')]=\frac{\eta}{\pi}\int_{-\infty}^\infty \mathrm{d}\omega\cos[\omega(t-t')]\\ &= \frac{\eta}{\pi}\int_{-\infty}^\infty \mathrm{d}\omega\left\{\cos[\omega(t-t')]+i\sin[\omega(t-t')]\right\}\end{aligned}$$

$$= \frac{\eta}{\pi}\int_{-\infty}^{\infty} \mathrm{d}\omega\, e^{i\omega(t-t')} = 2\eta\int_{-\infty}^{\infty} \mathrm{d}\omega\, e^{i(2\pi\omega)(t-t')} = 2\eta\,\delta(t-t'). \tag{3.19}$$

In the above expression, we have used the fact that the cosine function is an even function in order to extend the integration boundaries. Moreover, because of the odd property of the sine function, we have redefined the integration variable, and finally used a definition for the Dirac delta function. Thus, the last term on the left of Eq. (3.14) reduces to

$$\frac{d}{dt}\left[\int_0^t dt'\, 2\eta\,\delta(t-t')q(t')\right] = \eta\,\dot{q}(t), \tag{3.20}$$

in which we already recognize the friction term in the Langevin equation [49].

The last bit of work we have to do is on the right-hand side of Eq. (3.14). These two terms can be interpreted as a fluctuating force,

$$f(t) = \sum_k C_k \frac{1}{2\pi i}\int_{\gamma-i\infty}^{\gamma+i\infty} e^{st}\mathrm{d}s\left[\frac{\dot{q}_k(0)}{s^2+\omega_k^2} + \frac{sq_k(0)}{s^2+\omega_k^2}\right]. \tag{3.21}$$

By performing the inverse Laplace transform, this term becomes

$$f(t) = \sum_k C_k\left[\frac{\dot{q}_k(0)}{\omega_k}\sin(\omega_k t) + q_k(0)\cos(\omega t)\right]. \tag{3.22}$$

Now, we have to make some assumptions on the state of the bath. There are multiple options, as shown in Ref. [49]. Let us suppose that at $t = 0$, each oscillator is at thermodynamic equilibrium. We make use of the equipartition theorem from statistical physics, which states that each quadratic term in the Hamiltonian contributes $\frac{1}{2}k_{\mathrm{B}}T$ to the total energy. We then find

$$\begin{aligned}
&\langle q_k(0)\rangle = 0,\ \langle \dot{q}_k(0)\rangle = 0,\ \langle \dot{q}_k(0)q_k(0)\rangle = 0,\\
&\langle q_k(0)q_{k'}(0)\rangle = \frac{k_{\mathrm{B}}T}{m_k\omega_k^2}\delta_{k,k'},\\
&\langle \dot{q}_k(0)\dot{q}_{k'}(0)\rangle = \frac{k_{\mathrm{B}}T}{m_k}\delta_{k,k'}.
\end{aligned} \tag{3.23}$$

The thermodynamic average of $f(t)$ is trivial. The average of its square is calculated by employing the Ohmic spectral function

$$\langle f(t)f(t')\rangle = \sum_{k,k'} C_k C_{k'}\big[\frac{\langle \dot{q}_k(0)\dot{q}_{k'}(0)\rangle}{\omega_k\omega_{k'}}\sin(\omega_k t)\sin\big(\omega_{k'}t'\big) + \langle q_k(0)q_{k'}(0)\rangle\cos(\omega_k t)\cos\big(\omega_{k'}t'\big)\big]$$

$$
\begin{aligned}
&= \sum_k \frac{C_k^2 k_B T}{m_k \omega_k^2} \cos[\omega_k (t-t')] = \frac{2k_B T}{\pi} \int_0^\infty d\omega \, \frac{J(\omega)}{\omega} \cos[\omega(t-t')] \\
&= 2\eta k_B T \delta(t-t'),
\end{aligned} \tag{3.24}
$$

where we have used the identity $\sin u \sin v + \cos u \cos v = \cos(u-v)$, and afterwards we have taken the same steps employed in Eq. (3.19).

Putting the previous calculations together, we find

$$
M\ddot{q} + \eta \dot{q} + V'(q) = f(t), \quad \langle f(t) \rangle = 0, \quad \langle f(t) f(t') \rangle = 2\eta k_B T \delta(t-t'), \tag{3.25}
$$

which represents exactly the Langevin equation, introduced in Eq. (3.1). Hence, for the current set of assumptions and choice for the coupling, the microscopic Caldeira-Leggett model reproduces the classical Brownian motion. Other choices can also be made, such as different particle-bath couplings, a different spectral function $J \propto \omega^s$, $s > 0$, and so on, and different kinds of physics will emerge [52].

3.2.3 Integrating out the bath

To study the influence of the bath on the dynamics of the particle, the degrees of freedom of the harmonic-oscillator bath has to be integrated out in the equations. We will show how this is done, by following Ref. [51].

Ultimately, we are interested in the partition function Z, which is the trace over the density matrix

$$
\begin{aligned}
Z = \mathrm{tr}\, e^{-\beta H} &= \int dx \, \langle x | e^{-\beta H} | x \rangle = \int_{-\infty}^{\infty} dx \int_{q(0)=x}^{q(\hbar\beta)=x} Dq(\tau) \, e^{-\frac{1}{\hbar} S_E[q(\tau)]} \\
&= \int_{-\infty}^{\infty} dx \, \rho(x,x,\beta).
\end{aligned} \tag{3.26}
$$

Note that we can interpret Z also as the trace over the transition amplitude $\langle q | e^{-iHt/\hbar} | q \rangle$ taken at imaginary time $t = -i\hbar\beta$, where $\beta = 1/k_B T$ with T the temperature. This implies that it is natural to look at the Wick rotated (imaginary time, $t \to -i\tau$) path integral representation with the Euclidean action S_E.

For our system, the density matrix for the composite system in equilibrium is

$$
\rho(x, \mathbf{R}; y, \mathbf{Q}, \beta) = \langle x, \mathbf{R} | e^{-\beta H} | y, \mathbf{Q} \rangle \tag{3.27}
$$

$$
= \int_y^x \mathscr{D}q(\tau) \int_{\mathbf{Q}}^{\mathbf{R}} \mathscr{D}\mathbf{R}(\tau) \exp\left\{ -\frac{1}{\hbar} S_E[q(\tau), \mathbf{R}(\tau)] \right\}, \tag{3.28}
$$

where H is the Hamiltonian of the full system, $H = H_S + H_I + H_R + H_{CT}$. Here, x, y denote the particle's coordinates, and $\mathbf{R}, \mathbf{Q}$ are the bath coordinates. The Euclidean action is given by

$$\begin{aligned} S_E\left[q(\tau), \mathbf{R}(\tau)\right] &\equiv S_0 + S_{CT} + S_\Lambda \\ &= \int_0^{\hbar\beta} \mathrm{d}\tau \left[\frac{1}{2} M \dot{q}^2 + V(q) + \sum_k \frac{C_k^2}{2 m_k \omega_k^2} q^2 \right. \\ &\qquad \left. + \sum_k \left(C_k R_k q + \frac{1}{2} m_k \dot{R}_k^2 + \frac{1}{2} m_k \omega_k^2 R_k^2 \right) \right]. \end{aligned} \tag{3.29}$$

In the first line, S_0 corresponds to the action of the main system, S_{CT} to the part containing the counter-term, and S_Λ the remaining bath contribution. Note that all the time derivatives pick up an extra factor i due to the transformation to imaginary time. As a consequence, we find an overall minus sign in front of the Euclidean action, containing now strictly positive terms. We are interested in how the bare particle action changes due to the presence of the bath. In order to do this, we have to set $x = y$, $\mathbf{R} = \mathbf{Q}$, and integrate out the bath coordinates $\mathbf{R}(\tau)$. In other words, we want to compute the reduced density operator

$$\tilde{\rho}(x, y, \beta) \equiv \int_y^x \mathscr{D}q(\tau) \int_{-\infty}^{\infty} \mathrm{d}\mathbf{R} \int_{\mathbf{R}}^{\mathbf{R}} \mathscr{D}\mathbf{R}(\tau) \exp\left\{ -\frac{1}{\hbar} S_E\left[q(\tau), \mathbf{R}(\tau)\right] \right\}. \tag{3.30}$$

The general path integral solution for the forced harmonic oscillator is given in Ref. [53]. We consider a system with Lagrangian

$$L = \frac{1}{2} m \dot{q}^2(t) - \frac{1}{2} m \omega^2 q(t) + f(t) q(t), \tag{3.31}$$

where we require that $q(t)$ is a periodic function in the imaginary time representation, $q(\tau + \hbar\beta) = q(\tau)$. Hence, the kinetic term is partially integrated, where the boundary term $[q\dot{q}]_0^{\hbar\beta}$ vanishes. The action reads

$$S_E = \int_0^{\hbar\beta} \mathrm{d}\tau \left[\frac{m}{2} q(\tau) D_{\omega^2}(\tau, \tau') q(\tau') - q(\tau) f(\tau) \right], \tag{3.32}$$

with the functional matrix given by

$$D_{\omega^2}(\tau, \tau') \equiv (-\partial_\tau^2 + \omega^2) \delta(\tau - \tau'), \quad \tau - \tau' \in [0, \hbar\beta]. \tag{3.33}$$

The Euclidean Green's function is then

$$G_{\omega^2}(\tau,\tau') = G_{\omega^2}(\tau-\tau') = D^{-1}_{\omega^2}(\tau,\tau') = (-\partial_\tau^2+\omega^2)^{-1}\delta(\tau-\tau'). \tag{3.34}$$

We complete the square in the action with a variable shift

$$q(\tau) \to q(\tau) + \frac{1}{m} G_{\omega^2}(\tau,\tau') f(\tau). \tag{3.35}$$

Note that the measure remains unchanged. The action then becomes

$$S_E = \int_0^{\hbar\beta} \mathrm{d}\tau \frac{m}{2} q(\tau) D_{\omega^2}(\tau,\tau') q(\tau') - \frac{1}{2m}\int_0^{\hbar\beta}\mathrm{d}\tau\int_0^{\hbar\beta}\mathrm{d}\tau' f(\tau) G_{\omega^2}(\tau-\tau') f(\tau'). \tag{3.36}$$

Now, if $f(\tau)=0$, the partition function is the simple Gaussian result for the standard harmonic oscillator, namely

$$Z_\omega = \frac{1}{2\sinh(\beta\hbar\omega/2)}. \tag{3.37}$$

The generating functional for $f(\tau)$ then reads

$$Z[f(\tau)] = Z_\omega \exp\left[\frac{1}{2m}\int_0^{\hbar\beta}\mathrm{d}\tau\int_0^{\hbar\beta}\mathrm{d}\tau' f(\tau) G_{\omega^2}(\tau-\tau') f(\tau')\right], \tag{3.38}$$

where the Green's function is calculated as follows. First, the eigenfunctions of the operator $-\delta_\tau^2$ are $\exp(-i\omega_m\tau)$ with eigenvalues ω_m^2. Requiring periodic boundary conditions, the frequencies are recognized as Matsubara frequencies: $\omega_m = 2\pi m/\hbar\beta$, with $m\in\mathbb{Z}$. By definition, the eigenvalues for $G_{\omega^2}(\tau-\tau')$ are the inverse of those of $D_{\omega^2}(\tau,\tau')$. Hence, we write the function in a Fourier expansion

$$G_{\omega^2}(\tau) = \frac{1}{\hbar\beta}\sum_{m=-\infty}^{\infty}\frac{1}{\omega_m^2+\omega^2}e^{-i\omega_m\tau}. \tag{3.39}$$

If we take now the zero-temperature limit $T\to 0$, the Matsubara sum becomes an integral,

$$G_{\omega^2}(\tau) = \int\frac{\mathrm{d}\omega_m}{2\pi}\frac{1}{\omega_m^2+\omega^2}e^{-i\omega_m\tau} = \frac{1}{2\omega}e^{-\omega|\tau|}. \tag{3.40}$$

However, this step serves only a calculational purpose, as we are interested in the finite-temperature regime. We use the Poisson sum formula

$$\sum_m f(m) = \int \mathrm{d}\mu \sum_n e^{2\pi i\mu n} f(\mu), \tag{3.41}$$

and by choosing a delta function, we include an extra Poisson sum in the Matsubara integrand,

$$\sum_{\bar{m}=-\infty}^{\infty} \delta(\bar{m}-m) = \sum_{n=-\infty}^{\infty} e^{i2\pi nm} = \sum_{n=-\infty}^{\infty} e^{in\omega_m \hbar\beta}. \tag{3.42}$$

The Green's function then becomes a sum

$$G_{\omega^2}(\tau) = \frac{1}{2\omega}\sum_n e^{-\omega|\tau-n\hbar\beta|} = \frac{1}{2\omega}\frac{\cosh[\omega(\tau-\frac{\hbar\beta}{2})]}{\sinh\frac{\omega\hbar\beta}{2}}, \tag{3.43}$$

and the contribution to the action for the Caldeira-Leggett model then reduces to

$$S_\Lambda[q(\tau)] = \sum_k \frac{C_k^2}{4m_k\omega_k}\int_0^{\hbar\beta} \mathrm{d}\tau' \int_0^{\hbar\beta} \mathrm{d}\tau q(\tau)q(\tau')\frac{\cosh\left(\omega_k|\tau-\tau'|-\frac{\hbar\beta\omega_k}{2}\right)}{\sinh\left(\frac{\hbar\beta\omega_k}{2}\right)}. \tag{3.44}$$

If we define $q(\tau')$ to be a periodic function, such that outside the domain $0 \leq \tau' \leq \hbar\beta$: $q(\tau'+\hbar\beta) = q(\tau')$, we can take the boundaries to infinity and have to modify the integrand accordingly [54]. Formally, we have, with $T = \tau_b - \tau_a$,

$$\lim_{T\to\infty} \frac{\cosh(\omega|\tau-\tau'|-T/2)}{\sinh(T/2)} = \frac{e^{\omega|\tau-\tau'|-T/2}+e^{-\omega|\tau-\tau'|+T/2}}{e^{T/2}-e^{-T/2}} = e^{-\omega|\tau-\tau'|}. \tag{3.45}$$

The dissipation term in the action reduces to

$$S_\Lambda[q(\tau)] = \sum_k \frac{C_k^2}{4m_k\omega_k}\int_{-\infty}^{\infty} \mathrm{d}\tau' \int_0^{\hbar\beta} \mathrm{d}\tau q(\tau)q(\tau')e^{-\omega_k|\tau-\tau'|}. \tag{3.46}$$

Combining all these calculations, we find

$$\begin{aligned}\tilde{\rho}(x,y,\beta) &= \tilde{\rho}_0(\beta)\int_y^x Dq(\tau)\exp\left\{-\frac{1}{\hbar}S_E^{(0)}[q(\tau)] - \frac{1}{\hbar}S_{CT}[q(\tau)] - \frac{1}{\hbar}S_\Lambda[q(\tau)]\right\} \\ &= \tilde{\rho}_0(\beta)\int_y^x Dq(\tau)\exp\left\{-\frac{1}{\hbar}S_{\mathrm{eff}}[q(\tau)]\right\},\end{aligned} \tag{3.47}$$

where the effective action reads

$$S_{\mathrm{eff}}[q(\tau)] = S_E^{(0)}[q(\tau)] + S_{CT}[q(\tau)] + S_\Lambda[q(\tau)] \tag{3.48}$$

$$= \int_0^{\hbar\beta} \mathrm{d}\tau\left[\frac{1}{2}M\dot{q}^2 + V(q)\right] + \frac{1}{2}\int \mathrm{d}\tau' \int \mathrm{d}\tau K(\tau-\tau')\left[(q(\tau)-q(\tau')\right]^2, \tag{3.49}$$

with

$$K(\tau-\tau') \equiv \sum_k \frac{C_k^2}{4m_k\omega_k} e^{-\omega_k|\tau-\tau'|} = \frac{1}{2\pi}\int_0^\infty \mathrm{d}\omega J(\omega) e^{-\omega|\tau-\tau'|}. \tag{3.50}$$

In the second step, we have completed the square in order to cancel the counter-term in the action,

$$\begin{aligned}
&\frac{1}{2}\int \mathrm{d}\tau' \int \mathrm{d}\tau\, e^{-\omega_k|\tau-\tau'|}\left[(q(\tau)-q(\tau')\right]^2 \\
&\quad = \frac{1}{2}\int \mathrm{d}\tau' \int \mathrm{d}\tau\, e^{-\omega_k|\tau-\tau'|}\left[(q^2(\tau)-2q(\tau)q(\tau')+q^2(\tau')\right]^2,
\end{aligned} \tag{3.51}$$

where the second term is recognized in $S_\Lambda[q(\tau)]$. The first one is calculated as follows,

$$\begin{aligned}
\int_{-\infty}^{\infty}\mathrm{d}\tau' \int_0^{\hbar\beta} \mathrm{d}\tau\, q^2(\tau) e^{-\omega_k|\tau-\tau'|} &= \int_0^{\hbar\beta}\mathrm{d}\tau\, q^2(\tau)\left[\int_\tau^\infty \mathrm{d}\tau' e^{+\omega_k(\tau-\tau')} + \int_{-\infty}^{\tau}\mathrm{d}\tau' e^{-\omega_k(\tau-\tau')}\right] \\
&= \int_0^{\hbar\beta}\mathrm{d}\tau\, q^2(\tau)\left\{\left[-\frac{1}{\omega_k}e^{\omega_k(\tau-\tau')}\right]_\tau^\infty + \left[\frac{1}{\omega_k}e^{-\omega_k(\tau-\tau')}\right]_{-\infty}^{\tau}\right\} \\
&= \int_0^{\hbar\beta}\mathrm{d}\tau\, q^2(\tau)\left[0+\frac{1}{\omega_k}+\frac{1}{\omega_k}+0\right] = \int_0^{\hbar\beta}\mathrm{d}\tau\,\frac{2}{\omega_k}q^2(\tau),
\end{aligned} \tag{3.52}$$

and cancels partially the counter-term in the action. The third term is more difficult, because the integration also extends over $q(\tau)$. However, by transforming back to the initial boundaries $[0,\hbar\beta]$ this problem is then solved. Because of symmetry, it follows that the result has to be equal to that of the first term. The full calculation reads

$$\begin{aligned}
&\int_{-\infty}^{\infty}\mathrm{d}\tau' \int_0^{\hbar\beta}\mathrm{d}\tau\, q^2(\tau') e^{-\omega_k|\tau-\tau'|} \\
&\quad = \int_0^{\hbar\beta}\mathrm{d}\tau' \int_0^{\hbar\beta}\mathrm{d}\tau\, q^2(\tau')\frac{\cosh[\omega_k|\tau-\tau'|-\frac{\beta\hbar\omega_k}{2}]}{\sinh\left(\frac{\beta\hbar\omega_k}{2}\right)} \\
&\quad = \int_0^{\hbar\beta}\mathrm{d}\tau'\frac{q^2(\tau')}{\sinh\left(\frac{\beta\hbar\omega_k}{2}\right)}\left[\int_{\tau'}^{\hbar\beta}\mathrm{d}\tau\cosh[\omega_k(\tau-\tau')-\frac{\beta\hbar\omega_k}{2}]\right. \\
&\qquad\qquad \left. + \int_0^{\tau'}\mathrm{d}\tau\cosh[-\omega_k(\tau-\tau')-\frac{\beta\hbar\omega_k}{2}]\right] \\
&\quad = \int_0^{\hbar\beta}\mathrm{d}\tau'\frac{q^2(\tau')}{\sinh\left(\frac{\beta\hbar\omega_k}{2}\right)}\left\{\left[\frac{1}{\omega_k}\sinh[\omega_k(\tau-\tau')-\frac{\beta\hbar\omega_k}{2}]\right]_{\tau'}^{\hbar\beta}\right. \\
&\qquad\qquad \left. + \left[-\frac{1}{\omega_k}\sinh[-\omega_k(\tau-\tau')-\frac{\beta\hbar\omega_k}{2}]\right]_0^{\tau'}\right\}
\end{aligned}$$

$$= \int_0^{\hbar\beta} \mathrm{d}\tau' \frac{q^2(\tau')}{\omega_k \sinh\left(\frac{\beta\hbar\omega_k}{2}\right)} \left[\sinh\left(-\omega_k\tau' + \frac{\beta\hbar\omega_k}{2}\right) - \sinh\left(-\frac{\beta\hbar\omega_k}{2}\right) \right.$$
$$\left. - \sinh\left(-\frac{\beta\hbar\omega_k}{2}\right) + \sinh\left(\omega_k\tau' - \frac{\beta\hbar\omega_k}{2}\right) \right]$$
$$= \int_0^{\hbar\beta} \mathrm{d}\tau' \frac{2}{\omega_k} q^2(\tau'), \tag{3.53}$$

where we have used the identity $\sinh(-x) = -\sinh(x)$. The full result is given by

$$\frac{1}{2} \int \mathrm{d}\tau' \int \mathrm{d}\tau \sum_k \frac{C_k^2}{4m_k\omega_k} e^{-\omega_k|\tau-\tau'|} \left[(q(\tau) - q(\tau')\right]^2$$
$$= \int_0^{\hbar\beta} \mathrm{d}\tau \sum_k \frac{C_k^2}{2m_k\omega_k^2} q^2(\tau) + S_\Lambda[q(\tau)]. \tag{3.54}$$

These contributions indeed cancel the counter-term S_{CT}.

In the case of Ohmic dissipation, by using integration by parts, the kernel Eq. (3.50) becomes

$$K(\tau - \tau') = \frac{1}{2\pi} \int_0^\infty \mathrm{d}\omega\, \eta\, \omega\, e^{-\omega|\tau-\tau'|} = \frac{\eta}{2\pi} \frac{1}{(\tau - \tau')^2}, \tag{3.55}$$

and the effective action reads

$$S_{\mathrm{eff}}[q(\tau)] = \int_0^{\hbar\beta} \mathrm{d}\tau \left[\frac{1}{2}M\dot{q}^2 + V(q)\right] + \frac{\eta}{4\pi} \int \mathrm{d}\tau' \int \mathrm{d}\tau \frac{\left[(q(\tau) - q(\tau')\right]^2}{(\tau - \tau')^2}. \tag{3.56}$$

Thus, the correction on the action of the main system due to the linear interaction with the bath in the Ohmic case becomes the third term in Eq. (3.56). When τ approaches τ', the only way of avoiding a divergence in the integrand is to let $q(\tau)$ approach $q(\tau')$. This is exactly what friction does: it is much more profitable energetically for the particle to stay at the same position than being displaced. Thus, the bath in the Caldeira-Leggett model reproduces a friction-like contribution in the effective action.

Chapter 4

Bosonization of the Luttinger liquid

4.1 Introduction

Electrons in one dimension behave very differently compared to electrons living in higher-dimensional systems. An example of this difference is the characterization of excitations. In two dimensions, fermions are generally described by Fermi-liquid theory [55]. The Pauli exclusion principle forbids that one state is occupied by more than one electron, such that in the ground state subsequent energy levels are filled, until the highest energy state, which is the Fermi level. Excitations of this ground state can be characterized by their charge, momentum, and spin. If we now add interactions to the problem, these parameters and the statistics remain unchanged. However, electron properties like mass, velocity, etc. are renormalized due to the effect of the interactions. Excitations are therefore not anymore described in terms of the original fundamental electrons, but as quasi-particles, electrons 'dressed' with interactions. In one dimension, however, the Fermi liquid description breaks down, and there are no single-particle excitations. Imagine that we have a wire with electrons on it. Now, if we add an extra electron, the others get pushed to the sides. It creates a density fluctuation, which is a collective excitation of all the electrons in the wire. Generally, individual motion does not exist in 1D, only collective modes occur. One-dimensional electrons can be described by the Luttinger theory [11].

To see the difference between 1D and 2D on a more formal level, consider Fig. 4.1a. Here, the energy of a single particle and the spectrum of particle-hole excitations are plotted, measured with respect to the ground state, in one dimension. Because of the linear character of the dispersion around the Fermi points, the pair momentum near $k = 0$ is very narrow, so that the particle and hole excitations propagate coherently. A weak attraction between them produces a coherently propagating quasi-particle. Compare this to the two-dimensional case

in Fig. 4.1b. A particle-hole pair with momentum k can have a wide degeneracy of energies. Interactions are much less likely to form coherently propagating particle-hole pairs.

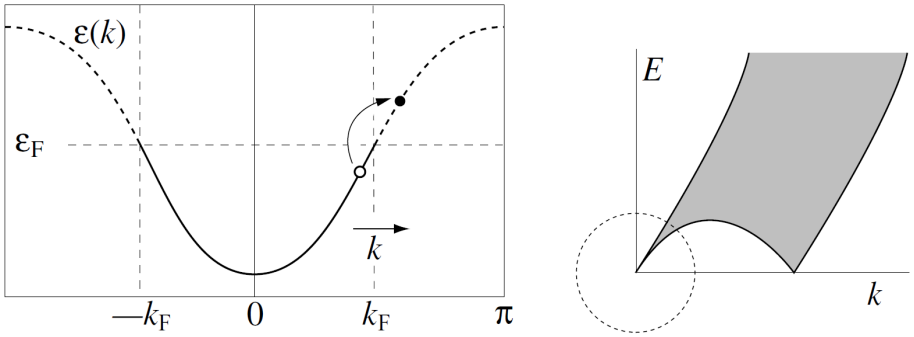

(a) The single-particle dispersion in 1D is shown on the left. Low-energy excitations exist of an electron leaving a state just below the Fermi level to a state just above it. On the right, the spectrum of particle-hole pairs with pair momentum k is depicted.

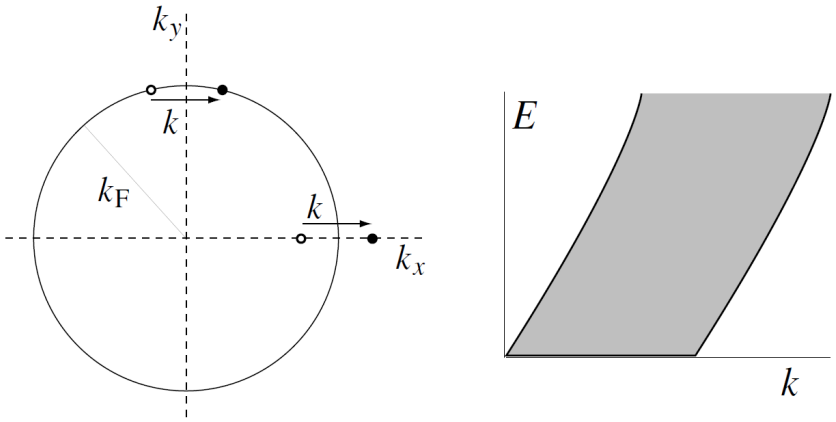

(b) Single particle excitation in 2D, shown in the two-dimensional momentum space (k_x,k_y) on the left. On the right, the particle-hole energy as a function of momentum is plotted. Already from $k = 0$ on, a range of energies is allowed for the pair, thus making coherent propagation of the pair unlikely.

Figure 4.1 Single particle excitations and the particle-hole dispersion in (a) 1D and (b) 2D. Figures taken from Ref. [56].

This peculiar behaviour of electrons in one dimension is also the basis for bosonization, which is one of the most widely used techniques in one-dimensional quantum physics. Because the low-energy particle-hole excitations are bosonic in character, a theory formulated in terms of fermionic fields can be reformulated in terms of bosonic fields, which opens up a new way to solving problems in one-dimensional fermionic systems. Though this also can

be done in higher dimensions [57, 58], the special feature of one dimension is that here, the bosonization mapping is exact [2, 56].

In this chapter, first we lay the groundwork for discussing fermionic theories in one dimension by describing the method of bosonization, and a few expressions that are needed further on will be calculated. Then, we derive the Luttinger-liquid Hamiltonian for a spinless fermionic chain. We discuss the free theory, various types of interactions, the chiral Luttinger liquid, which contains only modes propagating in one direction, and the helical Luttinger liquid, where the spin orientation is locked to the direction of motion because of the underlying time-reversal symmetry. Luttinger liquids take after bosonization the form of the sine-Gordon theories. We will show that a Luttinger liquid in presence of impurities on the edge can be mapped to a boundary sine-Gordon equation, which is a Gaussian theory with a cosine interaction at the boundary. Finally, we will show that in such a kind of theory with Luttinger parameter $K = \frac{1}{2}$, a Majorana zero-energy mode can be found at the edge of the chain. Note that throughout this chapter, we set $\hbar = 1$.

4.2 Bosonization

4.2.1 Introduction

Bosonization is a powerful technique in the areas of both condensed-matter and high-energy physics. It allows to reformulate problems in bosonic systems in terms of fermions, and vice versa. As such, it opens the path to new analytic solutions. The underlying idea is that fermionic particle-hole excitations are bosonic in character and therefore allow rewriting a strongly interacting fermionic (1+1)-dimensional theory into a bosonic free theory. The method the other way around is called fermionization. The earliest example of bosonization is given by the Jordan-Wigner transformation, where the equivalence between the anisotropic Heisenberg chain and a chain of interacting spinless fermions was shown in Ref. [59].

4.2.2 Dictionary

Approach

Starting from a fermionic field $\psi(x,t)$, the density operator is defined as $\rho = \psi^\dagger(x,t)\psi(x,t)$. It is interpreted as a creation and annihilation operator for an electron, but at the same time as two consecutive creation operators for an electron-hole pair. In the latter view, two coupled spin-$\frac{1}{2}$ particles are created. Together they can be viewed as a bosonic excitation of the field.

This is the main idea underlying bosonization. In this subsection, the approach by Sénéchal (Ref. [56]) is used.

The bosonization method roughly works as follows. First, a low-energy Fermi theory is written in terms of operators around the Fermi points k_F, such that the energy is linearized. The second step is to distinguish between left- and right-moving modes, so-called chiral components. Together, these modes are written as a spinor. Third, a formulation in terms of Bose fields satisfying fermionic commutation relations is needed. Finally, the Hamiltonian of interest is rewritten in terms of the free bosonic fields.

Complex coordinates

We start by considering complex coordinates z instead of x and t. The relation between the different coordinates is given by

$$z = -i(x - vt) = v\tau - ix, \quad \bar{z} = i(x + vt) = v\tau + ix, \tag{4.1}$$

and their corresponding derivatives are

$$\begin{aligned} \partial_t = iv(\partial_z + \partial_{\bar{z}}), \quad \partial_x = -i(\partial_z - \partial_{\bar{z}}) \\ \partial_z = -\frac{i}{2}\left(\frac{1}{v}\partial_t - \partial_x\right), \quad \partial_{\bar{z}} = -\frac{i}{2}\left(\frac{1}{v}\partial_t + \partial_x\right). \end{aligned} \tag{4.2}$$

Bosonization formula

We are now ready to study a Fermi field in terms of a Bose field. The standard expression for bosonization reads

$$\begin{aligned} \psi_L = \frac{1}{\sqrt{2\pi}} e^{+i\sqrt{4\pi}\phi_L(\bar{z})}, \quad \psi_L^\dagger = \frac{1}{\sqrt{2\pi}} e^{-i\sqrt{4\pi}\phi_L(\bar{z})}, \\ \psi_R = \frac{1}{\sqrt{2\pi}} e^{-i\sqrt{4\pi}\phi_R(z)}, \quad \psi_R^\dagger = \frac{1}{\sqrt{2\pi}} e^{+i\sqrt{4\pi}\phi_R(z)} \end{aligned} \tag{4.3}$$

Two subtleties should be discussed. First, the dimension of the Fermi operators here is $L^{1/2}$. This means that an extra factor $1/\sqrt{a}$ must be added for the normalization, where in the non-interacting case a equals the lattice constant. Second, if one is dealing with more than one species of fermions (e.g. working with spin degrees of freedom), Klein factors have to be introduced to ensure the proper fermionic anticommutation relations for the bosonized expressions [60]. They are Hermitian and obey the Clifford algebra

$$\{\eta_{L,\mu}, \eta_{L,\nu}\} = \{\eta_{R,\mu}, \eta_{R,\nu}\} = \delta_{\mu,\nu}, \quad \{\eta_{L,\mu}, \eta_{R,\nu}\} = 0. \tag{4.4}$$

One can now formulate a dictionary between interacting Fermi fields and decoupled massless Bose scalar fields, which is given in Table 4.1 [56, 2]. In the next sections, we will explicitly calculate some entries from the table.

Table 4.1 Bosonization dictionary. The procedure for replacing Fermi fields $\Psi(z)$ in terms of Bose fields $\Phi(z)$. In doing so, a crucial point is distinguishing between the left- (ψ_L) and right-moving modes (ψ_R). Similarly, the bosonic field Φ is separated into an analytic part $\phi_R(z)$ and an anti-analytic part $\phi_L(\bar{z})$ (so-called chiral components): $\Phi(z,\bar{z}) = \phi_R(z) + \phi_L(\bar{z})$ [56, 2].

Massless fermions	**Massless bosons**
Hamiltonian	
$i\left(\psi_R^\dagger \partial_x \psi_R + \psi_L^\dagger \partial_x \psi_L\right)$	$[\partial_z \Phi(z,\bar{z})]^2 + [\partial_{\bar{z}} \Phi(z,\bar{z})]^2$
Operators	
$\psi_R, \psi_R^\dagger$	$\frac{1}{\sqrt{2\pi}} e^{\mp i\sqrt{4\pi}\phi_R(z)}$
$\psi_L, \psi_L^\dagger$	$\frac{1}{\sqrt{2\pi}} e^{\pm i\sqrt{4\pi}\phi_L(\bar{z})}$
$\psi_R^\dagger \psi_R$	$-\frac{i}{\sqrt{\pi}} \partial_{\bar{z}} \Phi$
$\psi_L^\dagger \psi_L$	$\frac{i}{\sqrt{\pi}} \partial_z \Phi$
$\psi_R^\dagger \psi_L + \psi_L^\dagger \psi_R$	$\frac{1}{\pi} \cos\left[\sqrt{4\pi}\Phi(z,\bar{z})\right]$

Products of fermionic fields

The next move is to consider products of fermionic fields. They are more difficult to handle, because normal ordering of the operators is required. In principle, one can achieve normal ordering by expanding the operators, but another way of calculating the densities is, for instance, by point splitting. The exponentials have to be combined as follows [56]

$$e^{ia\phi(z)} e^{ib\phi(z')} = e^{ia\phi(z)+ib\phi(z')} e^{-ab\langle \phi(z)\phi(z')\rangle}, \tag{4.5}$$

where $\langle \dots \rangle$ denotes a ground-state expectation value if the left-hand side is a normal product, or a Green's function if it is a time-ordered product. The Green's function for free bosons is a standard result, which is calculated by compactifying the fields on a cilinder, and yields, [61, 62]

$$\langle \phi_R(z)\phi_R(z')\rangle = -\frac{1}{4\pi} \ln\left(z - z'\right). \tag{4.6}$$

The right-moving density is defined as

$$\rho_R = \psi_R^\dagger \psi_R = \lim_{\varepsilon \to 0} \left[\psi^\dagger(z+\varepsilon)\psi(z) - \langle \psi^\dagger(z+\varepsilon)\psi(z)\rangle \right], \tag{4.7}$$

where ε is some positive time that describes the normal ordering. The expectation value is

$$\begin{aligned}\langle \psi^\dagger(z)\psi(z')\rangle &= \int_{k>0}\frac{\mathrm{d}k}{2\pi}\int_{q>0}\frac{\mathrm{d}q}{2\pi}\langle 0|\,\alpha(k)\beta^\dagger(q)\,|0\rangle\, e^{-kz+qz'} \\ &= \int_{k>0}\frac{\mathrm{d}k}{2\pi}e^{-k(z-z')} = \frac{1}{2\pi}\frac{1}{z-z'},\end{aligned} \tag{4.8}$$

since $\langle 0|\,\alpha(k)\beta^\dagger(q)\,|0\rangle = \delta(k-q)$. Now, Eq. (4.7) can be calculated using the bosonization formula Eq. (4.3), by combining the exponentials according to Eq. (4.5), the Green's function in Eq. (4.6), and a Taylor expansion,

$$\begin{aligned}\rho_R &= \frac{1}{2\pi}\lim_{\varepsilon\to 0}\left[e^{i\sqrt{4\pi}\phi_R(z+\varepsilon)}e^{-i\sqrt{4\pi}\phi_R(z)} - \frac{1}{\varepsilon}\right] = \frac{1}{2\pi}\lim_{\varepsilon\to 0}\left[e^{i\sqrt{4\pi}[\phi_R(z+\varepsilon)-\phi_R(z)]}\frac{1}{\varepsilon} - \frac{1}{\varepsilon}\right] \\ &= \frac{1}{2\pi}\lim_{\varepsilon\to 0}\left[e^{i\varepsilon\sqrt{4\pi}\partial_z\phi_R(z)}\frac{1}{\varepsilon} - \frac{1}{\varepsilon}\right] = \frac{1}{2\pi}i\sqrt{4\pi}\partial_z\phi_R(z) = \frac{i}{\sqrt{\pi}}\partial_z\phi_R(z).\end{aligned} \tag{4.9}$$

Similarly, the left-moving density is

$$\rho_L = -\frac{i}{\sqrt{\pi}}\partial_{\bar{z}}\phi_L(\bar{z}). \tag{4.10}$$

Furthermore, for the bosonization of the Hamiltonian, we need to calculate $\psi^\dagger_{L/R}\partial_x\psi_{L/R}$. Again, we define

$$\psi^\dagger_R\partial_x\psi_R = -i\lim_{\varepsilon\to 0}\left[\psi^\dagger(z+\varepsilon)\partial_z\psi(z) - \langle\psi^\dagger(z+\varepsilon)\partial_z\psi(z)\rangle\right], \tag{4.11}$$

such that the derivative is written as

$$\partial_z\psi_R(x) = \lim_{\delta\to 0}\frac{\psi_R(z+\delta)-\psi_R(z)}{\delta}. \tag{4.12}$$

The Hamiltonian term becomes

$$\begin{aligned}\psi^\dagger_R\partial_z\psi_R &= -i\lim_{\varepsilon\to 0}\left[\psi^\dagger_R(z+\varepsilon)\partial_z\psi_R(z) - \langle\psi^\dagger_R(z+\varepsilon)\partial_z\psi_R(z)\rangle\right] \\ &= -i\lim_{\delta,\varepsilon\to 0}\frac{1}{\delta}\big\{\psi^\dagger_R(z+\varepsilon)\,[\psi_R(z+\delta)-\psi_R(z)] \\ &\qquad\qquad - \langle\psi^\dagger_R(z+\varepsilon)\,[\psi_R(z+\delta)-\psi_R(z)]\rangle\big\} \\ &= -i\lim_{\delta,\varepsilon\to 0}\frac{1}{\delta}\big[\psi^\dagger_R(z+\varepsilon)\psi_R(z+\delta) - \psi^\dagger_R(z+\varepsilon)\psi_R(z) \\ &\qquad\qquad - \langle\psi^\dagger_R(z+\varepsilon)\psi_R(z+\delta)\rangle + \langle\psi^\dagger_R(z+\varepsilon)\psi_R(z)\rangle\big].\end{aligned} \tag{4.13}$$

The last two ground-state expectation values have already been calculated. In order to calculate the first two products, we Taylor expand the Bose field around z with variable $\varepsilon = z' - z$,

$$\phi_R(z') = \phi_R(z) + \varepsilon\partial_z\phi_R(z) + \frac{\varepsilon^2}{2}\partial_z^2\phi_R(z) + \mathscr{O}(\varepsilon^3). \tag{4.14}$$

Now, the right-moving density becomes (to order ε^2, we choose to suppress the index R for now, as the argument z tells us we are dealing with the right-moving field, as opposed to $\bar{z}$ for the left-moving field)

$$\begin{aligned}\psi_R^\dagger(z')\psi_R(z) &= \frac{1}{2\pi}e^{i\sqrt{4\pi}\phi(z')}e^{-i\sqrt{4\pi}\phi(z)} = \frac{1}{2\pi\varepsilon}e^{i\sqrt{4\pi}[\phi(z+\varepsilon)-\phi(z)]} = \frac{1}{2\pi\varepsilon}e^{i\sqrt{4\pi}\varepsilon\partial_z\phi(z)} \\ &= \frac{1}{2\pi\varepsilon}\left\{1 + i\sqrt{4\pi}\varepsilon\partial_z\phi(z) - \frac{4\pi}{2}\varepsilon^2\left[\partial_z\phi(z)\right]^2 + \mathscr{O}(\varepsilon^3)\right\} \\ &= \frac{1}{2\pi\varepsilon} + i\frac{1}{\sqrt{\pi}}\partial_z\phi(z) - \varepsilon[\partial_z\phi(z)]^2 + \mathscr{O}(\varepsilon^2).\end{aligned} \tag{4.15}$$

The first product of Eq. (4.13) is

$$\psi_R^\dagger(z+\varepsilon)\psi_R(z+\delta) = \frac{1}{2\pi}e^{i\sqrt{4\pi}\phi(z+\varepsilon)}e^{-i\sqrt{4\pi}\phi(z+\delta)} = \frac{1}{2\pi(\varepsilon-\delta)}e^{i\sqrt{4\pi}[\phi(z+\varepsilon)-\phi(z+\delta)]}. \tag{4.16}$$

The full expression from Eq. (4.11) yields

$$\begin{aligned}\psi_R^\dagger(x)\partial_x\psi_R(x) &= -i\lim_{\delta,\varepsilon\to 0}\frac{1}{\delta}\left\{\frac{1}{2\pi(\varepsilon-\delta)}e^{i\sqrt{4\pi}[\phi(z+\varepsilon)-\phi(z+\delta)]} - \frac{1}{2\pi\varepsilon}\right. \\ &\qquad \left. - \frac{i}{\sqrt{\pi}}\partial_z\phi(z) + \varepsilon[\partial_z\phi(z)]^2 - \frac{1}{2\pi(\varepsilon-\delta)} + \frac{1}{2\pi\varepsilon}\right\} \\ &= -i\lim_{\delta\to 0}\frac{1}{\delta}\left\{-\frac{1}{2\pi\delta}e^{-i\sqrt{4\pi}\frac{\delta}{\delta}[\phi(z+\delta)-\phi(z)]} - \frac{i}{\sqrt{\pi}}\partial_z\phi(z) + \frac{1}{2\pi\delta}\right\} \\ &= -i\lim_{\delta\to 0}\frac{1}{\delta}\left\{-\frac{1}{2\pi\delta}e^{-i\sqrt{4\pi}\delta\partial_z\phi(z)] } - \frac{i}{\sqrt{\pi}}\partial_z\phi(z) + \frac{1}{2\pi\delta}\right\} \\ &= -i\lim_{\delta\to 0}\frac{1}{\delta}\left\{-\frac{1}{2\pi\delta}\left[1 - i\sqrt{4\pi}\delta\partial_z\phi(z) - 2\pi\delta^2[\partial_z\phi(z)]^2\right] - \frac{i}{\sqrt{\pi}}\partial_z\phi(z) + \frac{1}{2\pi\delta}\right\} \\ &= -i\lim_{\delta\to 0}\frac{1}{\delta}\left\{\frac{i}{\sqrt{\pi}}\partial_z\phi(z) + \delta[\partial_z\phi(z)]^2 - \frac{i}{\sqrt{\pi}}\partial_z\phi(z)\right\} \\ &= -i[\partial_z\phi(z)]^2 = i\pi\rho_R^2,\end{aligned} \tag{4.17}$$

where we have refermionized the expression in the last line, by using Eq. (4.7). Identically for the left-moving mode, we obtain

$$\psi_L^\dagger(x)\partial_x\psi_L(x) = i\pi\rho_L^2. \tag{4.18}$$

Mode expansion

For later use, a proper expansion of the Bose field Φ has to be defined. The field is massless, such that the zero-mode is ill-defined, and therefore it needs to be treated separately [56]. Furthermore, in order for bosonization to be properly defined, Φ should have an angular character, and the boson must be compactified on a circle of radius R. Consider the Fourier-mode expansion of Φ that satisfies the following conditions,

$$\Phi(x,t) = q + \frac{\pi_0 vt}{L} + \frac{\tilde{\pi}_0 x}{L} + \sum_{n>0}\frac{1}{\sqrt{4\pi n}}\left(a_n^\dagger e^{kz} + a_n e^{-kz} + \bar{a}_n^\dagger e^{k\bar{z}} + \bar{a}_n e^{-k\bar{z}}\right), \tag{4.19}$$

where q is the zero mode, π_0 and $\tilde{\pi}_0$ are the conjugate momenta. The wavevectors are quantized as $k = 2\pi n/L$, where L is the length of the chain. The creation and annihilation operators $\bar{a}_n$ are defined as $\bar{a}_n = a_{-n}$, such that only positive modes appear in the expansion. The operators satisfy the commutation rules

$$\left[a_n, a_m^\dagger\right] = \delta_{n,m}, \quad \left[\bar{a}_n, \bar{a}_m^\dagger\right] = \delta_{n,m}. \tag{4.20}$$

The zero mode is treated separately from the other modes. It is written explicitly as the combination of two pairs of canonical variables q and π_0, and $\tilde{q}$ and $\tilde{\pi}_0$, where $\tilde{q}$ does not appear in the original mode expansion, but will be used in the separation of left- and right-moving parts of the field. They are related by the commutation relations

$$[q, \pi_0] = i, \quad [\tilde{q}, \tilde{\pi}_0] = i. \tag{4.21}$$

The operator q is not single-valued, since it is an angular variable. Only exponentials $\exp(inq/R)$ are well defined. The Bose field Φ is separated in left- and right-moving parts $\phi_R(z)$ and $\phi_L(\bar{z})$, respectively. In terms of the mode expansion variables, they read

$$\phi_R(z) = Q + \frac{P}{2L}(vt - x) + \sum_{n>0}\frac{1}{\sqrt{4\pi n}}\left(a_n e^{-kz} + a_n^\dagger e^{kz}\right), \tag{4.22}$$

$$\phi_L(\bar{z}) = \bar{Q} + \frac{\bar{P}}{2L}(vt + x) + \sum_{n>0}\frac{1}{\sqrt{4\pi n}}\left(\bar{a}_n e^{-k\bar{z}} + \bar{a}_n^\dagger e^{k\bar{z}}\right), \tag{4.23}$$

with variables

$$Q = \frac{1}{2}(q - \tilde{q}), \quad P = \pi_0 - \tilde{\pi}_0, \quad [Q,P] = i,$$
$$\bar{Q} = \frac{1}{2}(q + \tilde{q}), \quad \bar{P} = \pi_0 + \tilde{\pi}_0, \quad \left[\bar{Q},\bar{P}\right] = i. \tag{4.24}$$

Dirac Hamiltonian

Let us consider the one-dimensional Dirac Hamiltonian, given by

$$H = -iv_{\mathrm{F}} \int \mathrm{d}x \left[\psi_R^\dagger(x)\partial_x\psi_R(x) - \psi_L^\dagger(x)\partial_x\psi_L(x)\right], \tag{4.25}$$

where the Dirac two-component spinor is $\Psi = (\psi_L, \psi_R)$, and v_F is the Fermi velocity. By using Eqs. (4.17) and (4.18) together, it can be bosonized to

$$H = \pi v_{\mathrm{F}} \int \mathrm{d}x \left(\rho_R^2 + \rho_L^2\right) = -v_{\mathrm{F}} \int \mathrm{d}x \left\{[\partial_z\Phi]^2 + [\partial_{\bar{z}}\Phi]^2\right\}. \tag{4.26}$$

The coordinates are rewritten using Eq. (4.2).

$$\begin{aligned} H &= -v_{\mathrm{F}} \int \mathrm{d}x \left\{[\partial_z\Phi]^2 + [\partial_{\bar{z}}\Phi]^2\right\} \\ &= -v_{\mathrm{F}} \int \mathrm{d}x \left\{\left[-\frac{i}{2}\left(\frac{1}{v_{\mathrm{F}}}\partial_t - \partial_{\bar{x}}\right)\Phi\right]^2 + \left[-\frac{i}{2}\left(\frac{1}{v_{\mathrm{F}}}\partial_t + \partial_x\right)\Phi\right]^2\right\} \\ &= \frac{v_{\mathrm{F}}}{2} \int \mathrm{d}x \left\{\left[\frac{1}{v_{\mathrm{F}}}\partial_t\Phi\right]^2 + [\partial_x\Phi]^2\right\}. \end{aligned} \tag{4.27}$$

This expression is the standard form of the free bosonic massless scalar field in two dimensions, also known as the Gaussian Hamiltonian,

$$H_0[\Phi] = \frac{v_{\mathrm{F}}}{2} \int \mathrm{d}x \left\{\Pi(x)^2 + [\partial_x\Phi(x)]^2\right\}, \tag{4.28}$$

where $\Pi(x)$ is the momentum canonically conjugated to $\Phi(x)$, and

$$\Pi = \frac{1}{v_{\mathrm{F}}}\partial_t\Phi, \quad \left[\Pi(x), \Phi(x')\right] = -i\delta(x - x'). \tag{4.29}$$

It is worth noting that often in literature, also a dual Bose field is defined as $\Theta = \phi_R - \phi_L$, and as a consequence, $\partial_x\Theta = -\Pi$.

4.3 Luttinger liquid

The Luttinger model was first introduced to describe the behaviour of interacting electrons in one dimension [11, 63]. It is based on the work done by Tomonaga [64], so that sometimes it still is referred to as the Tomonaga-Luttinger liquid.

In this section, we investigate the free Hamiltonian of a one-dimensional spinless fermionic chain. Subsequently, electron interactions are added to the problem. Next, we will consider the case of an impurity in the spinless Luttinger liquid, and we will investigate the system that preserves time-reversal symmetry and gives rise to the helical Luttinger liquid.

4.3.1 Noninteracting spinless electrons

In this section, we follow the introduction of Ref. [56]. A system consisting of noninteracting spinless fermions is described by the following microscopic Hamiltonian

$$H = \sum_k \varepsilon_k c_k^\dagger c_k, \tag{4.30}$$

where c_k is the annihilation operator at wavevector k, obeying the usual Fermi anti-commutation relations

$$\left\{c(k), c^\dagger(k')\right\} = \delta(k-k'), \quad \left\{c(k), c(k')\right\} = \left\{c^\dagger(k), c^\dagger(k')\right\} = 0. \tag{4.31}$$

The corresponding field operators are given by

$$\psi(x_j) = \frac{1}{\sqrt{N}} \sum_k e^{ikx_j} c_k, \quad c_k = \frac{1}{\sqrt{N}} \sum_{j=1}^{N} e^{-ikx_j} \psi(x_j), \tag{4.32}$$

where k increases with steps of $2\pi/L$, $L = Na$, $x_j = ja$, and a is the lattice constant. The energy of state k is denoted by ε_k. For example, a free electron gas has energy $\varepsilon_k = \hbar^2 k^2/2m$, whereas electrons hopping on a lattice have energy $\varepsilon_k = \cos(ka)$. At the ground state, all the energy levels up to the Fermi point ($|k| < k_\mathrm{F}$) are filled, and those above ($|k| > k_\mathrm{F}$) are empty.

Excitations from the ground state involve an electron hopping to a higher momentum state, leaving an empty state behind. These excitations are called particle-hole excitations. By switching on interactions in this system, several excitations are created and are located at momenta around the Fermi point. Thus, to investigate the low-energy behaviour, we have to expand the wavevectors around k_F. We define annihilation operators for electrons and holes,

respectively given by

$$\begin{aligned} \alpha_k &= c_{k_\mathrm{F}+k}, \quad \alpha_{-k} = c_{-k_\mathrm{F}-k}, \\ \beta_k &= c^\dagger_{k_\mathrm{F}-k}, \quad \beta_{-k} = c^\dagger_{-k_\mathrm{F}+k}, \end{aligned} \tag{4.33}$$

with k positive. Thus, α_k and β_k annihilate electrons and holes, respectively, around the right Fermi points, and similarly for α_{-k} and β_{-k} around the left Fermi point.

The energy is linearized around the left (minus sign) and right Fermi points: $\varepsilon_k = \pm v_\mathrm{F} k$, with v_F the Fermi velocity. Note that the energy now is defined with respect to the ground state energy $\varepsilon = v_\mathrm{F} k_\mathrm{F}$. At the same time, we have to introduce a momentum cut-off Λ to define the region where this approximation is valid. By doing so, we limit our approach to the contribution of low-energy states, and high-energy states far from the cut-off do not contribute. In the limit $\Lambda \to \infty$, only low-energy states contribute, which mathematically allows us to properly define field operators $\psi(x_j)$ in the low-energy limit.

In terms of the new operators, the Hamiltonian gets a contribution from the expansion around each Fermi point, and reads

$$\begin{aligned} H &\simeq \sum_{k=k_\mathrm{F}-\Lambda}^{k_\mathrm{F}+\Lambda} \varepsilon_k c^\dagger_k c_k + \sum_{k=-k_\mathrm{F}-\Lambda}^{-k_\mathrm{F}+\Lambda} \varepsilon_k c^\dagger_k c_k = \sum_{k=-\Lambda}^{\Lambda} \left[v_\mathrm{F} k c^\dagger_{k_\mathrm{F}+k} c_{k_\mathrm{F}+k} + (-vk) c^\dagger_{-k_\mathrm{F}-k} c_{-k_\mathrm{F}-k} \right] \\ &= \sum_{k>0}^{\Lambda} v_\mathrm{F} \left[k c^\dagger_{k_\mathrm{F}+k} c_{k_\mathrm{F}+k} + (-k) c^\dagger_{k_\mathrm{F}-k} c_{k_\mathrm{F}-k} + (-k) c^\dagger_{-k_\mathrm{F}+k} c_{-k_\mathrm{F}+k} + k c^\dagger_{-k_\mathrm{F}-k} c_{-k_\mathrm{F}-k} \right], \\ &= \sum_{k>0}^{\Lambda} v_\mathrm{F} k \left[\alpha^\dagger_k \alpha_k - \beta_k \beta^\dagger_k - \alpha^\dagger_{-k} \alpha_{-k} + \beta_{-k} \beta^\dagger_{-k} \right]. \end{aligned} \tag{4.34}$$

The operators β_k and $\beta^\dagger_k$ can be switched with the commutators, such that

$$\sum_{k>0} v_\mathrm{F} k \left[\alpha^\dagger_k \alpha_k + \beta^\dagger_k \beta_k - 1 - \alpha^\dagger_{-k} \alpha_{-k} - \beta^\dagger_{-k} \beta_{-k} + 1 \right] \tag{4.35}$$

and the Hamiltonian yields in the continuum limit,

$$H = \frac{L}{2\pi} \int_{-\Lambda}^{\Lambda} \mathrm{d}k \, v_\mathrm{F} |k| \left[\alpha^\dagger(k) \alpha(k) + \beta^\dagger(k) \beta(k) \right], \tag{4.36}$$

which is now written in terms of particle-hole excitation operators and is defined with respect to the non-excited ground state. The boundaries $[+\Lambda, -\Lambda]$ cover the areas around the left and the right Fermi points ($\pm k_\mathrm{F}$).

In position space, the procedure of expanding around both Fermi points amounts to expanding the electron field in slow-varying in space parts,

$$\begin{aligned}\psi(x_j) &\simeq \frac{1}{\sqrt{N}}\left(\sum_{k=k_\mathrm{F}-\Lambda}^{k_\mathrm{F}+\Lambda}+\sum_{k=-k_\mathrm{F}-\Lambda}^{-k_\mathrm{F}+\Lambda}\right)e^{ikx_j}c_k \\ &= \frac{1}{\sqrt{N}}\left[e^{ik_\mathrm{F}x_j}\sum_{k>0}\left(e^{ikx_j}\alpha_k+e^{-ikx_j}\beta_k^\dagger\right)+e^{-ik_\mathrm{F}x_j}\sum_{k<0}\left(e^{ikx_j}\alpha_k+e^{-ikx_j}\beta_k^\dagger\right)\right] \\ &= \frac{1}{\sqrt{a}}e^{ik_\mathrm{F}x_j}\psi_R(x_j)+e^{-ik_\mathrm{F}x_j}\psi_L(x_j). \end{aligned} \tag{4.37}$$

It is written in terms of the left- and right-moving fields $\psi_L(x)$ and $\psi_R(x)$ (we drop the index j for now), defined as

$$\psi_R(x)=\frac{1}{\sqrt{L}}\sum_{k>0}\left(e^{ikx}\alpha_k+e^{-ikx}\beta_k^\dagger\right),\quad \psi_L(x)=\frac{1}{\sqrt{L}}\sum_{k<0}\left(e^{ikx}\alpha_k+e^{-ikx}\beta_k^\dagger\right). \tag{4.38}$$

The fields obey the following anti-commutators

$$\left\{\psi_L(x),\psi_L^\dagger(x')\right\}=\delta(x-x'),\quad \left\{\psi_R(x),\psi_R^\dagger(x')\right\}=\delta(x-x'),\quad \left\{\psi_L(x),\psi_R^\dagger(x')\right\}=0. \tag{4.39}$$

The behaviour of $\psi_L(x)$ and $\psi_R(x)$ is slow-varying relative to the $\exp(ik_\mathrm{F}x)$, because they are defined in the regime where $|k|<<k_\mathrm{F}$. In the continuum limit they read

$$\begin{aligned}\psi_R(x) &= \frac{\sqrt{L}}{2\pi}\int_{k>0}\mathrm{d}k\left[e^{ikx}\alpha(k)+e^{-ikx}\beta^\dagger(k)\right], \\ \psi_L(x) &= \frac{\sqrt{L}}{2\pi}\int_{k<0}\mathrm{d}k\left[e^{ikx}\alpha(k)+e^{-ikx}\beta^\dagger(k)\right]. \end{aligned} \tag{4.40}$$

Time-dependence is added by multiplying with the phase $\exp(-iv|k|t)$, which translates to

$$\begin{aligned}\psi_R(z) &= \frac{\sqrt{L}}{2\pi}\int_{k>0}\mathrm{d}k\left[e^{-kz}\alpha(k)+e^{kz}\beta^\dagger(k)\right], \\ \psi_L(\bar{z}) &= \frac{\sqrt{L}}{2\pi}\int_{k<0}\mathrm{d}k\left[e^{k\bar{z}}\alpha(k)+e^{-k\bar{z}}\beta^\dagger(k)\right], \end{aligned} \tag{4.41}$$

where the coordinates defined in Eq. (4.1) are used. Note that the wavevectors of the left- and right-moving fields are still separated by roughly $2k_\mathrm{F}$. In terms of the left- and right-moving

fields, the total current is defined as

$$\begin{aligned} J &= \int \mathrm{d}x \left[\psi_L^\dagger(x)\psi_L(x) - \psi_R^\dagger(x)\psi_R(x)\right] \\ &= -\int \mathrm{d}x \frac{i}{\sqrt{\pi}} \left[\partial_z \phi_R(z) + \partial_{\bar{z}} \phi_L(\bar{z})\right] = \frac{1}{\sqrt{\pi} v_\mathrm{F}} \int \mathrm{d}x\, \partial_t \Phi(x,t), \end{aligned} \tag{4.42}$$

where time-dependence was introduced to bosonize the expression, and the derivative has been rewritten in real coordinates using Eq. (4.2). Similarly for the total charge, we obtain

$$\begin{aligned} Q &= \int \mathrm{d}x \left[\psi_L^\dagger(x)\psi_L(x) + \psi_R^\dagger(x)\psi_R(x)\right] = \int \mathrm{d}x \frac{i}{\sqrt{\pi}} \left[\partial_z \phi_R(z) - \partial_{\bar{z}} \phi_L(\bar{z})\right] \\ &= -\frac{1}{\sqrt{\pi}} \int \mathrm{d}x\, \partial_x \Phi(x,t) = -\frac{1}{\sqrt{\pi}} \left[\Phi(L) - \Phi(0)\right], \end{aligned} \tag{4.43}$$

where the time-dependence has been taken out in the end by putting $t = 0$.

The Dirac Hamiltonian can be found by using the expansion Eq. (4.37) in Hamiltonian Eq. (4.34),

$$H = -i v_\mathrm{F} \int \mathrm{d}x \left[\psi_R^\dagger(x)\partial_x \psi_R(x) - \psi_L^\dagger(x)\partial_x \psi_L(x)\right]. \tag{4.44}$$

The easiest way to show this is to start from the above and plug in Eq. (4.40). For notational clarity, the $k < 0$ and $k > 0$ indices of the integrals are omitted, $\alpha(k)$ is written as α_k, and when the integrands of the left- and right-moving modes are identical, the second is not shown fully, but indicated by $(\dots)$,

$$\begin{aligned} H &= -i v_\mathrm{F} \frac{L}{(2\pi)^2} \int \mathrm{d}x \Bigg[\int \mathrm{d}k \int \mathrm{d}k' \left(e^{-ikx}\alpha_k^\dagger + e^{ikx}\beta_k\right)(ik') \left(e^{ik'x}\alpha_{k'} - e^{-ik'x}\beta_{k'}^\dagger\right) \\ &\qquad - \int \mathrm{d}k \int \mathrm{d}k' \,(\dots) \Bigg] \\ &= \frac{v_\mathrm{F} L}{(2\pi)^2} \int \mathrm{d}x \Bigg[\int \mathrm{d}k \int \mathrm{d}k'\, k' \big(\alpha_k^\dagger \alpha_{k'} e^{-i(k-k')x} - \alpha_k^\dagger \beta_{k'}^\dagger e^{-i(k+k')x} \\ &\qquad + \beta_k \alpha_{k'} e^{i(k+k')x} - \beta_k \beta_{k'}^\dagger e^{i(k-k')x}\big) - \int \mathrm{d}k \int \mathrm{d}k'\, k' \,(\dots) \Bigg] \\ &= \frac{v_\mathrm{F} L}{2\pi} \Bigg[\int \mathrm{d}k \int \mathrm{d}k'\, k' \big(\alpha_k^\dagger \alpha_{k'} \delta(k-k') - \alpha_k^\dagger \beta_{k'}^\dagger \delta(k+k') \\ &\qquad + \beta_k \alpha_{k'} \delta(k+k') - \beta_k \beta_{k'}^\dagger \delta(k-k')\big) - \int \mathrm{d}k \int \mathrm{d}k'\, k' \,(\dots) \Bigg], \end{aligned}$$

where the Fourier transform of the delta function is used. Now, note that all terms with $\delta(k+k')$ yield zero, as the integrals only cover the positive (or negative, for the left-moving modes) values of k and k', and the combination $(k,-k)$ does not occur. The β_k operators can

be switched, and the two integrals are combined, for which the absolute value of k has to be employed. This gives

$$\begin{aligned} H &= \frac{v_F L}{2\pi}\left[\int_{k>0} \mathrm{d}k\, k\left(\alpha_k^\dagger \alpha_k - \beta_k \beta_k^\dagger\right) - \int_{k<0} \mathrm{d}k\, k\left(\alpha_k^\dagger \alpha_k - \beta_k \beta_k^\dagger\right)\right] \\ &= \frac{v_F L}{2\pi}\left[\int_{k>0} \mathrm{d}k\, k\left(\alpha_k^\dagger \alpha_k + \beta_k^\dagger \beta_k - 1\right) - \int_{k<0} \mathrm{d}k\, k\left(\alpha_k^\dagger \alpha_k + \beta_k^\dagger \beta_k - 1\right)\right] \\ &= \frac{L}{2\pi}\int \mathrm{d}k\, v_F |k| \left(\alpha_k^\dagger \alpha_k + \beta_k^\dagger \beta_k\right), \end{aligned} \tag{4.45}$$

which is identical to Eq. (4.34).

4.3.2 Interactions

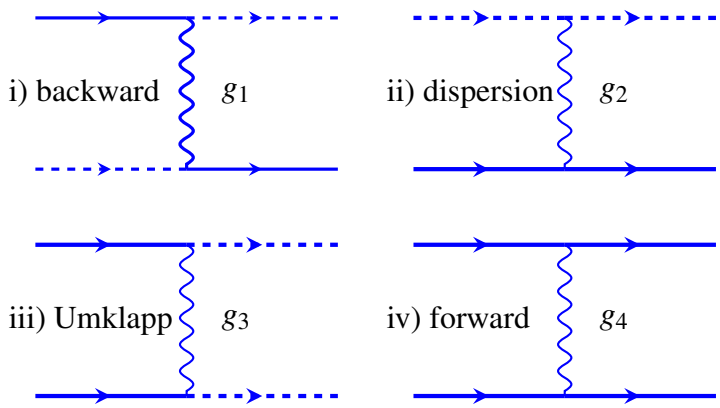

Figure 4.2 Electron-electron interactions in one dimension for right-moving (continuous) and left-moving (dashed) modes. The arrows indicate time. i) Backward scattering; a right-moving electron becomes left-moving and vice versa. ii) Dispersion; (left-) right-moving modes scatter off (right-) left-moving modes. iii) Umklapp; two (left-) right-moving electrons switch directions. iv) Forward scattering; the two particles keep moving in their original directions. In the diagram, spin indices are suppressed. Note that in i) and iii) the incoming electrons have opposed spins ($\uparrow$ and $\downarrow$ or vice versa), whereas in ii) and iv) all combinations of spin orientations of the incoming electrons are allowed. Figure taken from Ref. [56].

The general Hamiltonian of two-body interactions between electrons in one dimension reads

$$H_{int} = \frac{1}{2}\sum_{\sigma,\sigma'}\sum_{k_1,k_2,k_3} V_{\sigma,\sigma'} c_\sigma^\dagger(k_1) c_{\sigma'}^\dagger(k_2) c_{\sigma'}(k_3) c_\sigma(k_4), \tag{4.46}$$

with spin indices $\sigma = \uparrow, \downarrow$, and momentum conservation fixes the value of k_4. In the low-energy limit, all interactions occur close to the Fermi point. Four different types of interactions can be distinghuished: backward, dispersive, Umklapp, and forward scattering, all

graphically represented in Fig. 4.2. Each of them will be briefly discussed. The interactions are written in terms of the field operators $\psi_{a,\sigma}$, with $a = L,R$, and $\sigma = \uparrow,\downarrow$. The densities are denoted by $J_{a,\sigma} = \psi^{\dagger}_{a,\sigma}\psi_{a,\sigma}$. The charge and spin parts are decoupled because of spin-charge separation in 1D. The spinful Bose fields $\Phi_{\uparrow,\downarrow}$, needed to write down the bosonized expression for the interactions, are rewritten into spin and charge combinations

$$\Phi_c = \frac{1}{\sqrt{2}}\left(\Phi_\uparrow + \Phi_\downarrow\right), \quad \Phi_s = \frac{1}{\sqrt{2}}\left(\Phi_\uparrow - \Phi_\downarrow\right). \tag{4.47}$$

Backward scattering

The direction of motion is reversed, but the electrons keep their spin,

$$H_1 = v_{\mathrm{F}} g_1 \sum_\sigma \psi^{\dagger}_{R,\sigma}\psi_{L,\sigma}\psi^{\dagger}_{L,-\sigma}\psi_{R,-\sigma}. \tag{4.48}$$

Applying the bosonization formulas, we find

$$\begin{aligned} H_1 &= \frac{v_{\mathrm{F}} g_1}{(2\pi)^2}\sum_\sigma \eta_{R,\sigma}\eta_{L,\sigma}\eta_{L,-\sigma}\eta_{R,-\sigma}\exp\left[i\sqrt{4\pi}(\phi_{R,\sigma}+\phi_{L,\sigma}-\phi_{L,-\sigma}-\phi_{R,-\sigma})\right] \\ &= \frac{v_{\mathrm{F}} g_1}{(2\pi)^2}\left[\eta_{R,\uparrow}\eta_{L,\uparrow}\eta_{L,\downarrow}\eta_{R,\downarrow}e^{i\sqrt{8\pi}\Phi_s} + \eta_{R,\downarrow}\eta_{L,\downarrow}\eta_{L,\uparrow}\eta_{R,\uparrow}e^{-i\sqrt{8\pi}\Phi_s}\right] \\ &= \frac{v_{\mathrm{F}} g_1}{2\pi^2}\eta_{R,\uparrow}\eta_{L,\uparrow}\eta_{L,\downarrow}\eta_{R,\downarrow}\cos\left(\sqrt{8\pi}\Phi_s\right) = \frac{v_{\mathrm{F}} g_1}{2\pi^2}\cos\left(\sqrt{8\pi}\Phi_s\right), \end{aligned} \tag{4.49}$$

where we have used the anticommuting properties of the Klein factors $\eta_{a,\sigma}$, and the calculation of the Klein factor as shown in Ref. [56].

Dispersion

Density-density interaction of a left- and a right-moving particle. Afterwards, the particles keep moving with their respective directions and spin orientations,

$$H_{2,c} = v_{\mathrm{F}} g_{2,c}\left(J_{R,\uparrow} + J_{R,\downarrow}\right)\left(J_{L,\uparrow} + J_{L,\downarrow}\right), \tag{4.50}$$

$$H_{2,s} = v_{\mathrm{F}} g_{2,s}\left(J_{R,\uparrow} - J_{R,\downarrow}\right)\left(J_{L,\uparrow} - J_{L,\downarrow}\right), \tag{4.51}$$

where $J_{a,\sigma}$ denotes the electronic density. After bosonization, we find for the charge part,

$$H_{2,c} = \frac{v_{\mathrm{F}} g_{2,c}}{\pi}\sum_{\sigma,\sigma'}\partial_z\Phi_\sigma\partial_{\bar{z}}\Phi_{\sigma'} = \frac{2v_{\mathrm{F}} g_{2,c}}{\pi}\partial_z\Phi_c\partial_{\bar{z}}\Phi_c, \tag{4.52}$$

and similarly for the spin part

$$H_{2,s} = \frac{2v_{\mathrm{F}}g_{2,s}}{\pi}\partial_z\Phi_s\partial_{\bar{z}}\Phi_s. \tag{4.53}$$

Umklapp scattering

Two left-moving electrons become right-moving electrons, or vice versa,

$$H_3 = \frac{1}{2}v_{\mathrm{F}}g_3\sum_\sigma\left(\psi^\dagger_{R,\sigma}\psi^\dagger_{R,-\sigma}\psi_{L,\sigma}\psi_{L,-\sigma} + \mathrm{h.c.}\right). \tag{4.54}$$

Similar to the backward scattering, we obtain for the bosonized expression

$$\begin{aligned} H_3 &= \frac{v_{\mathrm{F}}g_3}{2(2\pi)^2}\big[\left(\eta_{R,\uparrow}\eta_{R,\downarrow}\eta_{L,\uparrow}\eta_{L,\downarrow} + \eta_{R,\downarrow}\eta_{R,\uparrow}\eta_{L,\downarrow}\eta_{L,\uparrow}\right) \\ &\quad\times e^{i\sqrt{4\pi}(\phi_{R,\uparrow}+\phi_{R,\downarrow}+\phi_{L,\uparrow}+\phi_{L,\downarrow})} + \mathrm{h.c.}\big] \\ &= \frac{v_{\mathrm{F}}g_3}{(2\pi)^2}\left[\eta_{R,\uparrow}\eta_{R,\downarrow}\eta_{L,\uparrow}\eta_{L,\downarrow}e^{i\sqrt{4\pi}\Phi_c} + \mathrm{h.c.}\right] = \frac{v_{\mathrm{F}}g_3}{2\pi^2}\cos\left(\sqrt{8\pi}\Phi_c\right). \end{aligned} \tag{4.55}$$

Forward scattering

Density-density interaction of two left-moving (right-moving) particles with different spin orientation. Afterwards, the particles keep moving with their respective directions and spin orientations,

$$H_{4,c} = \frac{1}{2}v_{\mathrm{F}}g_{4,c}\left[\left(J_{R,\uparrow}+J_{R,\downarrow}\right)^2 + \left(J_{L,\uparrow}+J_{L,\downarrow}\right)^2\right], \tag{4.56}$$

$$H_{4,s} = \frac{1}{2}v_{\mathrm{F}}g_{4,s}\left[\left(J_{R,\uparrow}-J_{R,\downarrow}\right)^2 + \left(J_{L,\uparrow}-J_{L,\downarrow}\right)^2\right]. \tag{4.57}$$

Similar to the bosonized dispersive scattering, we find that the charge part in terms of Bose fields is given by

$$\begin{aligned} H_{4,c} &= -\frac{v_{\mathrm{F}}g_{4,c}}{2\pi}\left[\left(\partial_z\Phi_\uparrow + \partial_{\bar{z}}\Phi_\downarrow\right)^2 + \left(\partial_{\bar{z}}\Phi_\uparrow + \partial_z\Phi_\downarrow\right)^2\right] \\ &= -\frac{v_{\mathrm{F}}g_{4,c}}{\pi}\left[(\partial_z\Phi_c)^2 + (\partial_{\bar{z}}\Phi_c)^2\right], \end{aligned} \tag{4.58}$$

and similarly for the spin part, we have

$$H_{4,s} = -\frac{v_{\mathrm{F}}g_{4,s}}{\pi}\left[(\partial_z\Phi_s)^2 + (\partial_{\bar{z}}\Phi_s)^2\right]. \tag{4.59}$$

Since the form of the Hamiltonian is the same as the Gaussian Hamiltonian in Eq. (4.26), this type of scattering effectively changes the speed v_F of the excitations.

4.3.3 Luttinger liquid

If one sets the interactions $g_1 = g_3 = 0$, such that the only type of interactions are density-density interactions, the resulting model is called the Luttinger liquid (LL). In bosonized form, the charge and spin degrees of freedom are fully separated:

$$H_{LL} = H_c[\Phi_c] + H_s[\Phi_s], \tag{4.60}$$

with

$$H_\mu = H_{0,\mu} + H_{2,\mu} + H_{4,\mu}, \tag{4.61}$$

where $\mu = c, s$, and

$$H_{0,\mu} = \int \mathrm{d}x \frac{v_\mathrm{F}}{2} \left[\Pi_\mu^2 + (\partial_x \Phi_\mu)^2\right] \tag{4.62}$$

$$H_{2,\mu} = \int \mathrm{d}x - \frac{v_\mathrm{F} g_{2,\mu}}{2} \left[\Pi_\mu^2 - (\partial_x \Phi_\mu)^2\right] \tag{4.63}$$

$$H_{4,\mu} = \int \mathrm{d}x \frac{v_\mathrm{F} g_{4,\mu}}{2} \left[\Pi_\mu^2 + (\partial_x \Phi_\mu)^2\right], \tag{4.64}$$

and combined

$$H_\mu = \int \mathrm{d}x \frac{v_\mu}{2} \left[K_\mu \Pi_\mu^2 + \frac{1}{K_\mu} (\partial_x \Phi_\mu)^2\right], \tag{4.65}$$

with

$$K_\mu = \sqrt{\frac{\pi - g_{2,\mu} + g_{4,\mu}}{\pi + g_{2,\mu} + g_{4,\mu}}}, \quad v_\mu = v_\mathrm{F} \sqrt{\left(1 + \frac{g_{4,\mu}}{\pi}\right)^2 - \left(\frac{g_{2,\mu}}{\pi}\right)^2}, \tag{4.66}$$

where K is called the Luttinger parameter. Observe that $g_2 \neq 0$ strictly decreases the excitation velocity, whereas $g_4 < 0$ decreases the velocity, and $g_4 > 0$ increases the velocity. A non-interacting system has $g_2 = g_4 = 0$ and $K = 1$, repulsive interactions are represented by $g_2, g_4 > 0$ and $K < 1$, and attractive interactions by $g_2, g_4 < 0$ and $K > 1$.

By rescaling the fields as

$$\Phi'_\mu = \frac{1}{\sqrt{K_\mu}} \Phi_\mu, \quad \Pi'_\mu \to \sqrt{K_\mu} \Pi_\mu, \tag{4.67}$$

brings us back to the Gaussian Hamiltonian Eq. (4.28). Therefore, in order to introduce interactions in a non-interacting theory, one only has to perform the reverse scaling of Eq. (4.67), and replace $v_\mathrm{F} \to v_\mu$. In short, an interacting electron theory is mapped to a free

boson theory, with general Luttinger liquid Hamiltonian

$$H_{LL} = \frac{v_{\mathrm{F}}}{2} \int \mathrm{d}x \left[K \Pi^2 + \frac{1}{K} (\nabla \Phi)^2 \right]. \tag{4.68}$$

If one adds Umklapp or backward scattering, this yields an additional cosine term and leads to the sine-Gordon equation, which will be the topic of the next section.

4.3.4 Impurity in the spinless Luttinger liquid

Now that we have discussed the free theory and interactions, we will consider the problem of an impurity in the spinless Luttinger liquid. The scattering process of the impurity can be divided into a forward and backward scattering process. The forward scattering can be transformed into the latter [2], and the latter will be bosonized. The resulting Hamiltonian is the same as the boundary sine-Gordon Hamiltonian. The presented calculation follows Ref. [2]. The Hamiltonian of the impurity scattering problem for spinless electrons is

$$H = H_{LL} + V, \tag{4.69}$$

where H_{LL} is the Luttinger liquid Hamiltonian. Note that in this section electron-electron interactions are not taken into account, only the interaction between the electrons and the impurity. The potential scattering operator is given by

$$V = \int \mathrm{d}x V(x) \psi(x) \psi(x), \tag{4.70}$$

where $V(x)$ represents some nonzero potential, localized in a region of finite radius a. In this calculation we take $V(x) = V\delta(x)$, i.e. the impurity is located at the origin.

The first step is to expand the electron field in slow-varying in space chiral parts, using the expansion Eq. (4.37). Second, the potential scattering operator Eq. (4.70) is divided into a forward and backward scattering part,

$$V = V_{fs} + V_{bs}, \tag{4.71}$$

where

$$V_{fs} = \int \mathrm{d}x V_{fs}(x) \left[\psi_R^\dagger(x) \psi_R(x) + (R \to L) \right], \tag{4.72}$$

while

$$V_{bs} = \int \mathrm{d}x V_{bs}(x) \left[\psi_R^\dagger(x) \psi_L(x) + \mathrm{h.c.} \right]. \tag{4.73}$$

The forward and backscattering amplitudes are related to the original scattering potential $V(x)$ by

$$V_{fs}(x) = V(x), \quad V_{bs}(x) = V(x)e^{2ik_F x}. \tag{4.74}$$

Third, the standard bosonization procedure is used, with help of the relations defined in Table 4.1,

$$\psi_R(x) = \frac{1}{\sqrt{2\pi a}} e^{i\sqrt{4\pi}\phi_R(x)}, \quad \psi_L(x) = \frac{1}{\sqrt{2\pi a}} e^{-i\sqrt{4\pi}\phi_L(x)}, \tag{4.75}$$

with $\phi_{L,R}$ the left- and right-moving Bose fields and a_0 the lattice constant. Together, they constitute the full Bose field

$$\Phi = \phi_L + \phi_R. \tag{4.76}$$

Fourth, interactions between electrons in the conduction band are manually inserted by rescaling the field,

$$\Phi(x) \to \sqrt{K}\Phi(x). \tag{4.77}$$

Here, K denotes the Luttinger liquid parameter. These steps bring us to the Hamiltonian

$$H = H_0[\Phi] + \sqrt{\frac{K}{\pi}} V_{fs} \partial_x \Phi(0) + \frac{V_{bs}}{\pi a} \cos\left[\sqrt{4\pi K}\Phi(0)\right], \tag{4.78}$$

where $H_0[\Phi]$ is the Gaussian Hamiltonian in Eq. (4.28). Because the forward scattering and backscattering processes are independent, the total Hamiltonian can be decomposed into two parts

$$H = H_{fs} + H_{bs}. \tag{4.79}$$

Moreover, they are related to different chiral fields. Consider the decomposition of the Bose field by parity with respect to the origin $x = 0$, written in terms of the left- and right-moving fields of Eq. (4.76),

$$\Phi(x)_\pm = \frac{1}{\sqrt{2}} [\Phi(x) \pm \Phi(-x)] = \phi_{R\pm}(x) + \phi_{L\pm}(x) \tag{4.80}$$

These fields are defined on the semi-axis $x > 0$, and satisfy $\phi_{R\pm}(0) = \phi_{L\pm}(0)$. This allows us to replace these fields by two new chiral right-moving fields, one of them being the even parity combination,

$$\varphi_p(x) = \begin{cases} \phi_{R+}(x) & \text{if } x > 0 \\ \phi_{L+}(-x) & \text{if } x < 0, \end{cases} \tag{4.81}$$

and the other one the odd parity combination

$$\varphi_q(x) = \begin{cases} \phi_{R-}(x) & \text{if } x > 0 \\ \phi_{L-}(-x) & \text{if } x < 0. \end{cases} \tag{4.82}$$

In terms of these new fields, the Bose field at the boundary reads

$$\Phi(0) = \sqrt{2}\varphi_p(0), \quad \partial_x\Phi(0) = \sqrt{2}\partial_x\varphi_q(0). \tag{4.83}$$

Now, Eq. (4.79) can be reformulated in terms of these fields,

$$H_{bs} = H_0[\varphi_p] + \frac{V_{bs}}{\pi a}\cos\left[\sqrt{8\pi K}\varphi_p(0)\right], \quad H_0[\varphi_p] = v\int \mathrm{d}x\,\left[\partial_x\varphi_p(x)\right]^2, \tag{4.84}$$

$$H_{fs} = H_0[\varphi_q] + \sqrt{\frac{2K}{\pi}}V_{fs}\partial_x\varphi_q(0), \quad H_0[\varphi_q] = v\int \mathrm{d}x\,\left[\partial_x\varphi_q(x)\right]^2. \tag{4.85}$$

4.3.5 Chiral and helical Luttinger liquid

The chiral Luttinger liquid contains modes that move either to the right or to the left direction. This means that backscattering of an impurity or by electron-electron interactions is not allowed. Considering only the right-moving mode, the Hamiltonian reads

$$H = \sum_{k>0} v_{\mathrm{F}}k\left(\alpha_k^\dagger\alpha_k + \beta_k^\dagger\beta_k\right), \tag{4.86}$$

and the fermion number is

$$N_F = \sum_{k>0}\left(\alpha_k^\dagger\alpha_k - \beta_k^\dagger\beta_k\right). \tag{4.87}$$

In the chiral case, this number is equivalent to the charge and the current, as all modes in the system move in the same direction. When we consider both the left and the right-moving modes, the Hamiltonian has the Gaussian form of Eq. (4.68). Chiral modes emerge, for instance, at the edge of the two-dimensional electron gas displayed in the integer or fractional quantum Hall effect [65].

There exists another important family of Luttinger liquids, called the helical Luttinger liquid (HLL). It describes one-dimensional conductors with spin-filtered transport [6]. For instance, the right-moving modes solely carry spin up, and the left-moving modes solely spin down, due to the presence of time-reversal symmetry. They have been predicted to exist in 2D edge states in topological insulators (Ref. [65]), 3D arrays of 1D nanowires, 1D semiconductor wires with strong Rashba spin-orbit interaction in an external magnetic field,

and in carbon nanotubes. If a HLL is brought close to a superconductor, it supports Majorana bound states at the edges [66, 67]. In 2015, their existence has been verified experimentally [68].

The linearized non-interacting Hamiltonian is given by

$$H^0_{HLL} = -iv_{\mathrm{F}} \int \mathrm{d}x \left[\psi^\dagger_{R,\uparrow}(x)\partial_x \psi_{R,\uparrow}(x) - \psi^\dagger_{L,\downarrow}(x)\partial_x \psi_{L,\downarrow}(x) \right]. \tag{4.88}$$

We see the similarity with the Dirac Hamiltonian for the Luttinger liquid Eq. (4.25). The strong spin-orbit coupling makes that the spin and chirality properties of the fields coincide. Rewriting the fields in terms of spinless fields makes the spin index redundant. Bosonizing this Hamiltonian, and writing $\Phi = \frac{1}{\sqrt{2}}(\phi_{R\uparrow} + \phi_{L\downarrow})$ and $\Theta = \frac{1}{\sqrt{2}}(\phi_{R\uparrow} - \phi_{L\downarrow})$, we find

$$H_{HLL} = \int \frac{\mathrm{d}x}{2\pi} v \left[\frac{1}{K_{HLL}} (\nabla\Phi)^2 + K_{HLL} (\nabla\Theta)^2 \right], \tag{4.89}$$

where the parameter K_{HLL} accounts for the interactions, and $v = v_{\mathrm{F}}/K_{HLL}$ denotes the velocity in the boson model [69].

The time-reversal symmetry of this system dictates that only two kinds of interactions are allowed: the forward and Umklapp scattering [69]. The Hamiltonian for an impurity at the boundary is rewritten to

$$H = \int \mathrm{d}x \frac{v}{2} \left[\frac{1}{K_{HLL}} (\nabla\Phi)^2 + K_{HLL} (\nabla\Theta)^2 \right] + \frac{v g_3}{2\pi^2} \cos\sqrt{8\pi K_{HLL}}\, \Phi(0), \tag{4.90}$$

where the cosine term is completely induced by the Umklapp term, given in Eq. (4.55), due to the time-reversal symmetry of the system. To account for density-density interactions in the chain, the parameters have been rescaled, such that $v_{\mathrm{F}} \to v$ and $\Phi(z) \to \sqrt{K}\Phi(z)$.

The expressions for the current Eq. (4.42) and charge Eq. (4.43) remain the same for this system, where only the locked spin index has to be added.

4.4 Boundary sine-Gordon model

In this section, we briefly discuss the boundary sine-Gordon (BSG) model. We will see that the BSG Hamiltonian is equivalent to the Hamiltonian describing the backscattering process of an impurity in the chiral spinless Luttinger liquid. For an overview of this theory, see Ref. [70]. Finally, we show that for a particular value of the Luttinger liquid parameter K, the BSG theory supports a zero-energy Majorana mode at the boundary.

4.4.1 Sine-Gordon theory

The sine-Gordon theory has Lagrangian density

$$L = \frac{1}{2}\left[(\partial_t \Phi)^2 + (\partial_x \Phi)^2\right] - 1 + \cos\Phi. \tag{4.91}$$

Its equation of motion is a variation on the standard linear wave equation and is given by

$$\partial_{tt} u(x,t) - \partial_{xx} u(x,t) + \sin u(x,t) = 0. \tag{4.92}$$

Though the equation stems from the 19$^{\text{th}}$ century, the discovery that the equation gives rise to soliton solutions caused it to be a topic of recent interest [71, 72]. The name is a play on the Klein-Gordon equation. The BSG model differs with respect to the sine-Gordon model by the interaction term being present only at the spatial boundary, and not in the bulk. The BSG model is exactly solvable [73].

4.4.2 Partition function of the BSG

The BSG Hamiltonian is given by

$$H_{\text{BSG}} = H_0 + \frac{V_{bs}}{\pi a}\cos\left[\sqrt{4\pi K}\Phi(0)\right]. \tag{4.93}$$

This is equivalent to the Hamiltonian solely describing backscattering off an impurity in the chiral spinless Tomonaga-Luttinger liquid Eq. (4.78). To study the BSG model into more detail, we investigate its action [2]. The partition function for the above Hamiltonian is the partition function Z for a field $\Phi(x,\tau)$,

$$Z = \int \mathrm{D}\Phi(x,\tau) e^{-S_0[\Phi(x,\tau)] - S_1[\Phi(0,\tau)]}, \tag{4.94}$$

where S_0 is the Gaussian action for a free bosonic massless scalar field in a two-dimensional Euclidean space,

$$S_0\left[\Phi(x,\tau)\right] = \frac{v}{2}\int_0^\beta \mathrm{d}\tau \int_{-\infty}^{\infty} \mathrm{d}x \left[(\partial_\tau \Phi)^2 + (\partial_x \Phi)^2\right], \tag{4.95}$$

where β is the inverse temperature $k_B T$, which now also plays the role of the time scale (as mentioned before, we set $\hbar = 1$). S_1 denotes the local action, describing the impurity

potential term at $x = 0$,

$$S_1[\Phi(0,\tau)] = -\frac{V_{bs}}{\pi a}\int_0^\beta \mathrm{d}\tau \cos\left[\sqrt{4\pi K}\Phi(0,\tau)\right]. \tag{4.96}$$

We are primarily interested in the dynamics of the impurity $\Phi(\tau) = \Phi(0,\tau)$, so we have to integrate out all $x \neq 0$ degrees of freedom of the local action. In order to do this, we employ a trick by using a Lagrange multiplier with the auxiliary field $\lambda(\tau)$. This leads us to writing

$$\delta[\Phi(0,\tau) - \Phi(\tau)] = \int \mathrm{D}\lambda(\tau)\exp\left\{i\int_0^\beta \lambda(\tau)\mathrm{d}\tau\,[\Phi(0,\tau) - \Phi(\tau)]\right\}. \tag{4.97}$$

We put its Fourier transform into the partition function and find

$$Z = \int \mathrm{D}\Phi(\tau)e^{-S_1[\Phi(\tau)]}\int \mathrm{D}\lambda(\tau)\exp\left\{-i\int_0^\beta \lambda(\tau)\mathrm{d}\tau\Phi(\tau)\right\}Z[\lambda(\tau)], \tag{4.98}$$

and

$$Z[\lambda(\tau)] = \int \mathrm{D}\Phi(\tau)\exp\left\{-S_0[\Phi(x,\tau)] + i\int_0^\beta \mathrm{d}\tau\lambda(\tau)\Phi(0,\tau)\right\}. \tag{4.99}$$

The general form of the generating functional is

$$Z[\eta(\xi)] = \int \mathrm{D}\phi\exp\left\{-S_0[\phi(\xi)] + \int \mathrm{d}\xi\,\phi(\xi)\eta(\xi)\right\} \tag{4.100}$$

$$= Z[0]\exp\left[\frac{1}{2}\eta(\xi)G(\xi,\xi')\eta(\xi')\right], \tag{4.101}$$

where $G(\xi,\xi')$ is the Green's function, and $\eta(\xi)$ a source field. We identify Eq. (4.99) as exactly such a generating functional with coordinate $\xi = \tau$, source field $\eta(x,\tau) = i\delta(x)\lambda(\tau)$, and using delta functions written as Fourier transforms. Then, Eq. (4.99) gives

$$Z[\lambda(\tau)] = Z[0]\exp\left[-\frac{1}{2\beta}\sum_\omega \lambda(\omega)G_0(\omega)\lambda(-\omega)\right], \tag{4.102}$$

where $G_0(\omega)$ is the Green's function of the Bose field in an infinite system,

$$G_0(\omega) = \int_{-\infty}^{\infty}\mathrm{d}q\frac{1}{2\pi}\frac{1}{v^{-1}\omega^2 + vq^2} = \frac{1}{2|\omega|}. \tag{4.103}$$

Finally, we perform the integration over $\lambda(\tau)$ and find

$$\int \mathrm{D}\lambda(\tau)\exp\left[-i\int \mathrm{d}\tau\lambda(\tau)\Phi(\tau) - \frac{1}{2\beta}\sum_\omega \lambda(\omega)G_0(\omega)\lambda(-\omega)\right] \tag{4.104}$$

$$= \exp\left[\frac{1}{2\beta}\sum_{\omega}\Phi(\omega)G_0(\omega)\Phi(-\omega)\right]. \tag{4.105}$$

The full action then reads

$$S = S_0 + S_1 + \frac{1}{2\beta}\sum_{\omega}\Phi(\omega)G_0(\omega)\Phi(-\omega). \tag{4.106}$$

4.4.3 Majorana mode in the BSG model

For a particular value of the Luttinger parameter K, the boundary sine-Gordon model supports a zero-energy Majorana mode at the edge. We follow here section 27.IV from Ref. [2].

In the particular case $K = \frac{1}{2}$, the boundary sine-Gordon equation Eq. (4.93) has a simple nonperturbative solution. First, the original Hamiltonian is replaced by

$$H_{\mathrm{BSG}} \to \overline{H}_{\mathrm{BSG}} = H_0[\Phi] + \frac{2V_{bs}}{\pi a} s_x \cos\left[\sqrt{4\pi}\Phi(0)\right], \tag{4.107}$$

where $H_0[\Phi]$ denotes the non-interacting bulk part of the Hamiltonian and $s_x = \pm 1/2$ is the x-component of the spin-1/2 operator. This trick is employed to write the theory in terms of a fermionic spinor instead of a bosonic scalar field. Mathematically speaking the Hilbert space is doubled, but the physics of the problem remains the same. Second, the Hamiltonian is re-fermionized,

$$s_+ = d^\dagger \quad (= s_x + i s_y), \tag{4.108}$$

$$\Psi(x) = \frac{1}{\sqrt{2\pi a}} e^{i\pi d^\dagger d} e^{i\sqrt{4\pi}\Phi(x)}, \tag{4.109}$$

where d is a Fermi operator and $\Psi(x)$ is a Fermi field. At this point, the importance of introducing s_x and the exponential of the number operator becomes clear: we have to map a Fermi spinor to a Bose scalar field, so we need to introduce a matrix representation. The Jordan-Wigner type product $d^\dagger d$ serves to ensure the proper commutation relations, and reads

$$d^\dagger d = \begin{pmatrix} 0 & 1-i \\ 1+i & 0 \end{pmatrix}\begin{pmatrix} 0 & 1+i \\ 1-i & 0 \end{pmatrix} = 2\begin{pmatrix} 1 & 0 \\ 0 & 1 \end{pmatrix}. \tag{4.110}$$

Furthermore, $\exp(2\pi i) = 1$, such that the extra exponential does not change the bosonization formula in Eq. (4.109). With the identities in Eqs. (4.108) and (4.109), the Hamiltonian yields

$$\overline{H}_{\mathrm{BSG}} = H_0[\Psi] + \frac{4V_{bs}}{\sqrt{2\pi a}}\frac{1}{2}\left(d^\dagger + d\right)\left[\Psi(0) + \Psi^\dagger(0)\right]. \tag{4.111}$$

Third, we introduce Majorana components of the Fermi fields. The real and imaginary components equal their Hermitian conjugate by construction

$$d = \frac{1}{\sqrt{2}}(v + iw), \tag{4.112}$$

$$\Psi(x) = \frac{1}{\sqrt{2}}\left[\xi(x) + i\zeta(x)\right]. \tag{4.113}$$

The Hamiltonian then becomes

$$\begin{aligned}\overline{H}_{\mathrm{BSG}} &= H_0[\xi,\zeta] + \frac{2V_{bs}}{\sqrt{2\pi a}}\frac{1}{\sqrt{2}}(v + iw + v - iw)\frac{1}{\sqrt{2}}\left[\xi(x) + i\zeta(x) + \xi(x) - i\zeta(x)\right] \\ &= H_0[\xi,\zeta] + \frac{2V_{bs}}{\sqrt{2\pi a}}\frac{1}{\sqrt{2}}2v\frac{1}{\sqrt{2}}2\xi(x) \\ &= H_0[\xi,\zeta] + \frac{2\sqrt{2}}{\sqrt{\pi a}}V_{bs}v\xi(0).\end{aligned} \tag{4.114}$$

Now, following Ref. [74], we show that this edge mode actually is a zero-energy Majorana mode. First, we discretize the theory, with

$$\xi(x) \to \frac{1}{\sqrt{2a}}\xi_j, \quad \zeta(x) \to \frac{1}{\sqrt{2a}}\zeta_j, \tag{4.115}$$

such that

$$\overline{H}_{\mathrm{BSG}} = H_0[\xi_j,\zeta_j] + \frac{2}{\sqrt{\pi a}}V_{bs}v\xi_0. \tag{4.116}$$

We observe that ζ_0 does not appear in the Hamiltonian. The interacting part of the Hamiltonian only depends on ξ_0, such that the ζ_j contribution is decoupled from the impurity. We have that $\zeta_0 = \zeta_0^\dagger$ by construction. Therefore, we recognize ζ_0 as a zero-energy Majorana mode, located on the edge.

Chapter 5

Equivalence between the boundary sine-Gordon theory and Caldeira-Leggett model

5.1 Introduction

In this section, the equivalence between the boundary sine-Gordon theory and the Caldeira-Leggett model for a particle on a one-dimensional lattice with Ohmic bath will be established. First, the field for the calculation is set up and some intuition is provided. Subsequently, the equivalence is shown in three steps. First, the bosonized BSG-Hamiltonian Eq. (4.93) is expanded in terms of bosonic creation and annihilation operators. Second, the Hamiltonian is transformed with a canonical rotation. Third, a mapping between the operators in the BSG Hamiltonian and the variables in the Caldeira-Leggett model is identified. All steps are separately discussed, and correspond to a subsection. The calculation presented here is for the spinless one-dimensional system with both left- and right-moving fermionic modes. The outline for the equivalence is given in Refs. [2, 4].

5.2 Intuitive approach

Action of the Caldeira-Leggett model

Before showing the equivalence, we would like to provide some intuition for the physics behind this mapping. The starting point is the Caldeira-Leggett Lagrangian Eq. (3.3). To study the effect of the dissipation, the degrees of freedom of the bath of harmonic oscillators $\{q_k, \dot{q}_k\}$ are integrated out. As a result, the action of the particle acquires an extra dissipation

term (Ref. [49])

$$S_{\text{diss}} = \int_{-\infty}^{\infty} \mathrm{d}\tau' \int_0^{\beta} \mathrm{d}\tau K(\tau - \tau') x(\tau) x(\tau'), \tag{5.1}$$

with the kernel

$$K(\tau - \tau') = \frac{1}{2\pi} \int_0^{\infty} \mathrm{d}\omega e^{-\omega|\tau - \tau'|} J(\omega), \tag{5.2}$$

and $J(\omega)$ the spectral function, as defined in Eq. (3.16). Note that in this case $m_k = 1$, $\hbar = 1$, and the factor of $1/2$ has been left out. In these equations, the similarity between this action with the dissipation term and the action of the boundary sine-Gordon model Eq. (4.106) already becomes apparent. Note that throughout this chapter, we set $\hbar = 1$.

Particle on a lattice

In order to understand the outcome of the equivalence, we study the localization of the particle due to the interaction with the bath. Consider a particle on a lattice with lattice constant a, such that $x = na$. The Hamiltonian contains only hopping terms and reads

$$H_0[x] = \bar{\omega} \sum_n \left(|na\rangle \langle (n+1)a| + \text{h.c.} \right), \tag{5.3}$$

where $\bar{\omega}$ is the bare tunneling amplitude.

Next, the high- and low-energy degrees of freedom of the environment, which are the bath oscillator frequencies, have to be separated. Generally, those with high energy can follow the particle adiabatically, whereas the low-energy ones cannot adjust to the moving particle, and hence do not influence the kernel. The two regimes are separated by the frequency ω_0, which denotes the actual renormalized tunneling amplitude [75]

$$\omega_0 = \bar{\omega} \left\langle na, \{x_q\} \middle| (n+1)a, \{x_q\} \right\rangle = \bar{\omega} \exp\left[-\frac{a^2}{2\pi} \int_{\omega_0}^{\infty} \frac{\mathrm{d}\omega}{\omega^2} J(\omega) \right]. \tag{5.4}$$

The overlap integral is calculated by using a path integral, with the lattice Hamiltonian and the correction for dissipation. In the Ohmic dissipation regime, the spectral function is linear in ω up to a bath cut-off frequency ω_c, as we encountered in Eq. (3.18). The integral reduces to

$$\omega_0 = \bar{\omega} \exp\left[-\frac{\eta a^2}{2\pi} \int_{\omega_0}^{\omega_c} \frac{\mathrm{d}\omega}{\omega} \right] = \bar{\omega} \exp\left[-\frac{\eta a^2}{2\pi} \ln\left(\frac{\omega_c}{\omega_0} \right) \right] = \bar{\omega} \left(\frac{\omega_0}{\omega_c} \right)^{\alpha}, \tag{5.5}$$

with the dissipation strength characterized by the dimensionless constant

$$\alpha = \frac{\eta a^2}{2\pi}. \tag{5.6}$$

The self-consistent equation for the renormalized tunneling amplitude Eq. (5.5) yields

$$\omega_0 = \begin{cases} \omega_c \left(\frac{\bar{\omega}}{\omega_c}\right)^{\frac{1}{1-\alpha}} & \text{for } \alpha < 1, \\ 0 & \text{for } \alpha > 1. \end{cases} \tag{5.7}$$

The latter property comes from the fact that ω_0 must increase as a function of $\bar{\omega}$, and $\alpha > 1$ would yield decreasing behaviour for increasing ω_0, which is unphysical. Hence, as the dissipation strength α increases, the effective tunneling amplitude decreases. At $\alpha = 1$ there is a crossover, beyond which the tunneling amplitude is zero and therefore the particle is localized. Thus, there are two kinematic regimes for the particle: diffusive motion for $\alpha < 1$, and localized for $\alpha > 1$.

5.3 Mode expansion

The first step for proving the equivalence is to expand the modes in the boundary sine-Gordon Hamiltonian Eq. (4.93), given by

$$H_{\mathrm{BSG}} = H_0 + \frac{V_{bs}}{\pi a} \cos\left[\sqrt{4\pi K}\Phi(0)\right], \tag{5.8}$$

in terms of bosonic creation and annihilation operators. Therefore the mode expansion Eq. (4.19) reads

$$\Phi(x,t) = q + \frac{\pi_0 v t}{L} + \frac{\tilde{\pi}_0 x}{L} + \sum_{n>0} \frac{1}{\sqrt{4\pi n}} \left(a_n^\dagger e^{kz} + a_n e^{-kz} + \bar{a}_n^\dagger e^{k\bar{z}} + \bar{a}_n e^{-k\bar{z}}\right), \tag{5.9}$$

where the Bose field $\Phi(x,t)$ is defined on a circle of circumference L.

Additionally, we define the operator

$$b_k = \frac{a_k + \bar{a}_k}{\sqrt{2}}, \tag{5.10}$$

where the factor of $1/\sqrt{2}$ makes sure the commutators of the operators b_k, $b_k^\dagger$ are normalized,

$$\left[b_k, b_{k'}^\dagger\right] = \delta_{k,k'}, \quad \left[b_k^\dagger, b_{k'}^\dagger\right] = [b_k, b_{k'}] = 0. \tag{5.11}$$

Furthermore, we introduce the rescaled phase variable θ

$$\theta = -\sqrt{4\pi K}\Phi_0, \tag{5.12}$$

where θ corresponds to the full zero mode (i.e. the first term of Eq. (4.19)), and $\Phi_0 \equiv q$, using the notation of Ref. [2]. It satisfies a commutation relation with J, which is the total electron current through the system, and has been introduced in Eq. (4.42),

$$[\theta, J] = 2i. \tag{5.13}$$

The origin of the factor 2 is the counting of the difference between the left- and right-moving modes, where changing the direction of one mode gives a difference of 2 in the current. Moreover, we will see that the bosonic operator J can be interpreted as a coordinate of a particle moving on a lattice with period 2, such that its allowed values are $J = 2n$, with n integer. To achieve the quantization $x \to 2n$, we change the canonical commutation relation $[x, p] = i$ to $[2n, p] = 2i$ to arrive at the above commutator. Note that the needed additional minus sign is a matter of convention.

Finally, the expansion of $\Phi(z)$ is evaluated at $z = 0$. This means that the impurity is located at the spatial boundary and is static, which yields

$$\Phi(0) = -\frac{\theta}{\sqrt{4\pi K}} + \sum_{k>0} \frac{1}{\sqrt{kL}} \left(b_k + b_k^\dagger \right). \tag{5.14}$$

The mode expansion can now be used in the Hamiltonian.

5.3.1 Cosine interaction

We plug the Fourier mode expansion Eq. (5.14) into the cosine term of Eq. (5.8), and find

$$\frac{V_{bs}}{\pi a} \cos[\sqrt{4\pi K}\Phi(0)] = \frac{V_{bs}}{\pi a} \cos\left[-\theta + \sum_{k>0} \sqrt{\frac{4\pi K}{kL}} \left(b_k + b_k^\dagger \right) \right]. \tag{5.15}$$

5.3.2 Non-interacting part

The Gaussian part of Eq. (5.8) is expanded, so that we find the bosonized Luttinger Hamiltonian (1D chain of non-interacting fermions), as found in the seminal work by Haldane [11].

Our starting point is the Gaussian Hamiltonian Eq. (4.26). We calculate the derivatives

$$\partial_z\Phi = -\frac{iP}{2L} + \sum_{k>0}\sqrt{\frac{k}{2L}}\left(a_k^\dagger e^{kz} - a_k e^{-kz}\right),$$
$$\partial_{\bar{z}}\Phi = -\frac{i\bar{P}}{2L} + \sum_{k>0}\sqrt{\frac{k}{2L}}\left(\bar{a}_k^\dagger e^{k\bar{z}} - \bar{a}_k e^{-k\bar{z}}\right),$$

their squares being

$$\begin{aligned}(\partial_z\Phi)^2 &= (\partial_z\Phi)^\dagger(\partial_z\Phi)\\ &= \left(\frac{P}{2L}\right)^2 + \sum_{k>0,k'>0}\frac{\sqrt{kk'}}{2L}\Big(a_k a_{k'}^\dagger e^{-(k-k')z} - a_k^\dagger a_{k'}^\dagger e^{(k+k')z}\\ &\quad - a_k a_{k'} e^{-(k+k')z} + a_k^\dagger a_{k'} e^{(k-k')z}\Big),\end{aligned} \tag{5.16}$$

$$\begin{aligned}(\partial_{\bar{z}}\Phi)^2 &= \left(\frac{\bar{P}}{2L}\right)^2 + \sum_{k>0,k'>0}\frac{\sqrt{kk'}}{2L}\Big(\bar{a}_k \bar{a}_{k'}^\dagger e^{-(k-k')\bar{z}} - \bar{a}_k^\dagger \bar{a}_{k'}^\dagger e^{(k+k')\bar{z}}\\ &\quad - \bar{a}_k \bar{a}_{k'} e^{-(k+k')\bar{z}} + \bar{a}_k^\dagger \bar{a}_{k'} e^{(k-k')\bar{z}}\Big).\end{aligned} \tag{5.17}$$

The double sums and exponentials are handled with the Fourier transform of a delta function

$$\delta_{k,k'} = \frac{1}{L}\int_0^L \mathrm{d}x\, e^{i(k-k')x}. \tag{5.18}$$

Note that all terms with factor $\delta_{k,-k'}$ become zero, since the summation only covers the positive values of k and k', and the combination $(k,-k)$ does not occur. The parts with operators a_n of both squared derivatives are put together, and reduce to

$$\begin{aligned}&\sum_{k>0}\frac{k}{2}\left(a_k a_k^\dagger + a_k^\dagger a_k + \bar{a}_k\bar{a}_k^\dagger + \bar{a}_k^\dagger\bar{a}_k\right) = \sum_{k>0}\frac{k}{2}\left(a_k a_k^\dagger + a_k^\dagger a_k + a_{-k}a_{-k}^\dagger + a_{-k}^\dagger a_{-k}\right)\\ &= \sum_k \frac{|k|}{2}\left(2a_k^\dagger a_k + 1\right) = \sum_k |k|\left(a_k^\dagger a_k + \frac{1}{2}\right),\end{aligned} \tag{5.19}$$

where $\bar{a}_k = a_{-k}$ is written out and the commutator $\left[a_k, a_k^\dagger\right] = 1$ is employed. Note that the second term does not depend on the bosonic operators, and represents an irrelevant shift in energy. Therefore, it is often left out in literature. Here, we keep the term, since it will be part of the mapping.

Since the first term of Eq. (5.16) does not depend explicitly on x, integration over x yields an extra factor L. The zero modes are rewritten with Eq. (4.24), such that

$$P^2 + \bar{P}^2 = (\pi_0 + \tilde{\pi}_0)^2 + (\pi_0 - \tilde{\pi}_0)^2 = 2\left(\pi_0^2 + \tilde{\pi}_0^2\right). \tag{5.20}$$

The full expanded Hamiltonian then reads

$$H = \frac{v}{2L}(\pi_0^2 + \tilde{\pi}_0^2) + v\sum_k |k| \left(a_k^\dagger a_k + \frac{1}{2}\right), \tag{5.21}$$

where v is the renormalized velocity of the model, given in Eq. (4.66).

The zero mode terms can be related to the charge Q and the electric current J. By using Eq. (4.43) and the Fourier-mode expansion Eq. (4.19), the charge reads

$$Q = -\frac{1}{\sqrt{\pi}}\left[\Phi(L,t) - \Phi(0,t)\right] = \frac{\tilde{\pi}_0}{\sqrt{\pi}}. \tag{5.22}$$

Similarly, by using Eq. (4.42) and the mode expansion Eq. (4.19), the current J reads

$$J = \frac{1}{\sqrt{\pi}v}\int \mathrm{d}x \partial_t \Phi(x,t) = \frac{\pi_0}{\sqrt{\pi}}, \tag{5.23}$$

where is used the property that $\Phi(x,t)$ is defined on a circle of circumference L, and therefore the only difference between $\Phi(0,t)$ and $\Phi(L,t)$ is in the value of the zero mode of the expansion.

The final Hamiltonian becomes

$$H = \frac{\pi v}{2L}(J^2 + Q^2) + v\sum_k |k| \left(a_k^\dagger a_k + \frac{1}{2}\right). \tag{5.24}$$

Scaling the Luttinger parameter $\sqrt{K}$ in the field Φ yields an extra factor K in the second term. The first part of the second term is rewritten by redefining $b_k = (a_k + a_{-k})/\sqrt{2}$,[1]

$$\begin{aligned}\sum_k |k| a_k^\dagger a_k = \ldots &= \sum_{k>0} k\left(a_k^\dagger a_k + a_{-k}^\dagger a_{-k} + a_k^\dagger a_{-k} + a_{-k}^\dagger a_k\right) \\ &= \sum_{k>0} k(a_k^\dagger + a_{-k}^\dagger)(a_k + a_{-k}) = \sum_{k>0} k b_k^\dagger b_k.\end{aligned} \tag{5.25}$$

[1] Please note that at the time of writing, this step is still unclear. We expect the calculation from Ref. [2] to be correct and follow its steps.

Interactions can be introduced by scaling the parameter K, with $J \to \sqrt{K}J$, and $Q \to \sqrt{K}^{-1}Q$. This can be seen from their derivation in Eqs. (5.22) and (5.23). Furthermore, in the above Hamiltonian, we set the charge of the excited states $Q = 0$, and because we work in the low-energy limit, this term may be neglected.

By taking all separate terms together, the expanded Hamiltonian reads

$$H_{\mathrm{BSG}} = \sum_{k>0} vk\left(b_k^\dagger b_k + \frac{1}{2}\right) + \frac{\pi K v}{2L}J^2 + \frac{V_{bs}}{\pi a}\cos\left[-\theta + \sum_{k>0}\sqrt{\frac{4\pi K}{kL}}\left(b_k + b_k^\dagger\right)\right]. \tag{5.26}$$

5.4 Rotation of basis

In the second step, the canonical transformation

$$U_{\mathrm{CL}} = \exp\left\{\frac{i}{2}\sqrt{4\pi K}\left[\Phi(0) - \Phi_0\right]J\right\} = \exp\left[i\sum_{k>0}\sqrt{\frac{\pi K}{kL}}\left(b_k + b_k^\dagger\right)J\right], \tag{5.27}$$

is used, and the Hamiltonian is transformed in the following way

$$\overline{H}_{\mathrm{BSG}} = U_{\mathrm{CL}} H_{\mathrm{BSG}} U_{\mathrm{CL}}^\dagger. \tag{5.28}$$

To calculate the rotation, the Baker-Campbell-Hausdorff formula is employed,

$$e^X Y e^{-X} = Y + [X,Y] + \frac{1}{2!}[X,[X,Y]] + \frac{1}{3!}[X,[X,[X,Y]]] + \ldots. \tag{5.29}$$

The required commutators are then calculated with Eq. (5.11) and give

$$\begin{aligned}\left[b_k + b_k^\dagger, -b_{k'}^\dagger + b_{k'}\right] &= -\left[b_k, b_{k'}^\dagger\right] + \left[b_k, b_{k'}\right] - \left[b_k^\dagger, b_{k'}^\dagger\right] + \left[b_k^\dagger, b_{k'}\right] \\ &= -\delta_{k,k'} + 0 - 0 - \delta_{k,k'} = -2\delta_{k,k'},\end{aligned} \tag{5.30}$$

$$\begin{aligned}\left[b_k + b_k^\dagger, b_{k'}^\dagger + b_{k'}\right] &= \left[b_k, b_{k'}^\dagger\right] + \left[b_k, b_{k'}\right] + \left[b_k^\dagger, b_{k'}^\dagger\right] + \left[b_k^\dagger, b_{k'}\right] \\ &= \delta_{k,k'} + 0 + 0 - \delta_{k,k'} = 0,\end{aligned} \tag{5.31}$$

$$\begin{aligned}\left[b_k, b_{k'}^\dagger b_{k'}\right] &= b_k b_{k'}^\dagger b_{k'} - b_{k'}^\dagger b_{k'} b_k = (\delta_{k,k'} + b_{k'}^\dagger b_k) b_{k'} - b_{k'}^\dagger b_{k'} b_k \\ &= \delta_{k,k'} b_{k'} + b_{k'}^\dagger b_{k'} b_k - b_{k'}^\dagger b_{k'} b_k = b_{k'}\delta_{k,k'},\end{aligned} \tag{5.32}$$

$$\begin{aligned}\left[b_k^\dagger, b_{k'}^\dagger b_{k'}\right] &= b_k^\dagger b_{k'}^\dagger b_{k'} - b_{k'}^\dagger b_{k'} b_k^\dagger = b_{k'}^\dagger b_k^\dagger b_{k'} - b_{k'}^\dagger b_{k'} b_k^\dagger \\ &= b_{k'}^\dagger (b_{k'} b_k^\dagger - \delta_{k,k'}) - b_{k'}^\dagger b_{k'} b_k^\dagger = -b_{k'}^\dagger \delta_{k,k'}, \end{aligned} \tag{5.33}$$

and

$$[b_k, J] = \left[b_k^\dagger, J\right] = 0, \quad [b_k, \theta] = \left[b_k^\dagger, \theta\right] = 0, \quad [\theta, J] = 2i. \tag{5.34}$$

5.4.1 First and second term

The rotation of the first term is given by

$$\begin{aligned} &U_{\mathrm{CL}} \sum_{k>0} vk \left(b_k^\dagger b_k + \frac{1}{2}\right) U_{\mathrm{CL}}^\dagger = \\ &\exp\Bigg[\underbrace{i \sum_{k>0} \sqrt{\frac{\pi K}{kL}} \left(b_k + b_k^\dagger\right) J}_{\equiv \xi}\Bigg] \underbrace{\sum_{k>0} vk \left(b_k^\dagger b_k + \frac{1}{2}\right)}_{\equiv \Delta} \exp\Bigg[\underbrace{-i \sum_{k>0} \sqrt{\frac{\pi K}{kL}} \left(b_k + b_k^\dagger\right) J}_{\equiv \xi}\Bigg]. \end{aligned} \tag{5.35}$$

We introduce the abbreviations ξ and Δ for notational ease and apply the Baker-Campbell-Hausdorff formula given in Eq. (5.29). In order to do so, the commutators between ξ and Δ have to be calculated, up until the order in which the result commutes with ξ. Subsequent higher-order contributions will vanish. Note that all commutators with the ground state energy $vk/2$ also vanish. The first commutator then reads

$$\begin{aligned} &\left[i \sum_{k>0} \sqrt{\frac{\pi K}{kL}} \left(b_k + b_k^\dagger\right) J\,,\, \sum_{k'>0} vk' b_{k'}^\dagger b_{k'}\right] = i \sum_{k>0} \sum_{k'>0} \sqrt{\frac{\pi K}{kL}} vk' J \left[b_k + b_k^\dagger\,,\, b_{k'}^\dagger b_{k'}\right] \\ &= i \sum_{k>0} \sum_{k'>0} \sqrt{\frac{\pi K}{kL}} vk' J \left(-b_{k'}^\dagger \delta_{k,k'} + b_{k'} \delta_{k,k'}\right) = i \sum_{k>0} \sqrt{\frac{\pi k K}{L}} vJ \left(-b_k^\dagger + b_k\right). \end{aligned} \tag{5.36}$$

The second commutator reads

$$\begin{aligned} &\frac{1}{2}\left[i \sum_{k>0} \sqrt{\frac{\pi K}{kL}} \left(b_k + b_k^\dagger\right) J\,,\, i \sum_{k'>0} \sqrt{\frac{\pi k' K}{L}} vJ \left(-b_{k'}^\dagger + b_{k'}\right)\right] \\ &= -\sum_{k>0} \sum_{k'>0} \frac{\pi K v}{2L} \sqrt{\frac{k'}{k}} J^2 \left[b_k + b_k^\dagger\,,\, -b_{k'}^\dagger + b_{k'}\right] \\ &= -\sum_{k>0} \sum_{k'>0} \frac{\pi K v}{2L} \sqrt{\frac{k'}{k}} J^2 \left(-2\delta_{k,k'}\right) = \sum_{k>0} \frac{\pi K v}{L} J^2. \end{aligned} \tag{5.37}$$

Since J commutes with itself and b_k, higher-order commutators will be zero. Thus, the complete expression becomes[2]

$$\begin{aligned} &U_{\mathrm{CL}} \sum_{k>0} vk \left(b_k^\dagger b_k + \frac{1}{2} \right) U_{\mathrm{CL}}^\dagger \\ &= \sum_{k>0} vk \left(b_k^\dagger b_k + \frac{1}{2} \right) + i \sum_{k>0} \sqrt{\frac{\pi k K}{L}} vJ \left(-b_k^\dagger + b_k \right) + \sum_{k>0} \frac{\pi K v}{L} J^2. \end{aligned} \tag{5.38}$$

The second term of the backscattering Hamiltonian transforms trivially, as J commutes with itself and the bosonic field operators

$$\left[i \sum_{k>0} \sqrt{\frac{\pi K}{kL}} \left(b_k + b_k^\dagger \right) J \,,\, \frac{\pi K v}{2L} J^2 \right] = 0. \tag{5.39}$$

Therefore, we have

$$U_{\mathrm{CL}} \frac{\pi K v}{2L} J^2 U_{\mathrm{CL}}^\dagger = \frac{\pi K v}{2L} J^2. \tag{5.40}$$

5.4.2 Third term

The third term of the backscattering boundary sine-Gordon Hamiltonian Eq. (5.8) transforms as

$$\begin{aligned} &U_{\mathrm{CL}} \frac{V_{bs}}{\pi a} \cos \left[-\theta + \sum_{k>0} \sqrt{\frac{4\pi K}{kL}} \left(b_k + b_k^\dagger \right) \right] U_{\mathrm{CL}}^\dagger \\ &= \exp \Bigg[\underbrace{ i \sum_{k>0} \sqrt{\frac{\pi K}{kL}} \left(b_k + b_k^\dagger \right) J }_{\equiv \xi} \Bigg] \frac{V_{bs}}{\pi a} \cos \Bigg[-\theta + \underbrace{ \sum_{k>0} \sqrt{\frac{4\pi K}{kL}} \left(b_k + b_k^\dagger \right) }_{\equiv \chi} \Bigg] \\ &\quad \times \exp \Bigg[\underbrace{ -i \sum_{k>0} \sqrt{\frac{\pi K}{kL}} \left(b_k + b_k^\dagger \right) J }_{\equiv \xi} \Bigg], \end{aligned} \tag{5.41}$$

where we have introduced the abbreviations ξ and χ for notational clarity.

To calculate this expression, we rewrite the cosine as

$$\cos(x) = \frac{1}{2} \left(e^{ix} + e^{-ix} \right). \tag{5.42}$$

[2] Note that in Ref. [2] the summation covers all values of k, and the first term should contain an extra factor vk to match the mapping. These seem to be typos, as they are not consistent with the above calculations.

The irrelevant prefactor is now left out of the calculation for clarity. Symbolically, the goal of this step is to calculate

$$e^{\xi}e^{i(-\theta+\chi)}e^{-\xi}+e^{\xi}e^{i(+\theta-\chi)}e^{-\xi}, \tag{5.43}$$

where ξ, χ, and θ are generic variables, with the first two defined above. In order to combine the exponentials, one must use the Zassenhaus formula for two possibly noncommutative operators X,Y [56],

$$e^{tX+tY}=e^{tX}e^{tY}e^{-\frac{t^2}{2!}[X,Y]}e^{\frac{t^3}{3!}(2[Y,[X,Y]]+[X,[X,Y]])}\dots \tag{5.44}$$

We have that

$$[\theta,\chi]\propto[\theta,b_k]+\left[\theta,b_k^{\dagger}\right]=0, \tag{5.45}$$

$$\begin{aligned}[\xi,\theta]&=\left[i\sum_{k>0}\sqrt{\frac{\pi K}{kL}}\left(b_k+b_k^{\dagger}\right)J\,,\,\theta\right]=i\sum_{k>0}\sqrt{\frac{\pi K}{kL}}\left(b_k+b_k^{\dagger}\right)[J\,,\,\theta]\\&=i\sum_{k>0}\sqrt{\frac{\pi K}{kL}}\left(b_k+b_k^{\dagger}\right)(-2i)=2\sum_{k>0}\sqrt{\frac{\pi K}{kL}}\left(b_k+b_k^{\dagger}\right),\end{aligned} \tag{5.46}$$

$$[\theta,[\xi,\theta]]=0, \tag{5.47}$$

$$[\xi,[\xi,\theta]]=2i\sum_{k>0}\sum_{k'>0}\frac{\pi K}{L}\sqrt{\frac{1}{kk'}}J\left[b_k+b_k^{\dagger},b_{k'}+b_{k'}^{\dagger}\right]=0, \tag{5.48}$$

$$\begin{aligned}[\xi,\chi]&=\left[i\sum_{k>0}\sqrt{\frac{\pi K}{kL}}\left(b_k+b_k^{\dagger}\right)J\,,\,\sum_{k'>0}\sqrt{\frac{4\pi K}{k'L}}\left(b_{k'}+b_{k'}^{\dagger}\right)\right]\\&=i\sum_{k>0}\sum_{k'>0}\frac{2\pi K}{L}\sqrt{\frac{1}{kk'}}J\left[b_k+b_k^{\dagger},b_{k'}+b_{k'}^{\dagger}\right]=0.\end{aligned} \tag{5.49}$$

From these results, it can be seen that subsequent higher-order commutators vanish as well. This implies that the Zassenhaus formula for our case reduces to

$$e^{tX}e^{tY}=e^{tX+tY}e^{\frac{t^2}{2!}[X,Y]}=e^{tX+tY+\frac{t^2}{2!}[X,Y]}. \tag{5.50}$$

Now, we will evaluate the expression in Eq. (5.43). By writing out symbolically the outcome of the first exponential of the cosine,

$$\begin{aligned}
&\exp(\xi)\exp(-i\theta+i\chi)\exp(-\xi)\\
&=\exp(\xi)\exp(-i\theta)\exp\left(i\chi-\xi+\frac{i}{2}\cancelto{0}{[\chi,-\xi]}\right)\\
&=\exp(\xi)\exp\left(-i\theta+i\chi-\xi+\cancelto{0}{\frac{i}{2}[-\theta,\chi]}+\frac{i}{2}[-\theta,-\xi]\right)\\
&=\exp\left(\xi-i\theta+i\chi-\xi+\frac{i}{2}[\theta,\xi]+\frac{1}{2}[\xi,-i\theta]+\cancelto{0}{\frac{1}{2}[\xi,i\chi]}+\cancelto{0}{\frac{1}{2}[\xi,-\xi]}+\cancelto{0}{\frac{1}{4}[\xi,i[\theta,\xi]]}\right)\\
&=\exp\left(-i\theta+i\chi+i[\theta,\xi]\right),
\end{aligned}\tag{5.51}$$

which reads in full

$$\exp\left[-i\theta+i\sum_{k>0}\sqrt{\frac{4\pi K}{kL}}\left(b_k+b_k^\dagger\right)-2i\sum_{k>0}\sqrt{\frac{\pi K}{kL}}\left(b_k+b_k^\dagger\right)\right]=\exp\left(-i\theta\right).\tag{5.52}$$

By proceeding similarly for the second part, we find

$$\begin{aligned}
&\exp(\xi)\exp(+i\theta-i\chi)\exp(-\xi)\\
&=\exp(\xi)\exp(i\theta)\exp\left(-i\chi-\xi+\frac{1}{2}\cancelto{0}{[-i\chi,-\xi]}\right)\\
&=\exp(\xi)\exp\left(i\theta-i\chi-\xi+\cancelto{0}{\frac{1}{2}[i\theta,-\chi]}+\frac{1}{2}[i\theta,-\xi]\right)\\
&=\exp\left(\xi+i\theta-i\chi-\xi-\frac{1}{2}[i\theta,\xi]+\frac{1}{2}[\xi,i\theta]+\cancelto{0}{\frac{1}{2}[\xi,-i\chi]}+\cancelto{0}{\frac{1}{2}[\xi,-\xi]}-\cancelto{0}{\frac{1}{4}[\xi,[i\theta,\xi]]}\right)\\
&=\exp\left(i\theta-i\chi-i[\theta,\xi]\right),
\end{aligned}\tag{5.53}$$

which reads in full

$$\exp\left[i\theta-i\sum_{k>0}\sqrt{\frac{4\pi K}{kL}}\left(b_k+b_k^\dagger\right)+2i\sum_{k>0}\sqrt{\frac{\pi K}{kL}}\left(b_k+b_k^\dagger\right)\right]=\exp\left(i\theta\right).\tag{5.54}$$

By combining both results, the rotated third term yields

$$\frac{V_{bs}}{2\pi a}\left(e^{i\theta}+e^{-i\theta}\right)=\frac{V_{bs}}{\pi a}\cos\theta.\tag{5.55}$$

5.4.3 Result

After the rotation, the boundary sine-Gordon Hamiltonian Eq. (5.8) reads

$$\begin{aligned}\overline{H}_{\mathrm{BSG}} = &\sum_{k>0} vk\left(b_k^\dagger b_k + \frac{1}{2}\right) + i\sum_{k>0}\sqrt{\frac{\pi kK}{L}}vJ\left(-b_k^\dagger + b_k\right) + \sum_{k>0}\frac{\pi Kv}{L}J^2 \\ &+ \frac{\pi Kv}{2L}J^2 + \frac{V_{bs}}{\pi a}\cos\theta. \end{aligned} \tag{5.56}$$

5.5 Mapping the variables

The above Hamiltonian can be understood as a particle on a lattice with a dissipative term. This identification also encourages us to welcome a new interpretation of J, that is, to view it as a coordinate of a fictitious particle. In order to do this, the bosonic creation and annihilation operators $b_k^\dagger$, b_k must be rewritten in terms of the bath oscillator coordinates x_k, p_k. The variables corresponding to the harmonic oscillators are identified by

$$\begin{aligned} x_k = \frac{i}{\sqrt{2m_k\omega_k}}(b_k - b_k^\dagger), \quad p_k = \sqrt{\frac{m_k\omega_k}{2}}(b_k^\dagger + b_k), \\ C_k = \sqrt{\frac{2\pi Kv^3k^2m_k}{L}}, \quad \omega_k = vk. \end{aligned} \tag{5.57}$$

5.5.1 First and second term

The first three terms of Eq. (5.56) give the contribution of the Caldeira-Leggett model Eq. (3.3). The first term corresponds to the energy of the harmonic oscillators in the bath. The second (first commutator) yields the coupling between the particle and the bath, and the third (second commutator) gives us the counter-term. This is most easily seen by working backwards,

$$\begin{aligned}\frac{1}{2m_k}p_k^2 + \frac{1}{2}m_k\omega_k^2x_k^2 &= \frac{vk}{4}(b_k^\dagger + b_k)(b_k + b_k^\dagger) + \frac{-i^2v^2k^2}{4vk}(b_k - b_k^\dagger)(b_k^\dagger - b_k) \\ &= \frac{vk}{2}\left(b_k^\dagger b_k + b_k b_k^\dagger\right) = \frac{vk}{2}\left(2b_k^\dagger b_k + 1\right) = vkb_k^\dagger b_k + \frac{vk}{2}, \end{aligned} \tag{5.58}$$

$$C_kx_kJ = -i\sqrt{\frac{2\pi Kv^3k^2m_k}{2m_kvkL}}(b_k^\dagger - b_k)J = -i\sqrt{\frac{\pi Kk}{L}}v(b_k^\dagger - b_k)J, \tag{5.59}$$

$$\frac{C_k^2}{2m_k\omega_k^2}J^2 = \frac{2\pi K v^3 k^2 m_k}{2m_k v^2 k^2 L}J^2 = \frac{\pi K v}{L}J^2. \tag{5.60}$$

The full identified expression reads

$$U_{\mathrm{CL}} \sum_{k>0} vk \left(b_k^\dagger b_k + \frac{1}{2}\right) U_{\mathrm{CL}}^\dagger = \sum_{k>0} \left(\frac{p_k^2}{2m_k} + \frac{1}{2}m_k\omega_k^2 x_k^2 + C_k x_k J + \frac{C_k^2}{2m_k\omega_k^2}J^2\right), \tag{5.61}$$

which now clearly equals the bath contribution in the Caldeira-Leggett model, Eq. (3.3).

The second term does not need to mapped, as it is already formulated in terms of J.

5.5.2 Third term

Continuous model

By remembering the definition $\theta = -\sqrt{4\pi K}\Phi_0$, we start our inspection from the following identity

$$\frac{V_{bs}}{\pi a}\cos\theta = \frac{V_{bs}}{\pi a}\cos\left(\sqrt{4\pi K}\Phi_0\right). \tag{5.62}$$

Assuming θ to be small, we expand the interaction term as

$$\frac{V_{bs}}{\pi a}\cos\theta \simeq \frac{V_{bs}}{\pi a}\left(1 + \frac{1}{2}\theta^2\right) = \frac{V_{bs}}{\pi a}\left(1 + 2\pi K\Phi_0^2\right), \tag{5.63}$$

where the constant gives just a change in the energy spectrum and thus is ignored.

In the mapping of the Caldeira-Leggett term in Eq. (5.61), we have seen that J plays the role of coordinate of a fictitious particle. If we look at the commutator $[\theta, J] = 2i$, we notice the similarity with the position-momentum Heisenberg commutator $[x, p] = \hbar i$ (throughout here, $\hbar = 1$). Recognizing J as a coordinate, the commutator then implies that we can view θ as some kind of momentum. However, since we lack a summation over θ, it is more appropriate to view the contribution quadratic in θ as a mass term, which here causes a shift in the energy spectrum.

Discrete lattice

It has been shown in Ref. [2] that the discrete case corresponds to an effective hopping term between two lattice sites J and $J+2$, where the lattice spacing 2 comes from the commutator in Eq. (5.13). The cosine interaction is written as

$$\frac{V_{bs}}{\pi a}\left[|J\rangle\langle J+2| + \text{h.c.}\right] \tag{5.64}$$

As we originally have defined J as the total electron current in Eq. (4.42), this also has a physical interpretation in terms of the original picture in the Luttinger liquid. If we count the number of left- and right-moving modes, their difference gives us the total electron current J. Any scattering event or interaction that leads to annihilating a left (right-)moving mode, and creating a right (left)-moving mode, changes the numerical value of J by 2. This allows us to think of the above term as a transition between two states, characterized by the numbers J and $J+2$.

5.5.3 Final result

The final result of this section is

$$\bar{H}_{\mathrm{BSG}} = \frac{V_{bs}}{\pi a}\left[|J\rangle\langle J+2| + \mathrm{h.c.}\right] + \frac{\pi K v}{2L}J^2 + \sum_k \left(\frac{p_k^2}{2m_k} + \frac{1}{2}m_k\omega_k^2 x_k^2 + C_k x_k J + \frac{C_k^2}{2m_k\omega_k^2}J^2\right). \tag{5.65}$$

Comparing the above with the tunneling Hamiltonian in Eq. (5.3), we observe that the scaled backscattering potential $V_{bs}/\pi a$ plays the role of the bare tunneling amplitude $\bar{\omega}$. The second term, which goes with the squared 'coordinate' J^2, acts a weak harmonic potential, which vanishes in the limit $L \to \infty$.

As a corollary of Eq. (5.57), we calculate the spectral function Eq. (3.16), which is required to be Ohmic (linear in ω),

$$\begin{aligned} J(\omega) &= \frac{\pi}{2}\sum_k \frac{C_k^2}{m_k\omega_k}\delta(\omega-\omega_k) = \frac{\pi}{2}\sum_k \frac{2\pi K v^3 k^2}{vkL}\delta(\omega-\omega_k) \\ &= \frac{\pi^2 vK}{L}\sum_k \omega_k\delta(\omega-\omega_k). \end{aligned} \tag{5.66}$$

In order to evaluate the delta function, we replace the summation by an integral,

$$\sum_k \to \frac{L}{2\pi}\int \mathrm{d}k, \tag{5.67}$$

and use $\delta(ax) = \delta(x)/|a|$, such that

$$J(\omega) = \frac{\pi^2 vK}{L}\frac{L}{2\pi}\int \mathrm{d}k\, k\,\delta\left(\frac{\omega}{v}-k\right) = \frac{\pi K}{2}\omega = \eta\omega, \tag{5.68}$$

where the friction coefficient reads $\eta = \frac{\pi K}{2}$. The dissipation strength Eq. (5.6) for lattice constant 2 then becomes

$$\alpha = \frac{2\eta}{\pi} = K. \tag{5.69}$$

5.6 Conclusion

In the above, we have shown that the boundary sine-Gordon theory is exactly equivalent to the Caldeira-Leggett theory for a particle on a one-dimensional lattice with an Ohmic bath. The coordinate of the dissipative particle is identified as the total electron current J, and its mass term is represented by the backscattering potential.

In fact, in chapter 4, it has been shown that the spinless double chiral Luttinger liquid with an impurity can be bosonized into the boundary sine-Gordon theory. Therefore, the equivalence extends to this system as well. As a consequence, this might imply that every Luttinger theory that can be rewritten into a BSG, also can be reformulated in terms of a dissipative system with a particle moving in one dimension. This is analyzed in the next chapter.

The different parameter regions of the BSG and CL models map to each other in the following way. Remember that in section 5.2, two kinematic regimes for the particle have been found: diffusive motion for dissipation strength $\alpha < 1$, and localized for $\alpha > 1$. With the identification Eq. (5.69), we connect this to the Luttinger parameter K. If $K < 1$, the backscattering is relevant, and J is delocalized. If $K > 1$, the backscattering is irrelevant, and J is localized. This means that if there is no backscattering, the total current is conserved. When the backscattering is switched on, the total current becomes a dynamic variable.

In Refs. [3, 4], an equivalence very similar to the one discussed in this chapter has been shown. Starting from the Caldeira-Leggett model with linear coupling to a fermionic particle in a periodic potential, the same rotation U_{CL} is applied. The resulting Hamiltonian is diagonal in the momentum basis of the fermionic creation and annihilation operators. Fixing a particular value of the particle momentum in the Hamiltonian then yields the BSG equation. There are three main differences with the approach in this chapter. First, we work from the BSG theory to the Caldeira-Leggett model instead of the other way around. Second, in the current work a more general definition of the field $\Phi(x,t)$ is used, since the zero modes are not taken into account in the literature. Third, the summation over all momenta yields a hopping in the full chain, whereas here a hopping between two states is found. These references have been found shortly before the end of this research project. It would be very interesting to reconcile both approaches, since only the form used in this work can be written as a Luttinger-liquid theory.

Chapter 6

Extension to the helical Luttinger liquid

6.1 Introduction

In chapter 4, the spinless double chiral Luttinger liquid with an impurity has been bosonized into the boundary sine-Gordon equation. In chapter 5, the equivalence between the boundary sine-Gordon equation and a particle on a one-dimensional chain with dissipation has been shown. In the last chapter, it has been remarked that therefore every Luttinger theory that can be rewritten into a BSG, also can be reformulated in terms of a dissipative system with a particle moving in one dimension. In this chapter, we extend this equivalence to the helical Luttinger liquid. Note that throughout this chapter, we set $\hbar = 1$.

6.2 Helical Luttinger liquid

The helical Luttinger liquid, introduced in section 4.3.5, contains both left- and right-moving fermionic modes, and the spin index is locked to the direction of motion. For example, all left-moving modes have spin up, and all right-moving modes have spin down. Bosonized, it yields a Gaussian Hamiltonian, given in Eq. (4.89), and with an Umklapp interaction at the boundary, it yields the boundary sine-Gordon equation, given in Eq. (4.90),

$$H_{HLL} = \int \mathrm{d}x\, v \left[\frac{1}{K} (\nabla\Phi)^2 + K(\nabla\Theta)^2 \right] + \frac{v g_3}{2(\pi a)^2} \cos\left[\sqrt{4\pi K}\, \Phi(0) \right], \tag{6.1}$$

where we defined

$$\Phi(z,\bar{z}) = \phi_{R,\uparrow}(z) + \phi_{L,\downarrow}(\bar{z}), \quad \Theta(z,\bar{z}) = \phi_{R,\uparrow}(z) - \phi_{L,\downarrow}(\bar{z}). \tag{6.2}$$

Note that these definitions change with a factor of $1/\sqrt{2}$ compared to those in Eq. (4.89). This specific choice makes sure that we start with the same boundary sine-Gordon equation as in Chapter 5. The assignment of spin indices to a direction of motion is arbitrary and this specific choice does not affect the calculation. This last expression is the starting point for this section, in which we will show the correspondence to the system of a dissipative particle on a lattice, analogously to that of the spinless Luttinger liquid in Chapter 5.

Mode expansion

We start with the mode expansion

$$\Phi(x,t) = q + \frac{\pi_0 v t}{L} + \frac{\tilde{\pi}_0 x}{L} + \sum_{k>0} \frac{1}{\sqrt{2kL}} \left(a^\dagger_{k,\uparrow} e^{kz} + a_{k,\uparrow} e^{-kz} + a^\dagger_{-k,\downarrow} e^{k\bar{z}} + a_{-k,\downarrow} e^{-k\bar{z}} \right), \quad (6.3)$$

which is exactly Eq. (4.19), but with additional spin indices. The creation and annihilation operators satisfy the commutation rules

$$\left[a_{k,\uparrow}, a^\dagger_{k',\uparrow} \right] = \delta_{k,k'}, \quad \left[a_{-k,\downarrow}, a^\dagger_{-k',\downarrow} \right] = \delta_{k,k'}, \quad \left[a_{k,\uparrow}, a^\dagger_{-k',\downarrow} \right] = 0. \quad (6.4)$$

The expressions for the current and the charge are calculated as before in Eqs. (4.42) and (4.43), respectively, and give

$$\begin{aligned} J &= \int \mathrm{d}x \left[\psi^\dagger_{L,\downarrow}(x) \psi_{L,\downarrow}(x) - \psi^\dagger_{R,\uparrow}(x) \psi_{R,\uparrow}(x) \right] \\ &= -\int \mathrm{d}x \frac{i}{\sqrt{\pi}} \left[\partial_z \phi_{R,\uparrow}(z) + \partial_{\bar{z}} \phi_{L,\downarrow}(\bar{z}) \right] = \frac{1}{\sqrt{\pi} v_\mathrm{F}} \int \mathrm{d}x \, \partial_t \Phi(x,t) = \frac{\pi_0}{\sqrt{\pi}}, \end{aligned} \quad (6.5)$$

$$\begin{aligned} Q &= \int \mathrm{d}x \left[\psi^\dagger_{L,\downarrow}(x) \psi_{L,\downarrow}(x) + \psi^\dagger_{R,\uparrow}(x) \psi_{R,\uparrow}(x) \right] = \int \mathrm{d}x \frac{i}{\sqrt{\pi}} \left[\partial_z \phi_{R,\uparrow}(z) - \partial_{\bar{z}} \phi_{L,\downarrow}(\bar{z}) \right] \\ &= -\frac{1}{\sqrt{\pi}} \int \mathrm{d}x \, \partial_x \Phi(x,t) = -\frac{1}{\sqrt{\pi}} \left[\Phi(L) - \Phi(0) \right] = \frac{\tilde{\pi}_0}{\sqrt{\pi}}, \end{aligned} \quad (6.6)$$

where time-dependence was introduced to bosonize the expression, and the derivative has been rewritten in real coordinates with Eq. (4.2). Furthermore, we denote the spin down operator by $a_{-k,\downarrow} = \bar{a}_k$, analogous to the procedure in Chapter 5, such that

$$b_k = \frac{a_{k,\uparrow} + a_{-k,\downarrow}}{\sqrt{2}} = \frac{a_k + \bar{a}_k}{\sqrt{2}}, \quad k > 0, \quad (6.7)$$

satisfying the commutation relations

$$\left[b_k, b_{k'}^\dagger\right] = \delta_{k,k'}, \quad [b_k, b_{k'}] = \left[b_k^\dagger, b_{k'}^\dagger\right] = 0. \tag{6.8}$$

If we rewrite the Hamiltonian Eq. (6.1) with the expansion in Eq. (6.3), we use that[1]

$$\begin{aligned}
&\sum_{k>0} k\left(a_{k,\uparrow}^\dagger a_{k,\uparrow} + a_{-k,\downarrow}^\dagger a_{-k,\downarrow} + 1\right) = \dots \\
&\quad = \sum_{k>0} k\left(a_{k,\uparrow}^\dagger a_{k,\uparrow} + a_{-k,\downarrow}^\dagger a_{-k,\downarrow} + a_{k,\uparrow}^\dagger a_{-k} + a_{-k,\downarrow}^\dagger a_{k,\uparrow} + \frac{1}{2}\right) \\
&\quad = \sum_{k>0} k\left(a_{k,\uparrow}^\dagger + a_{-k,\downarrow}^\dagger\right)\left(a_{k,\uparrow} + a_{-k,\downarrow}\right) + \frac{k}{2} = \sum_{k>0} k\left(b_k^\dagger b_k + \frac{1}{2}\right),
\end{aligned} \tag{6.9}$$

such that the expanded Hamiltonian reads

$$H = \sum_{k>0} vk\left(b_k^\dagger b_k + \frac{1}{2}\right) + \frac{\pi K v}{2L} J^2 + \frac{v g_3}{2(\pi a)^2} \cos\left[-\theta + \sum_{k>0} \sqrt{\frac{4\pi K}{kL}}\left(b_k + b_k^\dagger\right)\right], \tag{6.10}$$

which is exactly Eq. (5.26), the expanded Hamiltonian employed in Chapter 5.

Rotation of basis and mapping

The commutators given in Eq. (6.8) determine the outcome of the rotation of basis. They behave exactly in the same way as in section 5.4, so that the rotation gives the same result, and we can use the same mapping as before. We then arrive at

$$\overline{H}_{HLL} = \frac{v g_3}{2\pi a}\left[|J\rangle\langle J+2| + \text{h.c.}\right] + \frac{\pi K v}{2L} J^2 + \sum_k \left(\frac{p_k^2}{2m_k} + \frac{1}{2} m_k \omega_k^2 x_k^2 + C_k x_k J + \frac{C_k^2}{2m_k\omega_k^2} J^2\right). \tag{6.11}$$

6.3 Conclusion

We have shown that the helical Luttinger liquid is equivalent to a particle hopping on a one-dimensional lattice, which is in contact with a harmonic oscillator bath.

Generally speaking, we have seen that the required Hamiltonian for the correspondence is a boundary sine-Gordon Hamiltonian, i.e. a Gaussian Hamiltonian, with an interaction in the form of a cosine of the field Φ at the boundary. Any physical system giving rise to this kind of theory may be mapped in the same way, as long the commutation relations between

[1] Similar to Chapter 5, this step is currently unclear. We proceed analogously to the calculation in Ref. [2].

the bosonic field operators are satisfied. For the spinless Luttinger liquid, an impurity at the boundary or an Umklapp scattering at the boundary corresponds to the BSG theory. For the spinful Luttinger liquid, one has to take into account the spin-charge separation. If one takes a spinful Luttinger liquid with backward and Umklapp interaction at the boundary, this system will correspond to a double system of dissipative particles. For the helical Luttinger liquid, an impurity at the boundary or Umklapp does the trick, as we have seen in this chapter. For all equivalences concerned, the characteristics of the Luttinger liquid are preserved in the dissipative system and emerge in the system parameters v and K, as defined in Eq. (4.66).

Chapter 7

Extension to the sine-Gordon theory

7.1 Introduction

In Chapter 5, we have shown the equivalence between the boundary sine-Gordon theory and a dissipative particle on a lattice. The particular form of the basis rotation used makes sure that the Gaussian contribution can be interpreted as a Caldeira-Leggett bath and a weak harmonic potential. The cosine interaction at the boundary can be interpreted as hopping terms between two lattice sites. Now, one can wonder if the full sine-Gordon theory also may be mapped. The Gaussian part will still yield the Caldeira-Leggett bath, but the cosine interaction may yield another kind of lattice. This chapter shows the calculation of the cosine term, and discusses its interpretation in terms of a dissipative particle on a lattice. Note that throughout this chapter, we set $\hbar = 1$.

7.2 Equivalence in the sine-Gordon theory

The sine-Gordon Hamiltonian for a semi-infinite chain reads

$$H_{\mathrm{SG}} = H_0 + \frac{\mu}{\pi a}\int \mathrm{d}x \cos\left[\sqrt{4\pi K}\Phi(z)\right], \tag{7.1}$$

where H_0 is the Gaussian Hamiltonian introduced in Eq. (4.65),

$$H_0 = \int \mathrm{d}x \frac{v}{2}\left[K\Pi^2 + \frac{1}{K}(\partial_x\Phi)^2\right]. \tag{7.2}$$

It can be derived from the Lagrangian density given in Eq. (4.91), where μ denotes the interaction strength. Since the proof of equivalence for H_0 will go exactly as in Chapter 5, yielding

the Caldeira-Leggett contribution given in Eq. (5.61) and the weak harmonic potential given in Eq. (5.40), we will focus here instead solely on the cosine term.

7.2.1 Mode expansion

We use the same mode expansion as before, given in Eq. (4.19). The zero modes are expressed as current and charge with Eqs. (5.23) and (5.22). This gives

$$\Phi(x,t) = q + \frac{\sqrt{\pi}Jvt}{L} + \frac{\sqrt{\pi}Qx}{L} + \sum_{n>0} \frac{1}{\sqrt{4\pi n}} \left(a_n^\dagger e^{kz} + a_n e^{-kz} + \bar{a}_n^\dagger e^{k\bar{z}} + \bar{a}_n e^{-k\bar{z}} \right). \tag{7.3}$$

The cosine term reads, assigning symbolical abbreviations for later calculational use,

$$\cos\left[\sqrt{4\pi K}\Phi(x,t)\right] \equiv \cos\left(-\Theta + \Omega\right), \tag{7.4}$$

where Θ denotes the three zero mode terms, and Ω entails the k-dependence,

$$\begin{aligned} \Theta &\equiv -\sqrt{4\pi K}\left(q + \frac{\sqrt{\pi}Jvt}{L} + \frac{\sqrt{\pi}Qx}{L} \right), \\ \Omega &\equiv \sum_{k>0} \sqrt{\frac{2\pi K}{kL}} \left(a_k^\dagger e^{kz} + a_k e^{-kz} + \bar{a}_k^\dagger e^{k\bar{z}} + \bar{a}_k e^{-k\bar{z}} \right). \end{aligned} \tag{7.5}$$

7.2.2 Basis rotation

We use the same unitary rotation matrix as before in section 5.4,

$$U_{\mathrm{CL}} = \exp\left[i \sum_{k>0} \sqrt{\frac{\pi K}{kL}} \left(b_k + b_k^\dagger \right) J \right] \equiv \exp(\xi), \tag{7.6}$$

where ξ denotes the argument of the exponential. The Hamiltonian is transformed as follows,

$$\overline{H}_{\mathrm{SG}} = U_{\mathrm{CL}} H_{\mathrm{SG}} U_{\mathrm{CL}}^\dagger. \tag{7.7}$$

This procedure ensures that H_0 gives again the Caldeira-Leggett bath and the weak harmonic potential, as calculated in section 5.4. However, the calculation for the cosine interaction term has to be done explicitly. Symbolically, this amounts to calculating

$$\exp\left(\xi\right) \cos\left(-\Theta + \Omega\right) \exp\left(-\xi\right). \tag{7.8}$$

In order to do so, we use the Baker-Campbell-Hausdorff formula

$$e^X Y e^{-X} = Y + [X,Y] + \frac{1}{2!}[X,[X,Y]] + \frac{1}{3!}[X,[X,[X,Y]]] + \ldots. \tag{7.9}$$

In addition to the commutators in section 5.4, we need the following commutators

$$\begin{aligned}
&[b_k, a_{k'}] = \left[b_k^\dagger, a_{k'}^\dagger\right] = 0, \\
&\left[b_k, a_{k'}^\dagger\right] = -\left[b_k^\dagger, a_{k'}\right] = \frac{1}{\sqrt{2}}\left(\delta_{k,k'} + \delta_{k,-k'}\right), \\
&[\Theta, J] = [\theta, J] = 2i, \\
&\left[a_k^{(\dagger)}, J\right] = \left[a_k^{(\dagger)}, Q\right] = \left[a_k^{(\dagger)}, q\right] = 0,
\end{aligned} \tag{7.10}$$

and for later use, we calculate

$$\begin{aligned}
&\sum_{k>0}\sum_{k'>0}\left[a_k^\dagger e^{kz} + a_k e^{-kz} + \bar{a}_k^\dagger e^{k\bar{z}} + \bar{a}_k e^{-k\bar{z}}, b_{k'} + b_{k'}^\dagger\right] \\
&= \sum_{k>0}\sum_{k'>0} e^{kz}\left[a_k^\dagger, b_{k'}\right] + e^{-kz}\left[a_k, b_{k'}^\dagger\right] + e^{k\bar{z}}\left[\bar{a}_k^\dagger, b_{k'}\right] + e^{-k\bar{z}}\left[\bar{a}_k, b_{k'}^\dagger\right] \\
&= \sum_{k>0}\sum_{k'>0}\frac{1}{\sqrt{2}}\left(\delta_{k,k'} + \delta_{k,-k'}\right)\left(-e^{kz} + e^{-kz} - e^{k\bar{z}} + e^{-k\bar{z}}\right) \\
&= \sum_{k>0}\left(-e^{kz} + e^{-kz} - e^{k\bar{z}} + e^{-k\bar{z}}\right) = \sum_{k>0} e^{v\tau}\left(-e^{-ikx} + e^{ikx} - e^{ikx} + e^{-ikx}\right) \\
&= \sum_{k>0} e^{v\tau} \times 0 = 0,
\end{aligned} \tag{7.11}$$

where we used the relations in Eq. (4.1), and the fact that in the summations over $k, k' > 0$ the combination $(k, -k')$ does not occur. Furthermore, we have that

$$[\xi, \Theta] = i\sum_{k>0}\sqrt{\frac{\pi K}{kL}}\left(b_k + b_k^\dagger\right) [J, \Theta] = 2\sum_{k>0}\sqrt{\frac{\pi K}{kL}}\left(b_k + b_k^\dagger\right), \tag{7.12}$$

$$[\xi, [\xi, \Theta]] \propto \left[b_k + b_k^\dagger, b_{k'} + b_{k'}^\dagger\right] = 0, \tag{7.13}$$

$$[\Theta, [\xi, \Theta]] = 0, \tag{7.14}$$

$$[\Omega,[\xi,\Theta]] = \sum_{k>0}\sum_{k'>0}\sqrt{\frac{\pi K}{2kL}}\sqrt{\frac{\pi K}{k'L}}\left[a_k^\dagger e^{kz} + a_k e^{-kz} + \bar{a}_k^\dagger e^{k\bar{z}} + \bar{a}_k e^{-k\bar{z}}, b_{k'} + b_{k'}^\dagger\right]$$
$$= \sum_{k>0}\sum_{k'>0}\frac{\pi K}{\sqrt{2kk'}L\sqrt{2}}\left(\delta_{k,k'} + \delta_{k,-k'}\right)\left(-e^{kz} + e^{-kz} - e^{k\bar{z}} + e^{-k\bar{z}}\right) = 0, \quad (7.15)$$

$$[\xi,-\xi] \propto \left[b_k + b_k^\dagger, b_{k'} + b_{k'}^\dagger\right] = 0, \quad (7.16)$$

$$[\Theta,\Omega] = 0, \quad (7.17)$$

$$[\xi,\Omega] = i\sum_{k>0}\sum_{k'>0}\sqrt{\frac{\pi K}{kL}}\sqrt{\frac{\pi K}{2k'L}}\left[b_k + b_k^\dagger, a_{k'}^\dagger e^{k'z} + a_{k'}e^{-k'z} + \bar{a}_{k'}^\dagger e^{k'\bar{z}} + \bar{a}_{k'}e^{-k'\bar{z}}\right]$$
$$= i\sum_{k>0}\sum_{k'>0}\frac{\pi K}{\sqrt{2kk'}L\sqrt{2}}\left(\delta_{k,k'} + \delta_{k,-k'}\right)\left(e^{kz} - e^{-kz} + e^{k\bar{z}} - e^{-k\bar{z}}\right) = 0, \quad (7.18)$$

such that subsequent higher-order commutators will vanish. This implies that for the current calculation, the Zassenhaus formula reduces to

$$e^{tX}e^{tY} = e^{tX+tY}e^{\frac{t^2}{2!}[X,Y]} = e^{tX+tY+\frac{t^2}{2!}[X,Y]}. \quad (7.19)$$

Now, we set to the task of evaluating the expression in Eq. (7.8). The cosine is written as the sum of two exponentials. The first term yields, symbolically,

$$\begin{aligned}
&\exp(\xi)\exp(-i\Theta + i\Omega)\exp(-\xi)\\
&= \exp(\xi)\exp(-i\Theta)\exp\left(i\Omega - \xi + \frac{1}{2}\cancelto{0}{[i\Omega,-\xi]}\right)\\
&= \exp(\xi)\exp\left(-i\Theta + i\Omega - \xi + \frac{1}{2}\cancelto{0}{[-i\Theta,i\Omega]} + \frac{1}{2}[-i\Theta,-\xi]\right)\\
&= \exp\left(\xi - i\Theta + i\Omega - \xi + \frac{1}{2}[i\Theta,\xi] + \frac{1}{2}[\xi,-i\Theta]\right.\\
&\qquad \left. + \frac{1}{2}[\xi,i\Omega] + \frac{1}{2}\cancelto{0}{[\xi,-\xi]} + \frac{1}{4}\cancelto{0}{[\xi,[i\Theta,\xi]]}\right)\\
&= \exp\left(-i\Theta + i\Omega + i[\Theta,\xi]\right).
\end{aligned} \quad (7.20)$$

By substituting the symbols with Eqs. (7.5) and (7.6), we find

$$\exp\left[i\sqrt{4\pi K}\Phi(z) - 2i\sum_{k>0}\sqrt{\frac{\pi K}{kL}}\left(b_k + b_k^\dagger\right)\right] = \exp\left\{i\sqrt{4\pi K}\left[\Phi(z) - \Phi(0) + \Phi_0\right]\right\}, \tag{7.21}$$

where in the last part the expansion of $\Phi(z)$ at $z = 0$ is employed, given by Eq. (5.14).

We proceed similarly for the second part of the cosine, and find, compared to the above, a relative minus sign in the exponential. Together they are recombined into a cosine. The full expression from Eq. (7.8) reads

$$\cos\left\{\sqrt{4\pi K}\left[\Phi(z) - \Phi(0) + \Phi_0\right]\right\} = \cos\left\{\sqrt{4\pi K}\left[\Phi(z \neq 0) + \Phi_0\right]\right\}. \tag{7.22}$$

After the rotation, we find an expression with $\Phi(z \neq 0)$, while the field at the boundary changes from $\Phi(0)$ to the zero mode Φ_0. As a sanity check, note that if we take $z = 0$ in the result, we find exactly the term we found in the previous section for the rotated BSG.

The fact that the boundary field $\Phi(0)$ emerges in the rotated full sine-Gordon Hamiltonian might, at first glance, seem odd, because the sine-Gordon Hamiltonian contained no information about the boundary. However, this information originates from the particular form of the rotation matrix U_{CL}, given in Eq. (5.27). It has already been stressed that this precise form is needed to arrive at the Caldeira-Leggett bath. It contains J, which has a nontrivial commutator with the zero mode term Φ_0. Applied to the sine-Gordon theory, this causes the boundary term to be present after the rotation.

7.2.3 Mapping the variables

In Chapter 5, we have focused on the interpretation of the boundary edge mode. For simplicity, we now consider only the bulk part, and propose an interpretation in terms of the fictitious coordinate J. By re-fermionizing the interaction, we arrive at

$$\frac{\mu}{\pi a}\cos\left[\sqrt{4\pi K}\Phi(z \neq 0)\right] \to \mu\left[\psi_L^\dagger(x)\psi_R(x) + \psi_R^\dagger(x)\psi_L(x)\right], \tag{7.23}$$

where $\psi_L(x)$ and $\psi_R(x)$ correspond to the left- and right-moving fermionic modes in the bulk. If we count the number of left- and right-moving modes, their difference gives us the total electron current J. This means that the above hopping term changes the numerical value of J by 2 for every hopping event. This allows us to think of the above term as a transition between two states, characterized by the numbers J and $J+2$. Since the integral covers the

entire chain, we arrive at

$$\mu \sum_J \left(|J\rangle \langle J+2| + \text{h.c.} \right), \tag{7.24}$$

which is simply the standard Hamiltonian for a particle hopping on a one-dimensional lattice, with position J and lattice constant 2, and tunneling amplitude μ, given in Eq. (5.3).

The rotated bulk sine-Gordon Hamiltonian, by using the results in Eqs. (5.40) and (5.61) for the Gaussian part, is then given by

$$\overline{H}_{\text{SG}} = \mu \sum_J \left(|J\rangle \langle J+2| + \text{h.c.} \right) + \frac{\pi K v}{2L} J^2 + \sum_k \left(\frac{p_k^2}{2m_k} + \frac{1}{2} m_k \omega_k^2 x_k^2 + C_k x_k J + \frac{C_k^2}{2m_k \omega_k^2} J^2 \right). \tag{7.25}$$

It describes a system of a particle hopping on a one-dimensional chain with dissipation, given by an Ohmic Caldeira-Leggett bath, subject to a weak harmonic potential.

Chapter 8

Conclusion and outlook

In this thesis, we set out with the question: how can dissipation on a lattice, represented by the Caldeira-Leggett formalism, be connected to the appearance of zero-energy Majorana modes in a fermionic chain? The answer to this comes in three parts. First, Luttinger liquids with several types of interactions or impurities can be bosonized into a sine-Gordon theory. If the interaction or impurity is localized at the boundary, this reduces to the boundary sine-Gordon theory. Second, the boundary sine-Gordon and sine-Gordon theories can be mapped to a system with a dissipative particle on a lattice, using a mode expansion and a canonical transformation, where the dissipation is modelled as an Ohmic Caldeira-Leggett bath. Third, in the boundary sine-Gordon theory, a zero-energy Majorana mode appears at the boundary for a Luttinger parameter $K = \frac{1}{2}$.

Elaborating on the above, we have shown that Luttinger liquids with left- and right-moving modes can be bosonized into a Gaussian Hamiltonian with interactions. In this scheme, density-density type interactions yield a rescaling of theory parameters K and v_{F}. Adding other kinds of interactions, or an impurity, gives rise to an additional cosine in the bosonized Hamiltonian. Together, they take the form of (boundary) sine-Gordon theories. After the mapping, the transformed Gaussian part can be interpreted as a Caldeira-Leggett bath of harmonic oscillators, and a weak harmonic potential. The cosine interaction yields after fermionization a hopping term. Summarizing, the Luttinger liquid for electrons in one-dimension maps to a dissipative particle on a one-dimensional lattice. Any terms leading to a cosine interaction in the bosonic picture generate hopping terms for the particle. This includes the helical Luttinger liquid, which describes edge states in two-dimensional time-reversal invariant topological insulators. In this thesis, the calculation of the equivalence for the helical Luttinger liquid to the dissipative system, and the generalization of the equivalence to the full sine-Gordon theory, represent new work with respect to the literature.

A few problems remain before the equivalence can be put to work. First, the exact interpretation of the zero modes in the rotated interaction terms is not fully understood. In particular, in the mappings from both the boundary sine-Gordon and sine-Gordon theory, at this point the mapping from the cosine interaction term to the hopping terms on a discrete lattice can be understood intuitively, but not be made precise mathematically. Second, Refs. [3, 4] relate the boundary sine-Gordon theory to a particle on a periodic potential. However, their approach does not include the zero mode in the Fourier-mode expansion, necessary to describe a massless Bose field. Also, they write a summation over the momentum that appears in the cosine interaction. This summation prevents the mapping to a Luttinger liquid. Further study of the correspondence may connect these ideas to the more general approach in Ref. [2], in the sense that here the zero mode is included and that this formulation can be mapped to the Luttinger liquid. Combining the general approach of the latter and the lattice description of the former will be an important achievement, because in this way the equivalence between the Luttinger liquid and Caldeira-Leggett model may be made exact.

Before discussing possible implications of this work, the importance of dissipation has to be stressed. Experimentally, it is practically impossible to simulate a system as truly isolated from its environment. However, dissipation also can be taken advantage of. The first possible implication of the equivalence between the dissipative and Luttinger models is its use in studying the latter system. Currently, free electron systems can be simulated in experimental set-ups of cold atoms. Simulating strongly correlated systems, however, is not possible with the current technology. The correspondence may help in clarifying our understanding of the Luttinger liquid by increasing the possibilities for its experimental realizations.

Second, regarding possible applications, the study of dissipation in topological materials is an ongoing quest. The main goal is to experimentally observe zero-energy Majorana modes, and see if these are topologically protected. A good understanding of dissipation and its effect on these modes is essential for the development of topological quantum information. It has been proposed to use dissipation to engineer Majorana modes at the edges of a one-dimensional chain of electrons, using the Lindblad formalism [1]. In the current work, if the Cooper pairs that give rise to the superconducting gap in the Kitaev Hamiltonian can be incorporated into the description, the Kitaev chain can be coupled to a Caldeira-Leggett bath. Eventually, the results of Ref. [1] might be reproduced out of this formalism. Also, the action of a bosonized Kitaev chain written in Majorana operators and a thermal bath has been studied [76], and it might be very interesting to map this system to a Luttinger liquid and study the behaviour of the zero-energy Majorana modes at its edges.

Third, the equivalence that has been central in this thesis has been applied to the helical Luttinger liquid, but may apply to many other forms of the Luttinger liquid as well, as long

they can be bosonized into a sine-Gordon Hamiltonian. Also other forms of the sine-Gordon may be mapped. For example, cosine interactions depending on the dual Bose field also may be studied, so-called self-dual sine-Gordon models [77]. Since different kind of interactions in the sine-Gordon picture lead to different dissipative systems, extensions of this equivalence may allow to emulate the physics of systems that are difficult to probe experimentally by using many kinds of dissipative systems. Moreover, the particular form of rotation and mapping can be topics of further research. The currently employed rotation and mapping yield the Caldeira-Leggett bath out of a Gaussian Hamiltonian. One can imagine that other unitary transformations exist, for example, that give a Caldeira-Leggett bath that consists of two-state systems, uses a non-Ohmic spectral function, or couples nonlinearly to the main system. In this way, different models of dissipation may be mapped, and the equivalence may be generalized beyond the bath of harmonic oscillators in the Caldeira-Leggett formalism.

In conclusion, the field of condensed-matter physics remains a rich and expanding field of both experimental and theoretical physics, and is an excellent example of the wondrous character of Nature.

Chapter 9

Nederlandse samenvatting

Zoals Pablo Picasso schildert, proberen theoretisch natuurkundigen de wereld te schetsen: het doel is om in een paar penseelstreken het wezenlijke gedrag van de natuur te vangen. Dit is een precair evenwicht: worden er teveel effecten meegenomen, dan wordt het systeem te complex om op te lossen, maar worden er teveel eigenschappen weggelaten, dan benadert het model de werkelijkheid niet meer. Het opstellen van zo'n theorie kan op twee analytische manieren. Allereerst, door de relevante energieën te nemen bij elkaar te nemen, de zogenaamde Hamiltoniaan, en daar de exacte bewegingsvergelijkingen uit af te leiden. Het aantal systemen waarvoor dit kan is zeer gering. Gelukkig is er één model dat bijzonder vaak in de natuur voorkomt en dat ook exact op te lossen is: de harmonische oscillator, waarbij het belangrijkste kenmerk is dat alle energieën een kwadratische vorm hebben. Een voorbeeld hiervan is een eenvoudige slinger met een kleine uitwijking. De tweede manier is om een systeem te modelleren als een kleine variatie op zo'n exact oplosbaar model, met behulp van zogenaamde storingsrekening. Zwakke interacties tussen deeltjes kunnen hiermee goed worden beschreven, maar voor sterke interacties werkt dit niet meer. Een mogelijke oplossing is dan om de theorie te herformuleren zodat deze alsnog exact oplosbaar is. Uiteindelijk kan er nog worden gewerkt met een numerieke benadering door middel van computersimulaties.

De natuurkunde van gecondenseerde materie is een bijzonder omvangrijk veld en gaat over het macroscopisch en microscopische gedrag van materialen, en analyseert daarvoor grote verzamelingen van ionen, electronen en hun interacties. In de natuur kunnen twee soorten deeltjes onderscheiden worden aan de hand van spin, een intrinsieke eigenschap, zoals massa, die erg lijkt op impulsmoment. Er zijn fermionen, deeltjes met halftallig spin ($\frac{1}{2}$,$\frac{3}{2}$,etc.), en bosonen, deeltjes met heeltallig spin (0,1, etc.). Voor fermionen geldt het Pauli uitsluitingsprincipe, dat stelt dat fermionen zich met niet meer dan één tegelijk in dezelfde quantumtoestand kunnen bevinden. Bosonen kunnen zich wel allemaal in dezelfde quantumtoestand zitten. Elektronen zijn fermionen, en er kan dus slechts één elektron per

toestand zijn. Een voorbeeld van een veelbestudeerde materiaaleigenschap is elektrische geleiding, het transport van elektrische lading. Geleidende en isolerende eigenschappen van materialen kunnen worden verklaard aan de hand van de bandstructuur die uit de Hamiltoniaan volgt, d.w.z. de ligging van bezette en onbezette energieniveaus van elektronen. Omdat elektronen zich niet in dezelfde toestand kunnen bevinden, kunnen ze vanuit hun eigen energieniveau alleen naar een onbezet niveau bewegen. Liggen de vrije en bezette energieniveaus tegen elkaar aan, dan kan een electron makkelijk naar een hoger liggend energieniveau springen, en is het materiaal geleidend. Scheidt een grote afstand beide niveaus, de bandkloof, dan is het zeer lastig, en is het materiaal isolerend. Zo'n tien jaar geleden is gebleken dat topologie een grote rol speelt in het fasegedrag van materialen. In deze tak uit de wiskunde wordt bestudeerd welke eigenschappen van objecten hetzelfde blijven als ze geleidelijk worden veranderd. Het klassieke voorbeeld is dat van een donut en een koffiemok: allebei hebben ze één gat, en door het materieel te kneden kunnen ze in elkaar vervormd worden, zonder het gat dicht te maken. Dit wordt topologische gelijkheid genoemd. Ze zijn bijvoorbeeld niet gelijk aan een bord (geen gat) of een krakeling (twee gaten). Deze topologische eigenschappen blijken grote invloed te hebben op, bijvoorbeeld, het geleidende of isolerende karakter van materialen. Als nu de Hamiltoniaan van een bepaald systeem geleidelijk veranderd kan worden in dat van een ander systeem, dat wil zeggen zonder dat de bandkloof gesloten wordt, zijn zij topologisch aan elkaar gelijk. De eigenschappen van zo'n topologische fase zijn erg bijzonder. Normaal gesproken is een materiaal overal geleidend of overal isolerend, maar een topologische isolator heeft op de rand geleidende toestanden, terwijl binnen het materiaal alleen maar isolerende toestanden voorkomen. Het gedrag van topologische materialen wordt in onze onderzoeksgroep veelvuldig bestudeerd, en deze thesis maakt ook deel van uit van het onderzoek. Hoofdstuk 2 geeft een introductie in dit onderwerp.

Een bijzonder interessant topologisch systeem is de Kitaev-keten, een één-dimensionale topologische supergeleider, die gemodelleerd is als een lange rij elektronen met bepaalde interacties. Een supergeleider wordt onder andere gekenmerkt door een verdwijnende elektrische weerstand voor lage temperaturen. In het model blijkt dat aan de randen van de keten voor bepaalde parameterwaarden nul-energie Majorana-toestanden ('zero-energy Majorana modes') verschijnen. Normaal gesproken heeft elk deeltje een ander anti-deeltje (denk aan een elektron en een positron), maar het bijzondere van Majorana-deeltjes is dat ze gelijk zijn aan hun eigen anti-deeltje. Hoewel hun bestaan al honderd jaar geleden theoretisch is voorspeld, zijn ze tot op heden nog niet experimenteel waargenomen. Er is overigens een verschil tussen fundamentele Majorana-deeltjes en de Majorana-toestanden die in deze thesis worden beschreven. De wiskunde is voor beide hetzelfde, maar de eerste categorie

betreft fundamentele deeltjes en de tweede categorie betreft quasideeltjes, een combinatie van elektronen en interacties. Het doel van het bestuderen van deze deeltjes is allereerst het verkrijgen van fundamenteel begrip, maar daarnaast zijn er ook interessante praktische toepassingen. De eigenschappen van Majorana-toestanden komen namelijk van pas bij het bouwen van een quantumcomputer, met een rekenkracht die vele malen groter is dan die van onze huidige computers. De tweede helft van Hoofdstuk 2 gaat over de Kitaev-keten.

Eén van de hoofdrolspelers in deze thesis is dissipatie, waarmee de energie wordt bedoeld die verloren gaat als gevolg van een interactie tussen een systeem en zijn omgeving. In experimenten is dit vaak een groot probleem. Natuurkundige theorieën gaan doorgaans uit van een Hamiltoniaan, en de veronderstelling dat deze totale energie van een systeem behouden blijft. Dissipatie gooit echter roet in het eten, omdat het vaak nauwelijks mogelijk is om grootheden in een compleet geïsoleerd systeem te meten, en dissipatie er voor zorgt dat de theoretische beschrijving van het systeem moeilijk te vergelijken is met de experimentele resultaten. In de jaren ‘80 hebben Caldeira en Leggett een theorie ontwikkeld om dissipatie te beschrijven. In Hoofdstuk 3 wordt dit model besproken. De truc hier is om de omgeving, waar de energie heen lekt, ook op te nemen in de Hamiltoniaan, zodat het complete systeem gesloten is. Deze omgeving wordt beschreven door een warmtebad, d.w.z. een grote groep harmonische oscillatoren, die individueel gekoppeld zijn aan het systeem dat we eigenlijk willen bestuderen. Deze theorie is erg succesvol gebleken in het beschrijven van decoherentie en tunneling, twee belangrijke verschijnselen in de quantumwereld. Gelukkig is dissipatie niet alleen nadelig. Enkele jaren geleden is duidelijk geworden dat dissipatie ook kan worden gebruikt om topologische toestanden te maken. De typische interactie die nodig is in de Kitaev-keten om supergeleiding te modelleren en ook leidt tot het verschijnen van de nul-energie Majorana-toestanden, kan vervangen worden door dissipatie. Dit is zeer interessant, omdat daarmee het bijzondere gedrag van topologische systemen experimenteel veel toegankelijker wordt. Dit nieuwe gebruik van dissipatie vormde de voornaamste motivatie van dit onderzoek, en in eerste instantie zijn we begonnen met het doel om dissipatie in de Kitaev-keten te bestuderen.

Hoofdstuk 4 beschrijft de theorie van de Luttinger-vloeistof (vloeistof omdat deeltjes met interacties worden bekeken, in tegenstelling tot een gas waar de dichtheid van deeltjes zo laag is dat er nauwelijks interacties plaatsvinden), de standaard manier om één-dimensionale fermionische systemen te beschrijven. Hoewel fermionen en bosonen in het algemeen erg verschillend zijn, lijken ze in één dimensie veel op elkaar. Dit heeft er mee te maken dat hun verschillende eigenschappen vooral tot uiting komen als er twee worden omgewisseld, en in één dimensie kunnen twee deeltjes niet om elkaar heen bewegen. Dit is de basis van de bosonisatie-methode, waarmee het omschrijven van een één-dimensionale fermionische

theorie naar een bosonische theorie wordt bedoeld. Dit is een erg krachtige methode, omdat het mogelijk maakt om interacties tussen fermionen, die vaak wiskundig gecompliceerde theorieën opleveren, om te schrijven naar een Hamiltoniaan van bosonische harmonische oscillatoren. Zoals eerder gezegd, het systeem van een harmonische oscillator kan analytisch worden opgelost, zodat nu via een omweg een oplossing van het systeem gevonden kan worden. Op deze manier kan de Luttinger-vloeistoftheorie voor fermionen omgeschreven worden naar een vergelijkbaar eenvoudige Hamiltoniaan, de sinus-Gordon vergelijking, die nog een extra interactie bevat, wiskundig weergegeven door een cosinus. Als deze interactie alleen plaatsvindt op de rand van een keten die zich verder oneindig uitstrekt (voor wiskundig gemak kunnen we dan de andere rand negeren), dan vinden we de rand sinus-Gordon vergelijking ('boundary sine-Gordon equation'). Interessant is dat we in deze laatste theorie op de rand van de keten een nul-energie Majorana-toestand vinden voor een bepaalde parameterwaarde.

De kern van deze scriptie wordt gevormd door Hoofdstuk 5. Alle losse onderdelen van het eerste deel van de scriptie komen hierin samen. In dit hoofdstuk wordt getoond dat de Hamiltoniaan van de rand sinus-Gordon vergelijking en dat van een systeem dat een deeltje dat tussen twee posities kan springen onder de invloed van dissipatie in het Caldeira-Leggett model, met elkaar overeen komen. Dit bewijs gaat in drie stappen. Allereerst wordt het natuurkundig veld dat de deeltjes beschrijft herschreven in termen van excitaties, een zogenaamde Fourier-mode expansie. Daarna wordt de basis van de toestanden geroteerd, zodanig dat de energieniveaus van het systeem niet veranderen. Dit komt grofweg overeen met het veranderen van gezichtspunt. Stel je voor dat je langs een voetbalveld staat, en naar de andere kant van het veld loopt. Hoe je de spelers ziet verandert, maar de opstelling blijft hetzelfde. Ten derde gebruiken we verschillende formalismen die de quantum harmonische oscillator beschrijven om de Hamiltoniaan te interpreteren als dat van een deeltje op een rooster met dissipatie. Met de kennis van Hoofdstuk 4 kunnen we ook een Luttinger-vloeistof naar het dissipatieve systeem omschrijven.

Hoofdstukken 6 en 7 vertegenwoordigen mijn eigen originele bijdrage. De oorspronkelijke correspondentie gaat uit van systemen zonder spin en de rand sinus-Gordon vergelijking. In het eerste hoofdstuk wordt de equivalentie toegepast op 'helical' Luttinger-systemen, waarin spin wordt toegevoegd en de spinoriëntatie gekoppeld is aan de bewegingsrichting: naar links bewegende deeltjes hebben spin $+\frac{1}{2}$, en naar rechts bewegende deeltjes hebben spin $-\frac{1}{2}$ (of vice versa). Dit systeem beschrijft het gedrag van elektronen aan de rand van topologische isolatoren, en is daarom van theoretisch belang. Ik laat zien dat de correspondentie ook voor dit systeem geldt. In het tweede hoofdstuk generaliseer ik de correspondentie naar de volledige sinus-Gordon vergelijking. Het blijkt dat de Hamiltoniaan van dit systeem

gelijk is aan dat van een deeltje dat op een oneindig lange keten beweegt. Zulke systemen komen in de natuur veel meer voor dan deeltjes die maar tussen twee posities kunnen springen, en hiermee wordt de overeenkomst van de Hamiltonianen in Hoofdstuk 5 veel breder inzetbaar.

De kracht van de overeenkomst is dat het de energetische beschrijving van experimenteel moeilijk toegankelijke systemen van elektronen en hun interacties koppelt aan een systeem dat experimenteel makkelijk is om te meten, namelijk dat van een deeltje op een rooster met dissipatie. Uiteindelijk zou dit een middel kunnen zijn om de invloed van dissipatie op nul-energie Majorana-toestanden in de Kitaev-keten te bestuderen, als een extra perspectief tussen de vele aangezichten die Picasso ons in zijn werken laat zien.

Acknowledgements

I would like to express my gratitude to my supervisors. First, to Cristiane, the most enthusiastic and inspiring professor I have met in my studies. She was the teacher of two marvellous courses I took in the Bachelor's and Master's programmes, during which I have gotten to know the area of condensed matter theory, and its beautiful connection between highly abstract theories and down-to-earth experiments. I want to thank her for her guidance in this research project, and her always attentive and discerning attitude which made the limited time available nonetheless very productive. I remember the beautiful analog she once drew between theoretical physics and the paintings by Pablo Picasso. In both, one tries to capture the essentials of Nature, with just a few strokes of the brush.

Second, to Gian, the postdoc who has been my tireless daily supervisor. More than once, he would send me another interesting paper he just found at 3:00 am - at any time prepared to think along with my project. Together, we spent many hours every week discussing my questions and problems I encountered, from theoretical understanding to countless minus signs and factors of 2. After all, that is the life of a theoretical physicist. His vast knowledge of literature, the ability of focusing and persisting for hours (months, sometimes) on end to completely solve a problem, starting out as a seemingly small one, and taking my questions and suggestions for new steps very seriously, even if they turned out to be trivial or unattainable, have been extremely educational. Gian, grazie mille di tutto.

I enjoyed the numerous discussions in the group meetings, which occasionally evolved into rather heated debates, showing each of the group members' passion for the topic and research.

Finally, I want to thank my fellow Master's students. Coming from all over the globe, together we took two years of courses and worked side-to-side on our theses. Borrowing each other's collective intelligence from time to time, sharing victories and drawbacks, we completed our degrees, before flying out to the next fascinating place on earth. It has been a pleasure.

References

[1] S. Diehl, E. Rico, M. A. Baranov, and P. Zoller, "Topology by dissipation in atomic quantum wires," *Nature Physics*, vol. 7, no. 12, pp. 971–977, 2011.

[2] A. O. Gogolin, A. A. Nersesyan, and A. M. Tsvelik, *Bosonization and strongly correlated systems*. Cambridge University Press, 2004.

[3] F. Guinea, "Dynamics of a particle in an external potential interacting with a dissipative environment," *Physical Review B*, vol. 32, no. 11, p. 7518, 1985.

[4] F. Guinea, V. Hakim, and A. Muramatsu, "Diffusion and localization of a particle in a periodic potential coupled to a dissipative environment," *Physical review letters*, vol. 54, no. 4, p. 263, 1985.

[5] C. L. Kane and E. J. Mele, "Quantum Spin Hall Effect in Graphene," *Phys. Rev. Lett.*, vol. 95, p. 226801, Nov 2005.

[6] B. A. Bernevig, T. L. Hughes, and S.-C. Zhang, "Quantum spin Hall effect and topological phase transition in HgTe quantum wells," *Science*, vol. 314, no. 5806, pp. 1757–1761, 2006.

[7] M. König, S. Wiedmann, C. Brüne, A. Roth, H. Buhmann, L. W. Molenkamp, X.-L. Qi, and S.-C. Zhang, "Quantum Spin Hall Insulator State in HgTe Quantum Wells," *Science*, 2007.

[8] A. Y. Kitaev, "Unpaired Majorana fermions in quantum wires," *Physics-Uspekhi*, vol. 44, no. 10S, p. 131, 2001.

[9] V. Mourik, K. Zuo, S. M. Frolov, S. Plissard, E. Bakkers, and L. Kouwenhoven, "Signatures of Majorana fermions in hybrid superconductor-semiconductor nanowire devices," *Science*, vol. 336, no. 6084, pp. 1003–1007, 2012.

[10] S. Albrecht, A. Higginbotham, M. Madsen, F. Kuemmeth, T. Jespersen, J. Nygård, P. Krogstrup, and C. Marcus, "Exponential protection of zero modes in Majorana islands," *Nature*, vol. 531, no. 7593, pp. 206–209, 2016.

[11] F. D. M. Haldane, "'Luttinger liquid theory' of one-dimensional quantum fluids. I. Properties of the Luttinger model and their extension to the general 1D interacting spinless Fermi gas," *Journal of Physics C: Solid State Physics*, vol. 14, no. 19, p. 2585, 1981.

[12] A. Caldeira and A. J. Leggett, "Quantum tunnelling in a dissipative system," *Annals of Physics*, vol. 149, no. 2, pp. 374–456, 1983.

[13] A. O. Caldeira and A. J. Leggett, "Path integral approach to quantum Brownian motion," *Physica A: Statistical mechanics and its Applications*, vol. 121, no. 3, pp. 587–616, 1983.

[14] L. Landau, "Zur Theorie der phasenumwandlungen II," *Phys. Z. Sowjetunion*, vol. 11, pp. 26–35, 1937.

[15] K. v. Klitzing, G. Dorda, and M. Pepper, "New Method for High-Accuracy Determination of the Fine-Structure Constant Based on Quantized Hall Resistance," *Phys. Rev. Lett.*, vol. 45, pp. 494–497, Aug 1980.

[16] J. R. Hook, H. E. Hall, and H. E. Hall, *Solid state physics*. Wiley, 1991.

[17] Nanite (own work) via Wikimedia Commons, "Band structure diagrams for metal, etc. Inspired by Kittel's Introduction to Solid State Physics 7th Edition, chapter 7," 2013.

[18] J. Bardeen, L. N. Cooper, and J. R. Schrieffer, "Theory of superconductivity," *Physical Review*, vol. 108, no. 5, p. 1175, 1957.

[19] M.-K. Wu, J. R. Ashburn, C. Torng, P. H. Hor, R. L. Meng, L. Gao, Z. J. Huang, Y. Wang, and a. Chu, "Superconductivity at 93 K in a new mixed-phase Y-Ba-Cu-O compound system at ambient pressure," *Physical Review Letters*, vol. 58, no. 9, p. 908, 1987.

[20] K.-H. Bennemann and J. B. Ketterson, *Superconductivity: Volume 1: Conventional and Unconventional Superconductors, Volume 2: Novel Superconductors*. Springer Science & Business Media, 2008.

[21] E. H. Hall, "On a new action of the magnet on electric currents," *American Journal of Mathematics*, vol. 2, no. 3, pp. 287–292, 1879.

[22] D. Tong, "Lectures on the Quantum Hall Effect," *ArXiv e-prints*, June 2016.

[23] K. Von Klitzing, "The quantized Hall effect," *Reviews of Modern Physics*, vol. 58, no. 3, p. 519, 1986.

[24] M. Z. Hasan and C. L. Kane, "Colloquium: topological insulators," *Reviews of Modern Physics*, vol. 82, no. 4, p. 3045, 2010.

[25] C. Morais Smith, "The Quantum Hall Effect - An Introductory Course," *Personal Collection of C. de Morais Smith, Utrecht University, The Netherlands*.

[26] D. Thouless, M. Kohmoto, M. Nightingale, and M. Den Nijs, "Quantized Hall conductance in a two-dimensional periodic potential," *Physical Review Letters*, vol. 49, no. 6, p. 405, 1982.

[27] F. D. M. Haldane, "Model for a quantum Hall effect without Landau levels: Condensed-matter realization of the" parity anomaly"," *Physical Review Letters*, vol. 61, no. 18, p. 2015, 1988.

[28] D. C. Tsui, H. L. Stormer, and A. C. Gossard, "Two-Dimensional Magnetotransport in the Extreme Quantum Limit," *Phys. Rev. Lett.*, vol. 48, pp. 1559–1562, May 1982.

[29] R. B. Laughlin, "Anomalous Quantum Hall Effect: An Incompressible Quantum Fluid with Fractionally Charged Excitations," *Phys. Rev. Lett.*, vol. 50, pp. 1395–1398, May 1983.

[30] L. Fu and C. L. Kane, "Topological insulators with inversion symmetry," *Physical Review B*, vol. 76, no. 4, p. 045302, 2007.

[31] X.-L. Qi and S.-C. Zhang, "The quantum spin Hall effect and topological insulators," *Physics Today*, vol. 63, no. 1, pp. 33–38, 2010.

[32] I. K. Drozdov, A. Alexandradinata, S. Jeon, S. Nadj-Perge, H. Ji, R. Cava, B. A. Bernevig, and A. Yazdani, "One-dimensional topological edge states of bismuth bilayers," *Nature Physics*, vol. 10, no. 9, pp. 664–669, 2014.

[33] R. Resta, "Manifestations of Berry's phase in molecules and condensed matter," *Journal of Physics: Condensed Matter*, vol. 12, no. 9, p. R107, 2000.

[34] B. A. Bernevig and T. L. Hughes, *Topological insulators and topological superconductors*. Princeton University Press, 2013.

[35] T. Morimoto and A. Furusaki, "Topological classification with additional symmetries from Clifford algebras," *Physical Review B*, vol. 88, no. 12, p. 125129, 2013.

[36] A. P. Schnyder, S. Ryu, A. Furusaki, and A. W. W. Ludwig, "Classification of topological insulators and superconductors in three spatial dimensions," *Phys. Rev. B*, vol. 78, p. 195125, Nov 2008.

[37] S. Ryu, A. P. Schnyder, A. Furusaki, and A. W. Ludwig, "Topological insulators and superconductors: tenfold way and dimensional hierarchy," *New Journal of Physics*, vol. 12, no. 6, p. 065010, 2010.

[38] A. Altland and M. R. Zirnbauer, "Nonstandard symmetry classes in mesoscopic normal-superconducting hybrid structures," *Physical Review B*, vol. 55, no. 2, p. 1142, 1997.

[39] M. Sato and Y. Ando, "Topological Superconductors," *ArXiv e-prints*, Aug. 2016.

[40] J. Alicea, "New directions in the pursuit of Majorana fermions in solid state systems," *Reports on Progress in Physics*, vol. 75, no. 7, p. 076501, 2012.

[41] M. Leijnse and K. Flensberg, "Introduction to topological superconductivity and Majorana fermions," *Semiconductor Science and Technology*, vol. 27, no. 12, p. 124003, 2012.

[42] E. Majorana, "Teoria simmetrica dell'elettrone e del positrone," *Il Nuovo Cimento (1924-1942)*, vol. 14, no. 4, pp. 171–184, 1937.

[43] S. Nadj-Perge, I. K. Drozdov, J. Li, H. Chen, S. Jeon, J. Seo, A. H. MacDonald, B. A. Bernevig, and A. Yazdani, "Observation of Majorana fermions in ferromagnetic atomic chains on a superconductor," *Science*, vol. 346, no. 6209, pp. 602–607, 2014.

[44] J. C. Budich and E. Ardonne, "Equivalent topological invariants for one-dimensional Majorana wires in symmetry class *D*," *Phys. Rev. B*, vol. 88, p. 075419, Aug 2013.

[45] A. Karch, J. Maciejko, and T. Takayanagi, "Holographic fractional topological insulators in $2+1$ and $1+1$ dimensions," *Phys. Rev. D*, vol. 82, p. 126003, Dec 2010.

[46] C. Nayak, S. H. Simon, A. Stern, M. Freedman, and S. D. Sarma, "Non-Abelian anyons and topological quantum computation," *Reviews of Modern Physics*, vol. 80, no. 3, p. 1083, 2008.

[47] J. K. Pachos, *Introduction to topological quantum computation*. Cambridge University Press, 2012.

[48] P. Langevin, "Sur la théorie du mouvement brownien," *CR Acad. Sci. Paris*, vol. 146, no. 530-533, p. 530, 1908.

[49] A. O. Caldeira, *An introduction to macroscopic quantum phenomena and quantum dissipation*. Cambridge University Press, 2014.

[50] G. Lindblad, "On the generators of quantum dynamical semigroups," *Communications in Mathematical Physics*, vol. 48, no. 2, pp. 119–130, 1976.

[51] R. P. Feynman and F. L. Vernon, "The theory of a general quantum system interacting with a linear dissipative system," *Annals of physics*, vol. 24, pp. 118–173, 1963.

[52] U. Weiss, *Quantum dissipative systems*, vol. 10. World Scientific, 1999.

[53] H. Kleinert, *Path integrals in quantum mechanics, statistics, polymer physics, and financial markets*. World Scientific, 2009.

[54] R. P. Feynman, "Lectures on Statistical Mechanics," 1972.

[55] G. Giuliani and G. Vignale, *Quantum theory of the electron liquid*. Cambridge university press, 2005.

[56] D. Sénéchal, A.-M. Tremblay, and C. Bourbonnais, *Theoretical methods for strongly correlated electrons*. Springer Science & Business Media, 2006.

[57] R. Doretto, A. Caldeira, and S. Girvin, "Lowest Landau level bosonization," *Physical Review B*, vol. 71, no. 4, p. 045339, 2005.

[58] A. C. Neto and E. Fradkin, "Bosonization of the low energy excitations of fermi liquids," *Physical review letters*, vol. 72, no. 10, p. 1393, 1994.

[59] P. Jordan and E. P. Wigner, "About the Pauli exclusion principle," *Z. Phys*, vol. 47, no. 631, pp. 14–75, 1928.

[60] T. Giamarchi, *Quantum physics in one dimension*. Oxford university press, 2004.

[61] P. Mathieu and D. Sénéchal, *Conformal field theory*. Springer Science & Business Media, 1997.

[62] P. H. Ginsparg, "Applied conformal field theory," *arXiv preprint hep-th/9108028*, vol. 63, 1988.

[63] J. Luttinger, "An exactly soluble model of a many-fermion system," *Journal of Mathematical Physics*, vol. 4, no. 9, pp. 1154–1162, 1963.

[64] S.-I. Tomonaga, "Remarks on Bloch's method of sound waves applied to many-fermion problems," *Progress of Theoretical Physics*, vol. 5, no. 4, pp. 544–569, 1950.

[65] X.-G. Wen, "Chiral Luttinger liquid and the edge excitations in the fractional quantum Hall states," *Physical Review B*, vol. 41, no. 18, p. 12838, 1990.

[66] B. Braunecker, C. Bena, and P. Simon, "Spectral properties of Luttinger liquids: A comparative analysis of regular, helical, and spiral Luttinger liquids," *Phys. Rev. B*, vol. 85, p. 035136, Jan 2012.

[67] G. Dolcetto, M. Sassetti, and T. L. Schmidt, "Edge physics in two-dimensional topological insulators," *arXiv preprint arXiv:1511.06141*, 2015.

[68] T. Li, P. Wang, H. Fu, L. Du, K. A. Schreiber, X. Mu, X. Liu, G. Sullivan, G. A. Csáthy, X. Lin, *et al.*, "Observation of a helical Luttinger liquid in InAs/GaSb quantum spin Hall edges," *Physical review letters*, vol. 115, no. 13, p. 136804, 2015.

[69] C. Wu, B. A. Bernevig, and S.-C. Zhang, "Helical Liquid and the Edge of Quantum Spin Hall Systems," *Phys. Rev. Lett.*, vol. 96, p. 106401, Mar 2006.

[70] H. Saleur, S. Skorik, and N. Warner, "The boundary sine-Gordon theory: classical and semi-classical analysis," *Nuclear Physics B*, vol. 441, no. 3, pp. 421–436, 1995.

[71] S. Mandelstam, "Soliton operators for the quantized sine-Gordon equation," *Physical Review D*, vol. 11, no. 10, p. 3026, 1975.

[72] S. Coleman, "More about the massive Schwinger model," *Annals of Physics*, vol. 101, no. 1, pp. 239–267, 1976.

[73] S. Ghoshal and A. Zamolodchikov, "Boundary S matrix and boundary state in two-dimensional integrable quantum field theory," *International Journal of Modern Physics A*, vol. 9, no. 21, pp. 3841–3885, 1994.

[74] M. Müller and A. A. Nersesyan, "Classical impurities and boundary Majorana zero modes in quantum chains," *arXiv preprint arXiv:1603.01037*, 2016.

[75] A. J. Leggett, S. Chakravarty, A. Dorsey, M. P. Fisher, A. Garg, and W. Zwerger, "Dynamics of the dissipative two-state system," *Reviews of Modern Physics*, vol. 59, no. 1, p. 1, 1987.

[76] P. Matthews, P. Ribeiro, and A. M. García-García, "Dissipation in a Simple Model of a Topological Josephson Junction," *Physical review letters*, vol. 112, no. 24, p. 247001, 2014.

[77] P. Lecheminant, A. O. Gogolin, and A. A. Nersesyan, "Criticality in self-dual sine-Gordon models," *Nuclear Physics B*, vol. 639, no. 3, pp. 502–523, 2002.